

TESLA - COLLABORATION

A Proposal to Construct and Test Prototype Superconducting RF Structures for Linear Colliders



March 1993, TESLA 93-01

**A Proposal to Construct and Test
Prototype Superconducting R.F. Structures
for Linear Colliders**

(April 1992)

The following individuals have participated in the work leading to this proposal:

CERN

D.Bloess
G.Geschonke
E.Haebel
H.Kugler
H.Lengeler
W.Pirkl
H.Riege

CORNELL

H.Padamsee
M.Tigner

TH DARMSTADT

R.Wanzenberg

FERMILAB

M.Champion
P.L.Colestock
H.Edwards
D.Finley
J.Kerby
K.Koepke
T.Nicol
R.Pasquinelli
J.Peoples
T.Petersen

INFN FRASCATI S.Tazzari

KFK KARLSRUHE K.P.Jüngst

UNIV. KARLSRUHE H.Steinhart

INFN MILANO C.Pagani

SACLAY B.Aune
 B.Bonin
 J.Cavedon
 J.Gastebois
 M.Jablonka
 F.Juster
 E.Klein
 P.Leconte
 A.Mosnier
 P.Paillier
 A.Patoux

GESAMTHOCHSCHULE WUPPERTAL
 A.Michalke
 G.Müller
 D.Reschke

DESY

I.Borchardt
W.Bothe
B.Dwersteg
G.Enderlein
A.Gamp
S.Herb
G.Horlitz
H.Kaiser
M.Leenen
H.Lierl
A.Matheisen
G.Meyer
W.D.Möller
B.Petersen
D.Proch
P.Schmüser
J.Sekutowicz
D.Trines
B.H.Wiik
S.Wolff

CONTENTS

1.	Introduction	1
2.	State of the Art	5
	2.1 Performance of Superconducting RF Systems	5
	2.2 Prospects for Improved Cavity Performance	9
3.	Project Overview	18
4.	Prototype Module	34
	4.1 Cavity	34
	4.2 Tuner and Couplers	43
	4.3 Cryostat	53
	4.4 Production and Assembly	70
5.	Test Facility	83
	5.1 General Layout	83
	5.2 Injector	83
	5.3 Cryogenics	90
	5.4 RF System	97
	5.5 Diagnostics	109
	5.6. Experimental Programme	112
6.	Further R & D Towards TESLA Goals	116
	Appendix 1	118
	Appendix 2	128

1. Introduction

The study of e^+e^- interactions has yielded a wealth of information on the basic constituents of matter and on the forces which act between these constituents. This is due to the inherent simplicity of the annihilation process. The incoming electrons and positrons annihilate to form a time like electroweak current with well defined quantum numbers $J^{PC} = 1^{--}$ which in turn couples directly to the basic constituents of matter. Thus the cross sections are well known and the annihilation process leads to a well defined final state topology. New particles can therefore be easily found and their properties unambiguously determined in a clean environment. Conversely a negative search can be used to define mass limits on new particles. It is thus desirable to extend e^+e^- experiments beyond LEP energies. Indeed an e^+e^- collider which covers the mass range between the W^+W^- pair production threshold and 500 GeV with luminosities in excess of $10^{33} \text{ cm}^{-2} \text{ s}^{-1}$ will have a rich physics programme complementary to the programme at the large hadron colliders.

Experiments at such an e^+e^- collider would allow us to:

- Explore the mass region around the Fermi mass scale of 250 GeV in detail. This is the natural scale for new phenomena to occur.
- Study the production and the decay of $t\bar{t}$ pairs.
- Carry out stringent tests of the standard model.
- Find the Higgs boson if its mass is less than 350 GeV and determine its properties. At these collider energies the favoured minimal supersymmetric extension of the Higgs model can either be confirmed or excluded.
- Search for new physics. Candidates are pair production of supersymmetric particles with mass less than 250 GeV, production of new leptons with mass up to the kinematic limit or a search for evidence of compositeness at the scale of 200 TeV.

There is a consensus that the energy range in e^+e^- collisions beyond LEP can only be explored by the use of linear colliders. However, to reach the energy and luminosity listed above requires to extend the performance of the Stanford Linear Collider by 4-5 orders of magnitude in luminosity and by a factor of 5 in energy. There are several proposals how to achieve this goal.

- SLAC, KEK and Novosibirsk/Serpukhov propose to use a warm traveling wave structure at 11.4 GHz and a gradient in the order of 50 MV/m. Several bunches spaced 1 ns apart are accelerated within the 80 ns long RF pulse.

Despite these attractive features relatively little effort has gone into establishing the technological base for a superconducting linear accelerator. The reason for this reluctance is the high cost per MV of acceleration derived from the cost and performance of superconducting cavities in storage rings. A price often quoted is 40.000 \$/MV which is based on an accelerating gradient of 5 MV/m and a cost of 200.000 \$ per meter of cavity.

The maximum accelerating gradient, which theoretically is around 50 MV/m for a Nb cavity is in general limited to lower values by field emission from localized regions of the cavity surface. In the last few years there has been dramatic progress both in our understanding of the field emission mechanism and in its cures. Both high temperature processing of cavities in vacuum or high RF power processing consistently yields multicell cavities with accelerating gradients between 15 MV/m and 20 MV/m. To reduce the cost per MV further we have designed a cryostat housing eight 9-cell 1.3 GHz cavities complete with tuners, power couplers and higher order mode couplers. Preliminary cost estimates indicate that with this design and a gradient of 25 MV/m the cost may be below 2000 \$/MV.

To demonstrate that this goal can indeed be achieved we propose to build four 12 m long cryostats each with eight 9-cell cavities at 1.3 GHz. The cavities are complete with tuners, higher order mode couplers and power couplers. With these first cavities we aim at reaching an accelerating gradient of at least 15 MV/m at $Q_0 = 3 \cdot 10^9$. The static heat load should be less than 1 W/m, i.e. at least a fivefold improvement of presently quoted values.

Once the cavities have been built and tested at liquid helium temperatures with high power we propose to inject and accelerate high current, high density electron bunches through the structure and demonstrate the performance of the accelerator.

In parallel we also propose to process a large number of Nb cavities to demonstrate that cavities with the performance required to construct linear colliders can be reliably and reproducibly manufactured. Basic research at various laboratories aimed at improving the performance of superconducting cavities will continue.

It is the aim of this proposal to create the technical basis for the construction of a 300 GeV to 500 GeV linear collider including a reliable cost estimate. If approved early in 1992 we believe that this work can be completed by 1996.

The present report is structured as follows:

The state of the art in RF superconductivity and the prospects of meeting the design goals of the test facility are discussed in chapter 2. An overview of the project is given in chapter 3. The design, construction and assembly of the cavities, the auxiliaries and the cryostat are outlined in chapter 4. The layout and the various components of the test facility are discussed in chapter 5 including the foreseen experimental programme. An outline of the basic research programme at the various laboratories aimed at improving the cavity performance can be found in chapter 6.

2. State of the Art

2.1 Performance of Superconducting RF Systems

Superconducting RF (SRF) technology is mature enough today to make significant and wide-ranging contributions to accelerators for particle physics, nuclear physics and free electron lasers. Application of SRF cavities is in progress at more than 25 laboratories around the world. Industrial capability has grown to meet the needs for application of SRF technology in future large accelerator projects.

To provide precision beams of heavy ions for nuclear physics research, linacs to boost the energy from existing electrostatic tandem van de Graafs have been one of the most successful applications of SRF technology since 1978. Pioneered at Argonne and SUNY, Stony Brook, 5 booster facilities are now operating, utilizing over 50 meters of superconducting resonators at gradients of 2 - 3 MV/m, logging over 100.000 hours of operating experience.

In the last few years, more than 70 meters of niobium cavities have been installed in high energy colliders: TRISTAN, LEP and HERA, logging more than 10.000 hours of operation at gradients around 5 MV/m. This should be compared to copper RF systems running in the same machines at ~ 1 MV/m. Based on these successes, plans to install over 300 meters of SRF cavities to double the energy of LEP are proceeding vigorously. Besides the energy upgrade possibilities, SRF cavities are considered attractive for high luminosity factories, such as CESR-B at Cornell. The higher voltage capability of SRF cavities, together with their large beam holes and smooth iris geometries, allow a substantial reduction in machine impedance.

Superconducting recirculating linacs are in use for electron accelerators for nuclear physics. A 3-pass 130 MeV machine utilizing 8 meters of niobium cavities recently turned on at TH Darmstadt (Darmstadt/Wuppertal collaboration). When completed in 1994, CEBAF in the U.S. will use 180 meters of Nb cavities. The superconducting linac injector for this machine is already operating at 45 MeV. Saclay has established a pilot SC linac (MACSE) and successfully accelerated a 10 MeV beam. In addition to lower power consumption, a SRF linac offers special advantages for nuclear physics in the form of continuous (100% duty cycle) beams of high average current (100 - 200 μ A) and excellent

beam quality.

The first free electron laser (FEL) was demonstrated with the high quality 50 MeV electron beam from the pioneering superconducting linac (SCA) at Stanford University. Because good beam quality is essential for short wavelength FELs, SRF linacs make excellent drivers. Now several FEL projects using SC linacs are underway, such as at INFN Frascati and JAERI, Japan.

Total installed voltage over the years for both ion and electron accelerators is plotted in Fig. 2.1. In all, more than 100 meters of niobium accelerating structures have been built and tested for electron accelerators. A large number of these structures were made by industry. In acceptance tests these structures reach an average accelerating field of 9 MV/m (Fig. 2.2) with Q values over $2 \cdot 10^9$.

Key aspects responsible for this performance are the anti-multipactor cell shape, and the high thermal conductivity niobium to stabilize against premature breakdown of superconductivity from small imperfections (defects). Niobium producing industry has responded admirably to the needs of the RF superconductivity community by increasing the purity and thereby the thermal conductivity of niobium by an order of magnitude in the last decade.

In summary, RF superconductivity has become an important technology for particle accelerators. Practical structures with attractive performance levels have been developed for a variety of applications. Operating experience shows that the design accelerating fields can be maintained for long periods. Substantial progress has been made in understanding field limitations and in inventing cures through better cavity geometries, materials and processes. The technical and economic potential of RF superconductivity makes it a candidate for future accelerators at the energy frontier.

However, in order to base the construction of the next linear collider on this technology the cost per MV of accelerating voltage must be reduced drastically. The prospects for improving the cavity performance while lowering the production cost are discussed next.

- | | |
|-----------------------------|-----------------------------|
| A: Stanford | F: Karlsruhe |
| B: Cornell | G: Argonne |
| C: Darmstadt | H: Stony Brook |
| D: CERN, Cornell, DESY, KEK | I: Florida State |
| E: KEK | J: University of Washington |
| | K: Saclay |
| | L: Argonne PII |

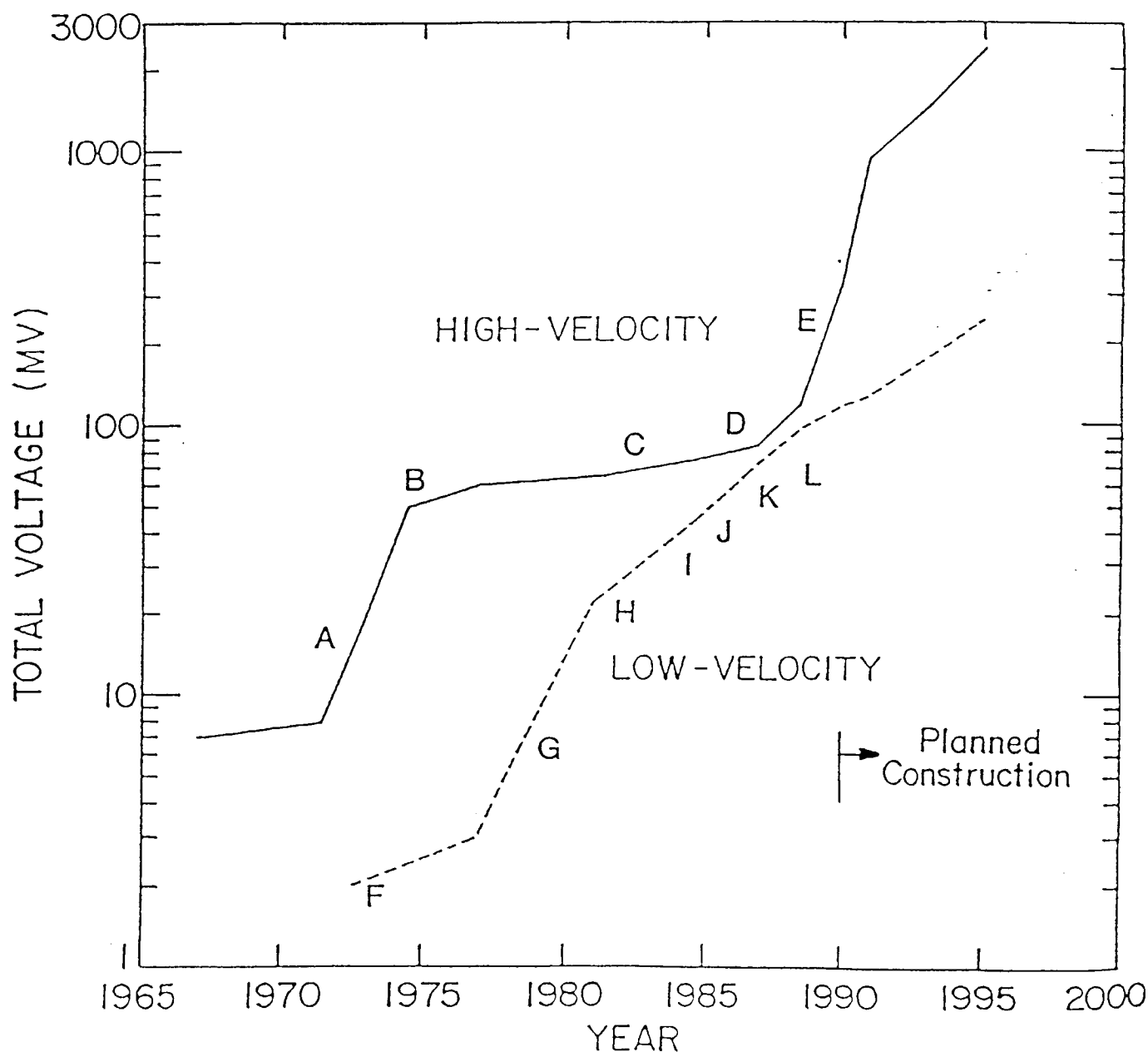


Fig. 2.1 Integrated, accumulative voltage in test and/or operation of superconducting cavities with beam.

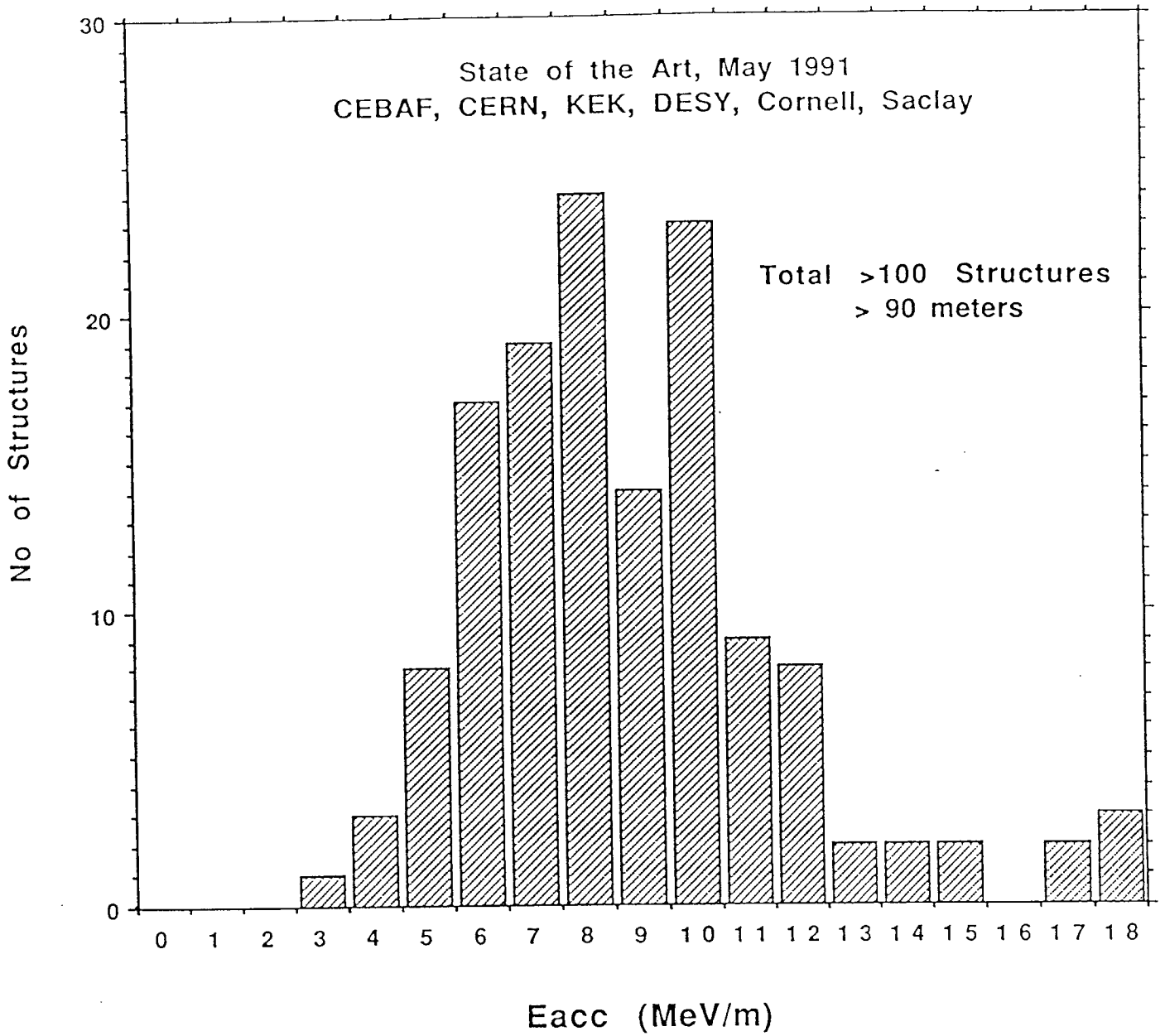


Fig. 2.2 State of the Art in Accelerating Gradients reached with standard chemical treatments. The data were obtained from the measurements of fully equipped structures in vertical cryostats.

2.2 Prospects for Improved Cavity Performance

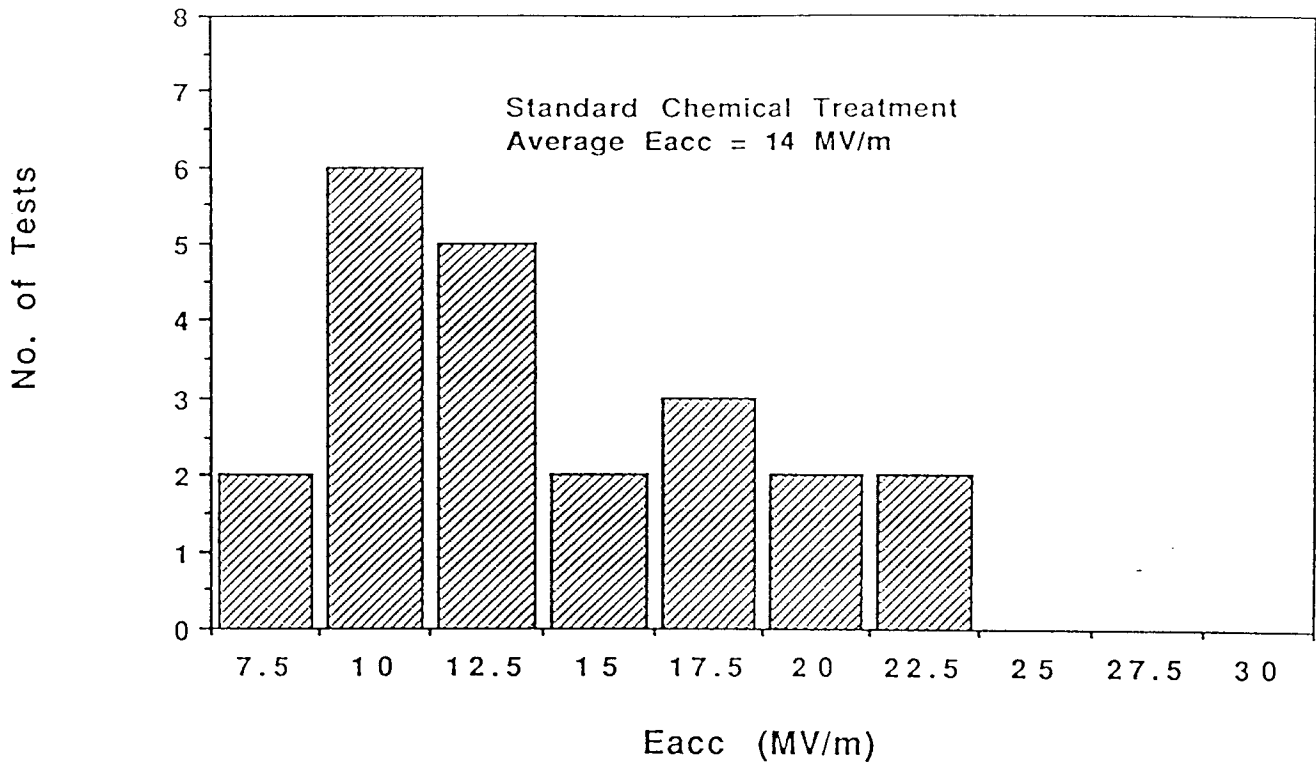
Today, the main obstacle to reliably achieving gradients above 10 MV/m is recognized to be the tenacious problem of field emission. In RF cavities, field emitted electrons are accelerated and strike the cavity surfaces causing heating, lowering of the Q and emission of bremsstrahlung X-rays. The enhanced emission is known to occur from isolated sites. Studies in which such sites are located by a DC probe, and subsequently examined by surface analytic tools, show that the enhanced emission is associated with μm size contaminant particles, or with inclusions. These studies confirm the critical importance of dust free environments, clean materials and clean test systems for preparation of emission free surfaces.

Two new approaches to overcome field emission in RF cavities have been studied extensively and have been used to effect significant improvement.

Encouraged by early results from DC field emission studies, there has been considerable exploration of the influence of high temperature annealing in a good vacuum for the final stage of SRF cavity preparation. In the DC studies, conducted at the University of Geneva, niobium samples scanned for emission sites were high temperature annealed and subsequently rescanned, all without removal from UHV. Above 1200°C the density of emitters was drastically reduced. Surfaces of cm^2 size which do not emit up to 100 MV/m were repeatedly obtained above 1400°C . Together with the emission, particles associated with emission were also observed to disappear, presumably by evaporation or dissolution. Artificially introduced emitters such as graphite particles could also be eliminated by heat treatment.

Using one-cell 1.5 GHz Nb cavities, a substantial reduction in emission was confirmed at Cornell for heat treatments between $1400\text{-}1500^{\circ}\text{C}$ and periods between 4-8 hours. During the heat treatment, the outer wall of the cavity must be coated with Titanium to prevent the purity of the cavity wall from degrading in the furnace. Fig. 2.3 shows that the average accelerating field reached in 9 separate heat treatments at 1500°C was 26 MV/m (assuming $E_{\text{pk}} / E_{\text{acc}} = 2$), with the record of 30 MV/m. Lower temperature heat treatments ($1200\text{-}1350^{\circ}\text{C}$) were also found useful in reducing emission but less substantially. More detailed studies that localize individual emission sites and determine

1.5 GHz, 1-cell
8 cavities, 18 Tests



1.5 GHz, 1-cell

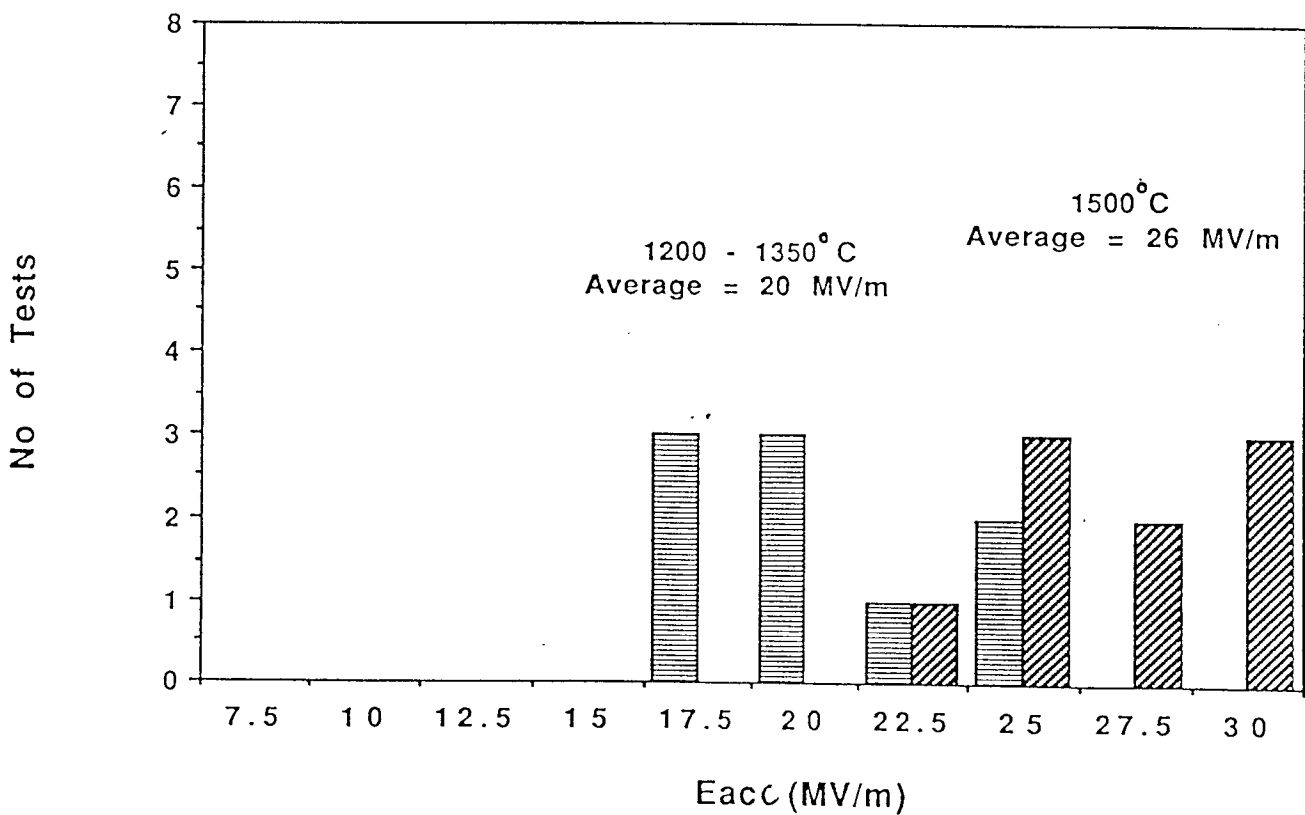


Fig. 2.3 A comparison of results on 1 cell, 1.5 GHz cavities at Cornell prepared by standard chemical treatment (upper) with those prepared by heat treatment (lower).

their emission characteristics are based on measurements of the cavity wall temperature increases caused by impinging electrons, i.e. temperature maps. Maps accompanying the 1.5 GHz one-cell cavity tests show an order of magnitude reduction in emitter density by comparison with the chemically prepared surface.

To summarize, with this specially developed heat treatment technique to reduce emission, one-cell cavities now regularly reach accelerating fields of 25 MV/m, needed for TESLA.

Heat treatment tests on multi-cell cavities have started. 5-cell and 9-cell cavities at 3 GHz are heat treated at Wuppertal, while 6-cell cavities at 1.5 GHz are heat treated at Cornell. In most tests accelerating fields > 15 MV/m are now more the rule rather than the exception, as shown in Fig. 2.4. This work is still in progress.

Important additional benefits are derived from heat treatment. The Ti protection coating is effective in improving the purity of the cavity wall by a factor of 2 or more, providing increased stabilization against thermal breakdown. Heat treatment homogenizes the material and ensures high thermal conductivity everywhere. Finally, above 1400°C , any hydrogen trapped in the wall during the chemical cleaning stage is completely removed, so that there are no problems with Q degradation from hydrogen, a difficulty that is often observed after chemical etching.

The second promising technique for overcoming field emission uses short pulses of high RF power to process a superconducting cavity. This technique is labelled HPP for high pulsed power. In regular testing of superconducting cavities at low power (10-100 W, cw), emission is often observed to reduce slightly, especially when the RF is increased for the first time. Eventually however, emission becomes stable and no further progress is realized. In most cases the test is terminated when the maximum available RF power is applied.

For many years, in processing structures used for heavy ion accelerators at Argonne and elsewhere, 1 - 2 kW of pulsed (msec) RF power was found more effective than the usual cw method. A study conducted at SLAC explored the use of 1 - 2 MW of peak power pulses of 1 - 2 μsec on 3 GHz 1-cell niobium cavities. It was shown possible to reach accelerating fields of 27 to 35 MV/m for 1 μsec . However, because of the fixed input power coupling system used, it was not possible to determine if the benefits from the high power exposure would extend to long pulses needed for TESLA or for cw operation.

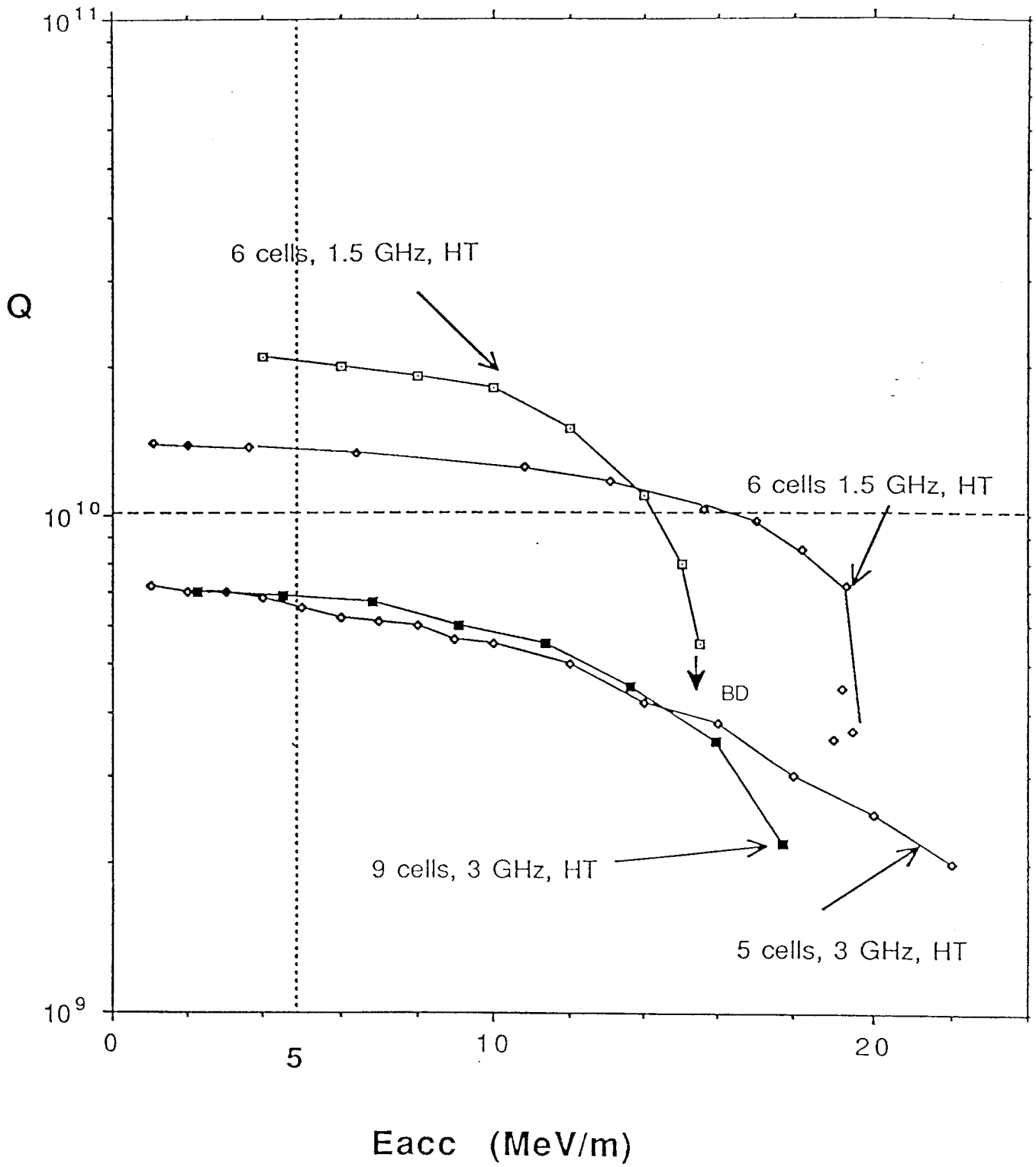


Fig. 2.4 Q versus E_{acc} for all heat treated multicell cavities (Cornell and Wuppertal).

Based on the encouraging results from these experiments, a wider exploration of the HPP technique was conducted at Cornell. The test setup was designed with variable input coupling without breaking the cavity vacuum. This method has proved quite effective.

With pulses up to 1 msec long and peak RF power between 2 and 50 kW, the onset of field emission in 6 cw tests on several 1-cell 3 GHz cavities was moved up by 50%. The maximum fields reached in these tests were $E_{acc} = 17 - 27$ MV/m(cw), with weak emission remaining. Q values over 10^{10} at $E_{acc} = 20$ MV/m were found possible after HPP.

Once again, single cell tests with HPP have demonstrated with a totally different technique the feasibility of the TESLA goal of 25 MV/m.

Extension of tests on HPP to multi-cell structures has also started at Cornell, using a 9-cell 3 GHz cavity. Five separate tests have been carried out, each time after preparing the cavity anew with standard chemical treatment. In all five tests, field emission limited the initial performance of the cavity as shown in three examples of Fig. 2.5. In each case the field emission limitation was overcome with pulsed power processing using 100 kW. The very first test was limited to $E_{acc} = 16$ MV/m by thermal breakdown which was attributed to the low RRR = 200. After improving the RRR to 400 at Wuppertal by a post-purification process, the next four tests reached $E_{acc} = 17$ to 20 MV/m. Most recently, a 6th test was carried out after exposing a processed surface to dust-free air for 24 hours. On retesting, it was possible to reach $E_{acc} = 18$ MV/m without any further processing.

An understanding of the HPP solution to field emission is taking shape. Microscopic examinations of dissected 1-cell cavities indicate that emitter extinction takes place by an explosive process. Presumably, at a high enough electric field, the local field emission current density exceeds 10^8 A/cm², shown by calculations to be sufficient to reach melting temperatures near the emitter. Subsequent visual inspection reveals crater-like holes with 5 - 10 μ m in diameter, and often nearby regions of molten remnants of the contaminant responsible for emission (see Fig. 2.6). The features found suggest the occurrence of a RF spark.

The key to successful processing is to establish a high electric field at the emission site, even for a short time (μ sec), so that the local emission current density can be elevated

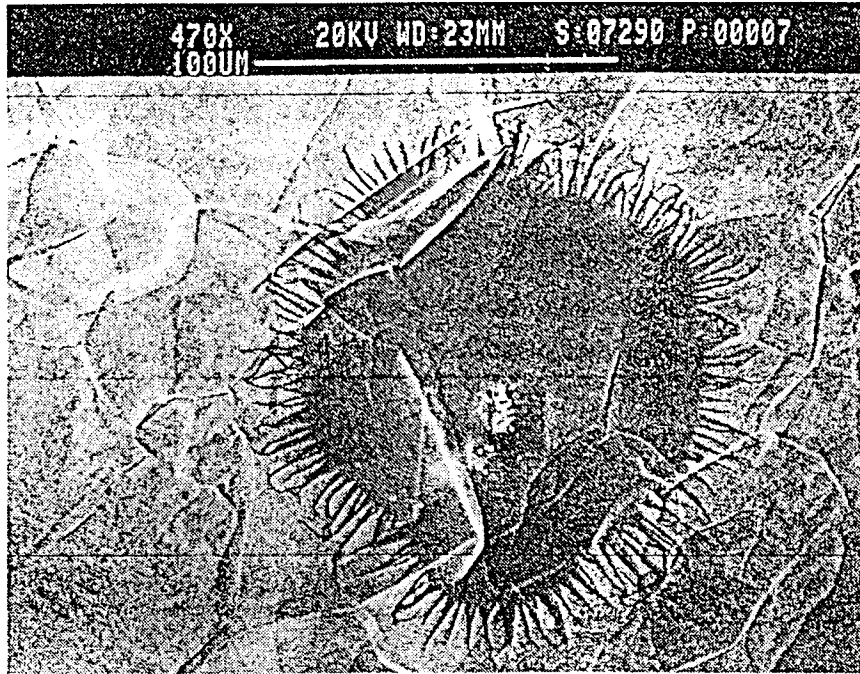


Fig. 2.6 Microscopic examination of cavity surface after HPP processing.

to the intensity necessary to initiate the explosive process, which extinguishes the emission. Only those emitters that reach the explosive current density will process. Others will continue to quiescently emit current. Fields reached during the processing stage are typically 50% higher than the maximum cw operating levels.

Both HT and HPP techniques when applied to multi-cell structures permit gradients of 15-20 MV/m, within the goals for the test facility. We expect the HPP technique to be much more effective at the lower frequency of 1.3 GHz chosen for TESLA, bringing closer the goal of $E_{acc} = 25$ MV/m. The limitation of HPP at 3 GHz tried so far has been shown, by careful thermometry measurements, to arise from a global thermal breakdown at the high magnetic field region of the cavity. When the magnetic field near the equator reaches 1300-1400 Oersted, the surface temperature rises unstably, i.e. a global thermal breakdown is initiated. This limits the maximum electric field accessible at the iris region for processing away emitters.

Recently a 2-cell, 3 GHz accelerating cavity with a more favorable H_{pk}/E_{pk} ratio was processed with HPP to reach a surface electric field of 100 MV/m cw. This result confirmed that if the thermal breakdown limitation is avoided, the HPP technique is inherently capable of processing emission to surface fields corresponding to $E_{acc} = 50$ MV/m in a well designed accelerating structure ($E_{pk}/E_{acc} = 2$). At the TESLA frequency of 1.3 GHz, the surface resistance is lowered by the square of the RF frequency ratio, eliminating global thermal breakdown and thus increasing the effectiveness of the HPP technique.

The HPP technique offers the possibility of cleaning up residual emission, which makes it more attractive, considering the likelihood that a clean cavity surface may suffer contamination during installation or operation in an accelerator. Auxiliary benefits of the HT technique are also valuable, so that a furnace will remain a necessary item for the preparation of Nb cavities, even if the HPP technique eventually supplants the HT approach.

Today it is even occasionally possible to reach 18 MV/m with standard chemical surface preparation techniques. This encourages us to expect that, with better understanding and improvements, even these standard techniques may in the future approach the desired performance. As discussed in the R & D section 6, areas of improvement already targeted are: filtering of acids, chemical treatments in a dust-free room, high pressure (100 bar)

water rinsing after chemistry, automated chemistry to preserve uniform treatment from cavity to cavity and to minimize contamination, and measures to improve the cleanliness of the vacuum system of the RF test set-up.

Apart from efforts to develop techniques to withstand higher surface electric fields, several efforts are underway to improve the structure geometry so that the ratio of E_{pk}/E_{acc} is reduced to below 2.0. Typical values for existing structures range from 2.1 to 2.6. Geometries with E_{pk}/E_{acc} down to $\simeq 2$ have been devised and are under study. Experience to date indicates that 10% - 20% improvements gained by a better geometry will directly translate to the same percentage higher gradients, as the limiting performance is usually set by the surface electric field.

3. Project Overview

It is the aim of this project to establish the technological base needed to construct and operate a high energy e^+e^- linear collider made of superconducting RF cavities and to demonstrate that this collider can be realized in cost effective manner and that its performance meets the design goals. We will first focus our efforts on the production and test of high performance superconducting RF cavities and the development of a cost effective low heat leak cryostat. The result of this work will also be of use to existing accelerator facilities like for example HERA and for the high energy high duty cycle electron facility now under discussion in the European Nuclear Physics community.

The various steps needed to meet this objective are summarized below:

- We first intend to erect clean rooms and install and commission the required surface treatment and test facilities at DESY and then to process and test 40 industrially produced 9-cell 1.3 GHz solid Niobium cavities including couplers and tuners.
- In parallel to the cavity programme we will design, construct and test low cost, low heat leak prototype cryomodules. Specifically we propose to construct four 12 m long cryomodules and install into each eight 1 m long 9-cell cavities including all the auxiliaries.
- We then intend to connect the four cryomodules into a string and subsequently to cool the string down to 1.9 K and to power the cavities. This part will address the problems which may arise when installing modules in a tunnel environment. It will further permit a test of the basic cooling concept, measurement of the static heat load, a first commissioning test of the RF system and a measurement of the high field properties of the installed cavities.
- As a final test we propose to accelerate an electron beam through the string of cryomodules and to measure the beam properties before and after acceleration. The layout of this test facility is shown in Fig. 3.1. It contains the four 12 m long cryomodules, the RF and Helium refrigeration system, an injector, a low and high energy beam analysis system and adequate diagnostic equipment.

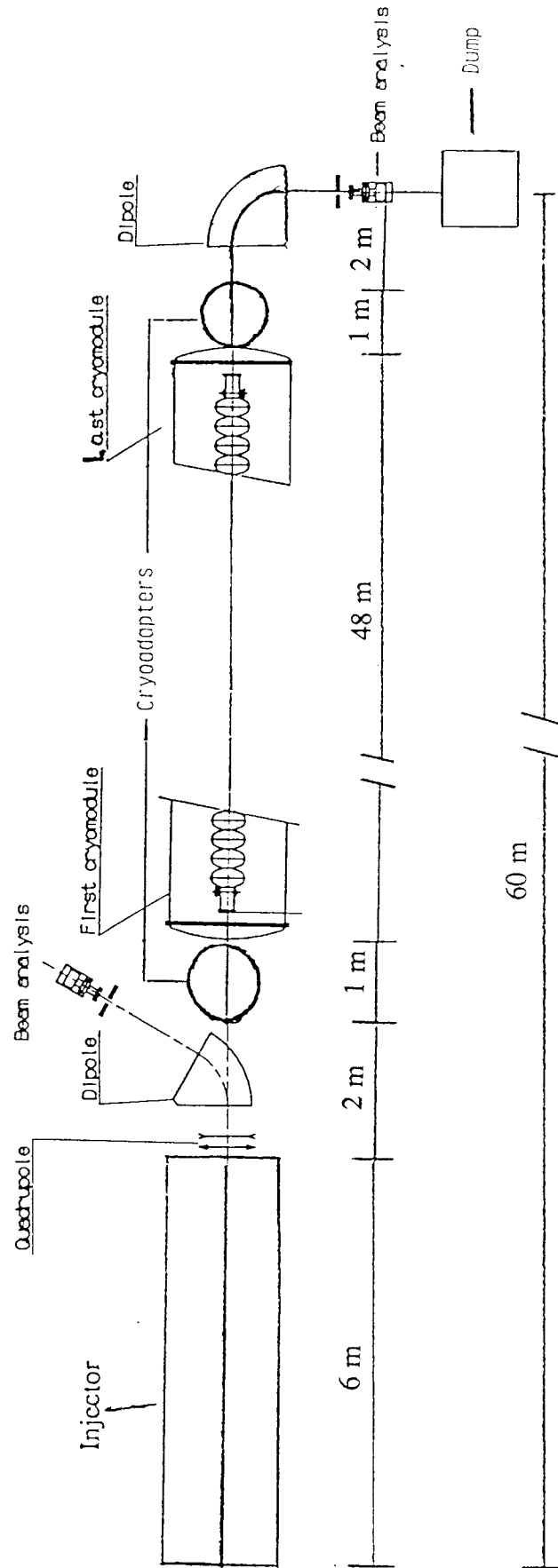


Fig. 3.1 Schematic layout of Test Facility including an injector, 4 cryomodules and beam analysis systems.

In the overview we will summarize the choice of parameters and discuss the steps needed to realize this project in more detail.

The Cavity

To develop the surface treatment methods and the fabrication procedures required to produce multicell superconducting cavities on an industrial scale with a performance matching the design goals of a linear collider, we propose to construct and test forty 9-cell 1.3 GHz solid Niobium cavities. A longitudinal cut through a 9-cell cavity is shown in Fig. 3.2 and its parameters are listed in Table 3.1.

The cavities will be made of high purity solid Niobium in order to preserve the option of annealing the cavities in high vacuum at a temperature of 1500⁰ C.

The choice of operating frequency for the SC cavities is influenced by a number of considerations involving shunt impedances, higher order mode losses, wake fields, alignment and jitter tolerances and cost.

Optimizing with these considerations a frequency choice of 1.3 GHz to 1.5 GHz is to be preferred as compared to 3 GHz or even higher frequencies. High power, high duty cycle 1.3 GHz klystrons are commercially available and we have hence chosen this frequency.

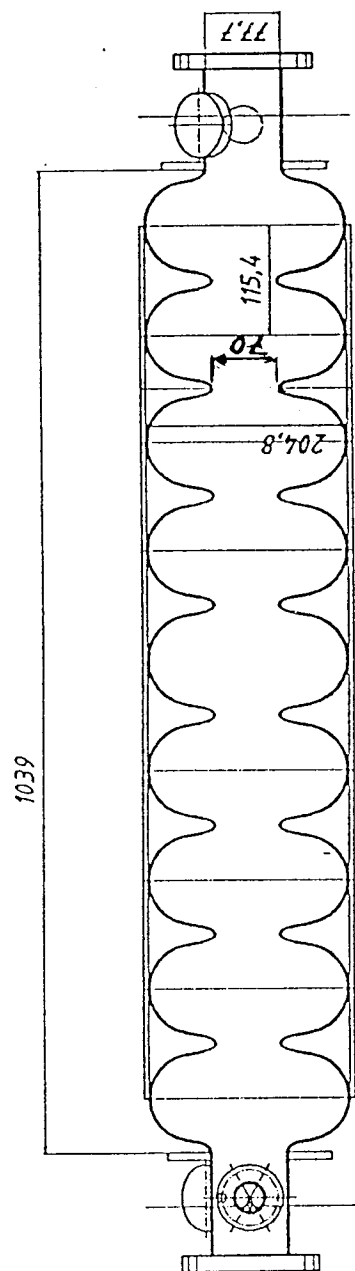


Fig. 3.2 9-cell Nb-cavity of 1.3 GHz with reinforcement bars and coupler ports.

Table 3.1 - Cavity Parameters* (for test setup)

Frequency	1.3 GHz
Number of cells/cavity	9
Iris opening	70 mm
Q_o at operating field	$3 \cdot 10^9$
R / Q	973 Ohm/m
Accelerating field	> 15 MV/m
E_{pk} / E_{acc}	2.0
B_{pk} / E_{acc}	4.2 mT/MV/m
Cell to cell coupling	1.85%
Operating temperature	1.9 K
HOM $k_{ }$ ($\sigma_z = 2$ mm)	5.75 V/pC/m
Total heat load of 12 m cryomodule at 2 K	1.35 W/m
RF peak power per unit length	125 kW/m
Beam and RF time structure	(see Fig. 3.3)
Cavity length	1.035 m
Q_{ext}	$3 \cdot 10^6$

* The parameters quoted are for a nominal gradient of 15 MV/m. However all subsystems will be designed for operation at gradients up to 25 MV/m.

For cost reasons the largest possible number of cells per cavity has been chosen. Trapped HOM modes and the achievable external Q for the most dangerous HOM modes limit this number to nine.

The cavity shape and in particular the iris opening is a trade-off between the number of cells per cavity, a low ratio of peak surface field to accelerating field, the power deposited by the beam at cryogenic temperatures, the coupling between cells and the induced wake fields. An iris aperture of 70 mm has been chosen, and the cavity has transversally a round shape at the iris region and an elliptic shape at the equator region. The cells are connected by four stiffening bars for stabilization against mechanical vibrations,

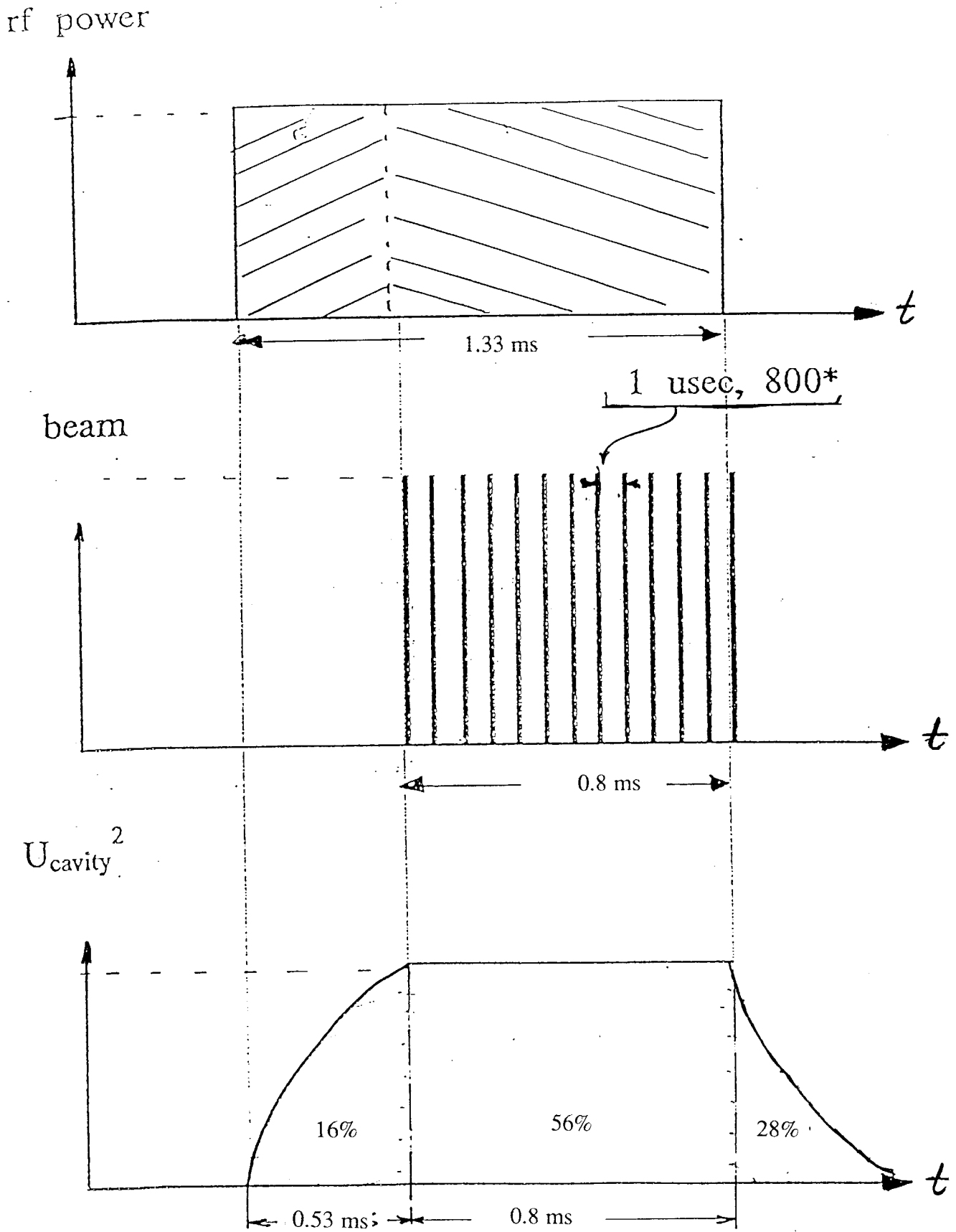
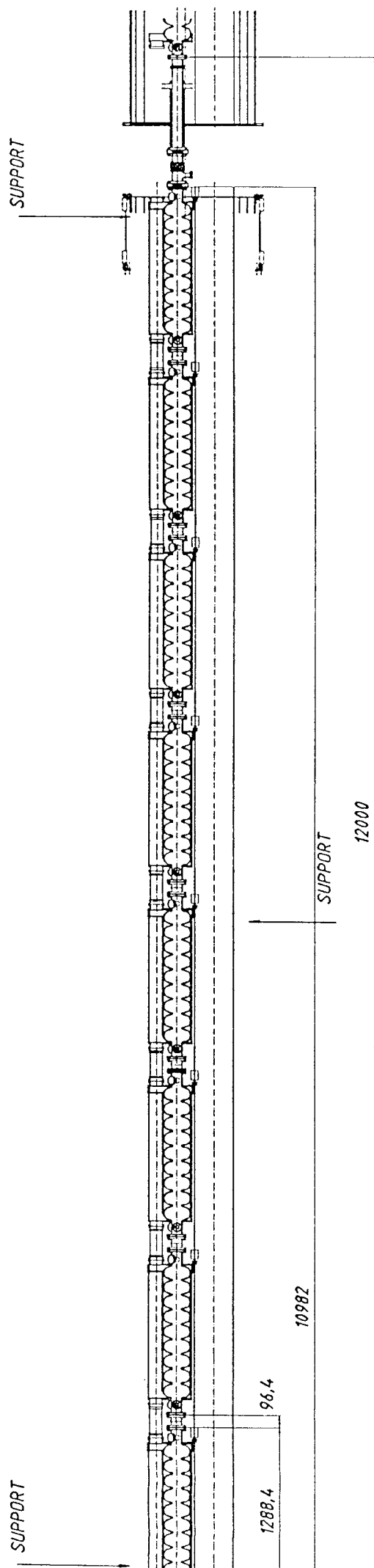


Fig. 3.3 Time structure of RF pulse, beam and stored energy. The percentage of RF losses for the different parts of the cycle is given.

a)



b)

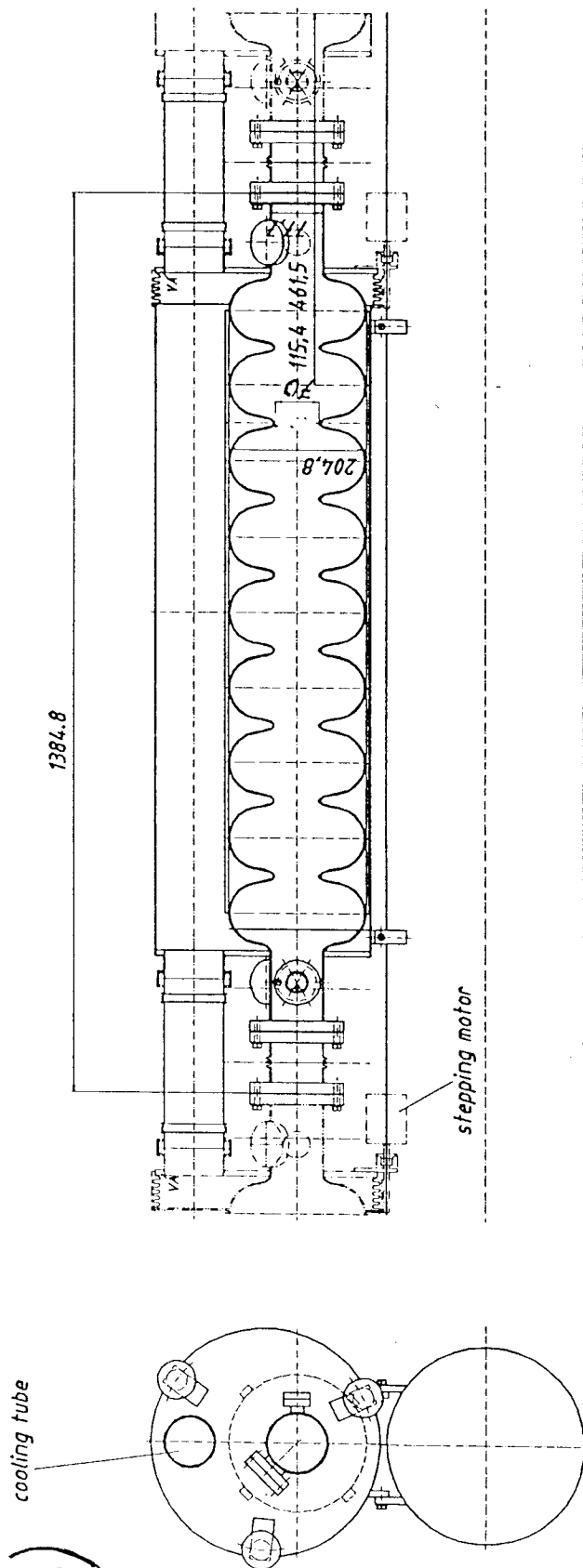


Fig. 3.4

- a) String of eight 9-cell cavities with He-vessels contained in one cryomodule.
- b) One SC cavity with its He-vessel and supporting (He-return) tube.

It is expected that this solution will provide good accessibility to all cavity parts, an absolutely crucial aspect if the high gradient and quality factors of the SC cavities are to be conserved during mounting and assembly.

At present the support and fixing system for the cavities will allow a movement of cavities during cooldown with respect to the outer vacuum vessel. With a fixpoint at the middle of a cryomodule the outer cavities will be displaced by 15 mm. This poses a particular problem for the main RF couplers which are fixed to the outer vacuum vessel. Two coupler designs are under study which will allow for this displacement. For safety reasons a two-window design has been chosen for the power input line.

Higher order mode couplers are located at the beam tubes between cavities. They will be connected via flexible RF cables to RF loads fixed to the 70 K shield.

A particular problem of linear colliders with their short bunch length ($\sigma_z = 2$ mm) is the large part of HOM power which is not damped by the HOM couplers but leaves the cavities via the beam tube. It is planned to absorb this power every 12 m at the location foreseen for the quadrupoles at a temperature of 70 K.

Inside the cryostat there are two aluminium radiation shields. The inner shield will be cooled by the 4.5 K return line, the outer one is at 70 K. Calculations show that the static heat leak at 2 K is less than 1 W/m, at least a fivefold improvement compared to present performance.

The assembly of the eight cavities onto the 300 mm support tube will be done in the class 100 cleanroom as well as the installation of the auxiliaries including connection pipes between the cavities and the manual gate valves at either end of the module. After this task the cavities are sealed against the outside environment and the rest of the installation will be performed under normal workshop conditions.

Installation and Cold Test of the Cryomodules

We plan to assemble a string of four cryomodules in Hall 3 on the DESY site (Fig. 3.5). This will address the problems which may occur when installing modules in a

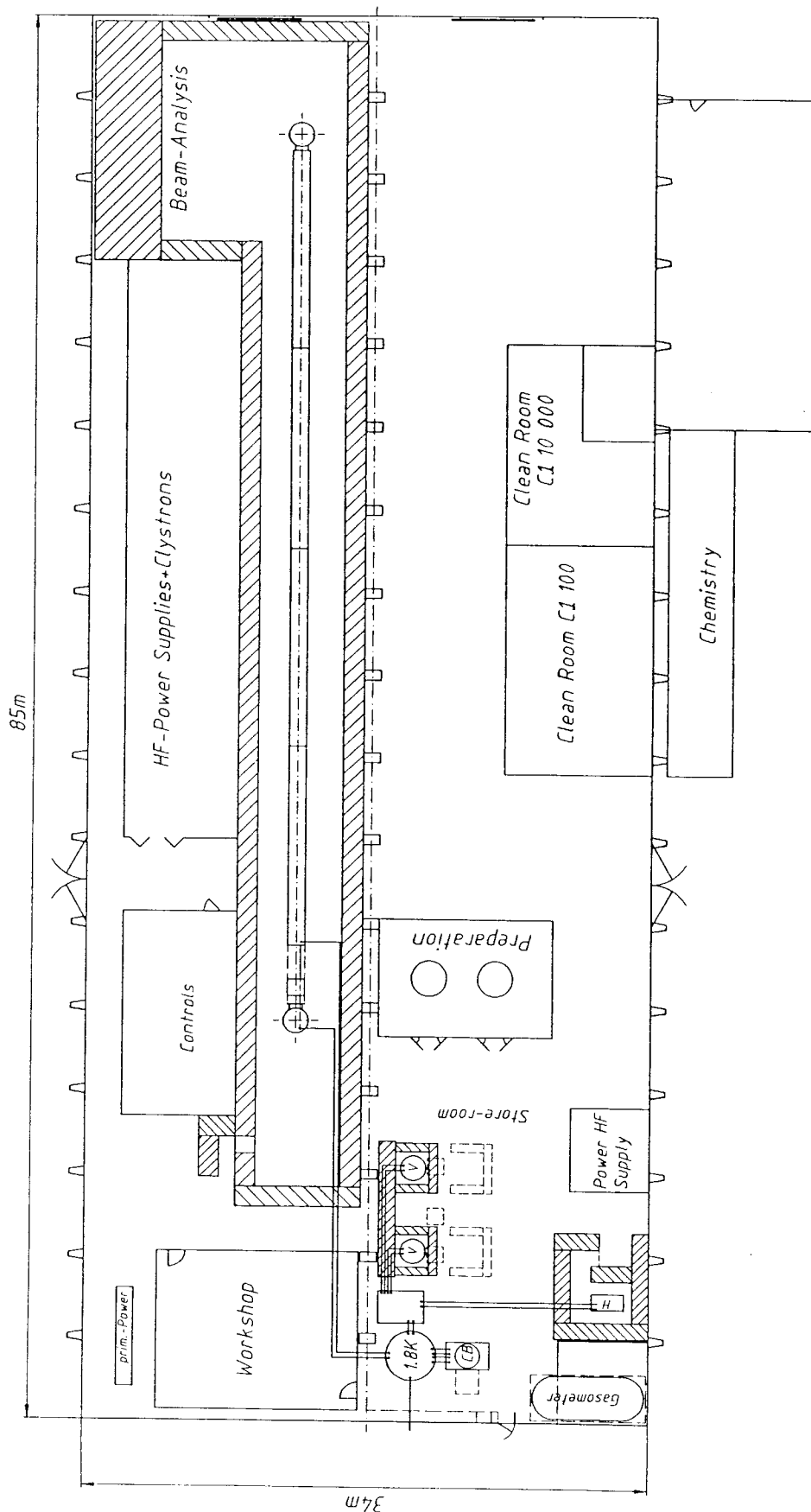


Fig. 3.5 DESY site for test facility. Shown are the 1.8 K He distribution box, 2 vertical test cryostats, one horizontal test cryostat and the cryomodule test set-up (~ 60 m length).

tunnel environment. We furthermore will connect the string to the refrigeration plant and test the basic cooling concept including a measurement of the static heat load. We then plan to power the cavities to test the layout of the RF system and determine the high field properties of the cavities.

At present bath cooling at a temperature of 1.9 K is foreseen. Additional cooling circuits at 4.5 K and 70 K will be needed for cold shields, quadrupole cooling and HOM absorbers every 12 meters at the location of the quadrupoles. The estimated heat loads are 65 W at 1.8 K including an estimated 20 W for the static heat load, 70 W at 4.5 K and 340 W between 70 K and 80 K. These requirements can be met by modifying an existing 900 W 4.4 K plant for operation at 1.8 K. After modification the plant will provide 200 W, 600 W and 2000 W at respective 1.8 K, 4.5 K and 70 K to 80 K. The plant is installed in Hall 3 resulting in short transferlines. The proposed cryogenic system is rather simple, since it does not involve extra filling circuits and no extra safety lines as would be needed for indirect cooling. Cooldown and warmup presents no special problems.

The RF power system consists of the high power klystron with its associated wave guide distribution to the superconducting cavities, the cavity input coupler and the modulator with its associated dc power supply and pulse transformer providing the klystron beam current. In addition low level and high level controls are necessary to maintain the appropriate phase and amplitude of the individual cavities relative to each other and to the beam. A schematic layout is shown in Fig. 3.6.

The RF power needed for one 9-cell cavity at full beam intensity is 125 kW at the design gradient of 15 MV/m. Two 1.3 GHz klystrons, each capable of delivering 4.5 MW during pulse lengths up to two ms at a 10 Hz repetition rate are foreseen for the 4 cryomodules.

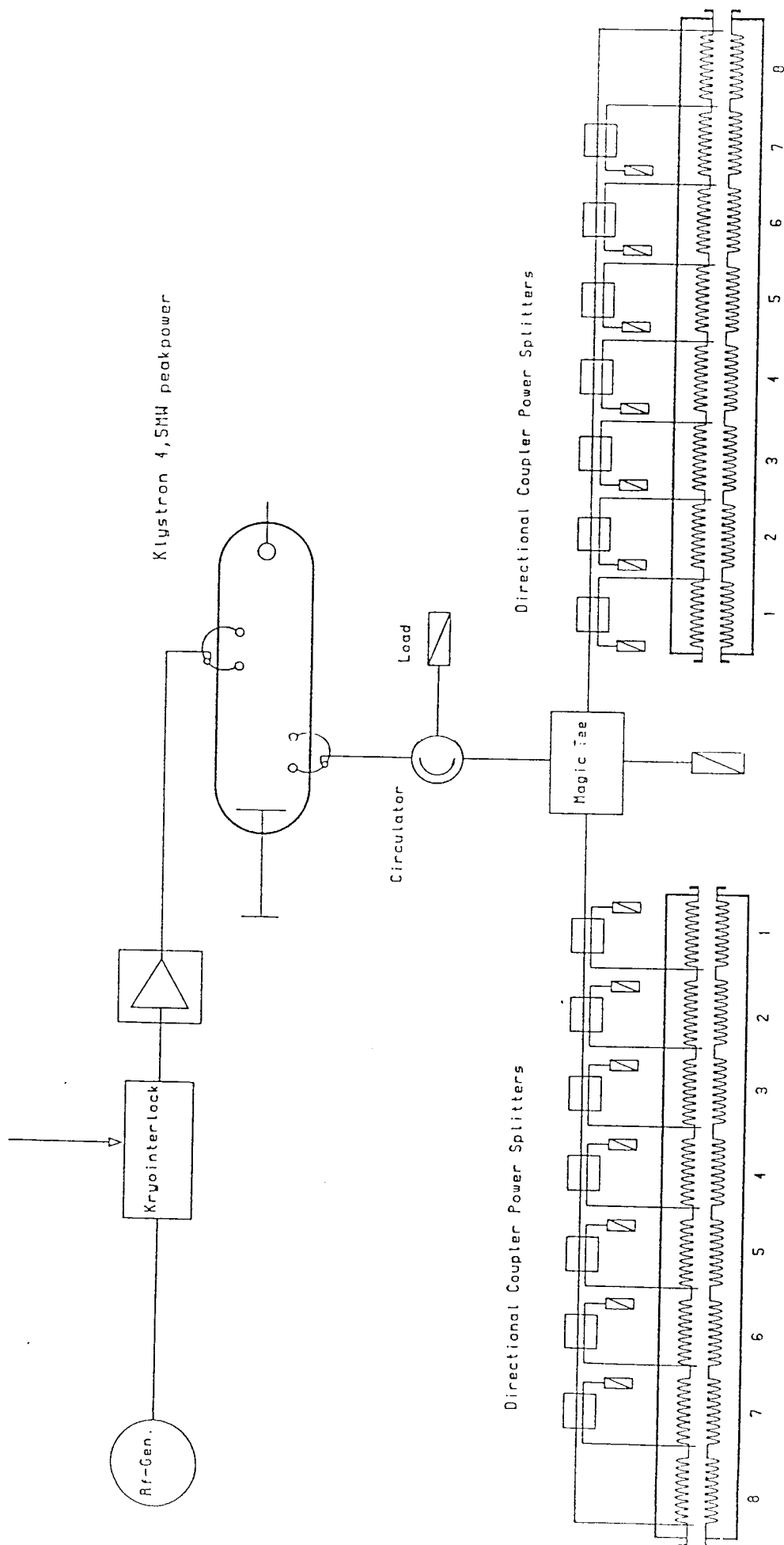


Fig. 3.6 Layout of RF system with one 4.5 MW peak power klystron feeding 16 sc cavities.

Date		Name		Projekt: Future		Erst- / gleiche / Nr.		Z. Mass. / Ort	
Gen. 1	22.11.91	A. Kaiser							
Gen. 2	22.11.91	A. Gess							

Test with Beam

A preliminary list of parameters for a 500 GeV e^+e^- collider mode of superconducting RF cavities can be found in Table 3.2.

Table 3.2 - Selected Linac Parameters

Center of Mass Energy	500 GeV
Luminosity*	$2.5 \cdot 10^{33} \text{ cm}^{-2} \text{ s}^{-1}$
Gradient	25 MV/m
Peak RF Power	208 kW/m
Active Length	20 km
Particles / Bunch	$5 \cdot 10^{10}$
Length of Beam pulse	800 μs
Bunch spacing	1 μs
Repetition Rate	10 Hz
Invariant emittance $\gamma \epsilon_{x,y}$	$20 / 1 \cdot 10^{-6} \text{ m} \cdot \text{rad}$
β -functions at IP	10/5 mm
Horizontal beam size	639 nm
Vertical beam size	101 nm
Bunch Length	2 mm
Horizontal Disruption Parameter	2.5
Vertical Disruption Parameter	15.8
Beamstrahlung Parameter Υ	0.016
Fractional Energy loss	0.0176

* without disruption enhancement

With present day accelerating gradients and quality factors cryogenic losses are too high for CW operation. Therefore a pulsed operation with a duty cycle of the order of 1% is necessary to keep investment and operation costs of the refrigerator at an affordable level. Note that the total charge accelerated and hence the luminosity is not affected by the duty

cycle.

The RF pulse length, bunch spacing and bunch population have been fixed as a compromise between cryogenic losses, peak RF power, the amount of dumped RF energy and higher order mode damping.

In the preliminary design of a 500 GeV e^+e^- collider listed above, each beam pulse has a length of 800 μ sec and contains 800 bunches with a bunch population of $5 \cdot 10^{10}$.

The very large bunch distance allows damping of higher order modes at a level corresponding to external Q's of 10^5 to 10^6 . Dampings of this strength have already been realized for many applications in SC cavities. The large bunch spacing ($l = 300$ m) also avoids unwanted bunch crossings at the interaction region.

A pulse repetition rate of 10 Hz has been selected as part of the parameter optimisation. This leads to a beam duty cycle of 0.8% and an average beam current of 65 μ A.

To demonstrate this performance and to gain operational experience we propose to add an electron injector and beam analysis stations located before and after the string of cryomodules. The test facility, as shown in Fig. 3.1 will be approximately 60 m long and it will include four superconducting quadrupole magnets needed to focus the beam.

Two types of injectors are foreseen.

We first plan to study the problems related to acceleration, energy-resolution and beam stability. To this end we will use an injector designed to accelerate $800 \cdot 5 \cdot 10^{10}$ electrons within a 1 ms long pulse but with the charge split into bunches of $3 \cdot 10^7$ e/bunch. These beam characteristics are rather standard and the injector should not present a special problem.

We next plan to study problems related to high bunch charge - i.e. wake fields, HOM dissipation and transmission and, more generally, beam instabilities.

Presently we are evaluating various schemes which are designed to deliver 800 bunches spaced at 1 μ sec with a bunch population of more than $2 \cdot 10^{10}$ electrons and with

The integration of all cold He-lines inside the cryostats and the simplification of He-line plumbing has also reduced the costs as compared to conventional Helium distribution systems.

It is also hoped that a good accessibility of all cavity and cryostat parts will favour automated handling and welding during assembly.

Another cost saving will be realized by the use of large peak power klystrons, enabling the feeding of many cavities by one klystron. This will lead to a reduction of the control and regulation circuits. Further cost reduction will be possible if more than one klystron can be powered by a common power supply.

Finally a reduction of operation costs is also expected since for example the proposed cryostat has a computed static heat leak of less than 1.0 W/m, far below the values common up to now.

4. Prototype Module

4.1 Cavity

Designing the cavity shape is a trade-off between several conflicting requirements:

- The number of cells per cavity should be high to reduce structure cost
- the ratio of peak surface fields to accelerating field should be minimized
- a strong coupling between cells should be achieved
- the higher order modes should be properly damped to avoid multibunch instabilities
- the dissipated power in the low temperature helium bath should be as low as possible
- the aperture should be large for lower wake fields.

Choice of Cell Geometry

An elliptic shape in the iris region (Fig. 4.1) and a round shape in the equator region (longitudinal cross section) give the lowest peak surface electric and magnetic fields for a fixed accelerating gradient. The choice of the iris aperture is of outstanding importance because it has repercussions on the gradient capability, the cavity dissipation, the power deposited by the beam (HOM losses) at cryogenic temperature and the wake fields. Table 4.1 below shows the fundamental mode parameters and the HOM loss factor for two bunchlengths and for a small and a large iris aperture cavity at 1.3 GHz. The numbers in Table 4.1 were obtained from model calculations using URMEL and TBCI.

1.3 GHZ 9-cell resonator

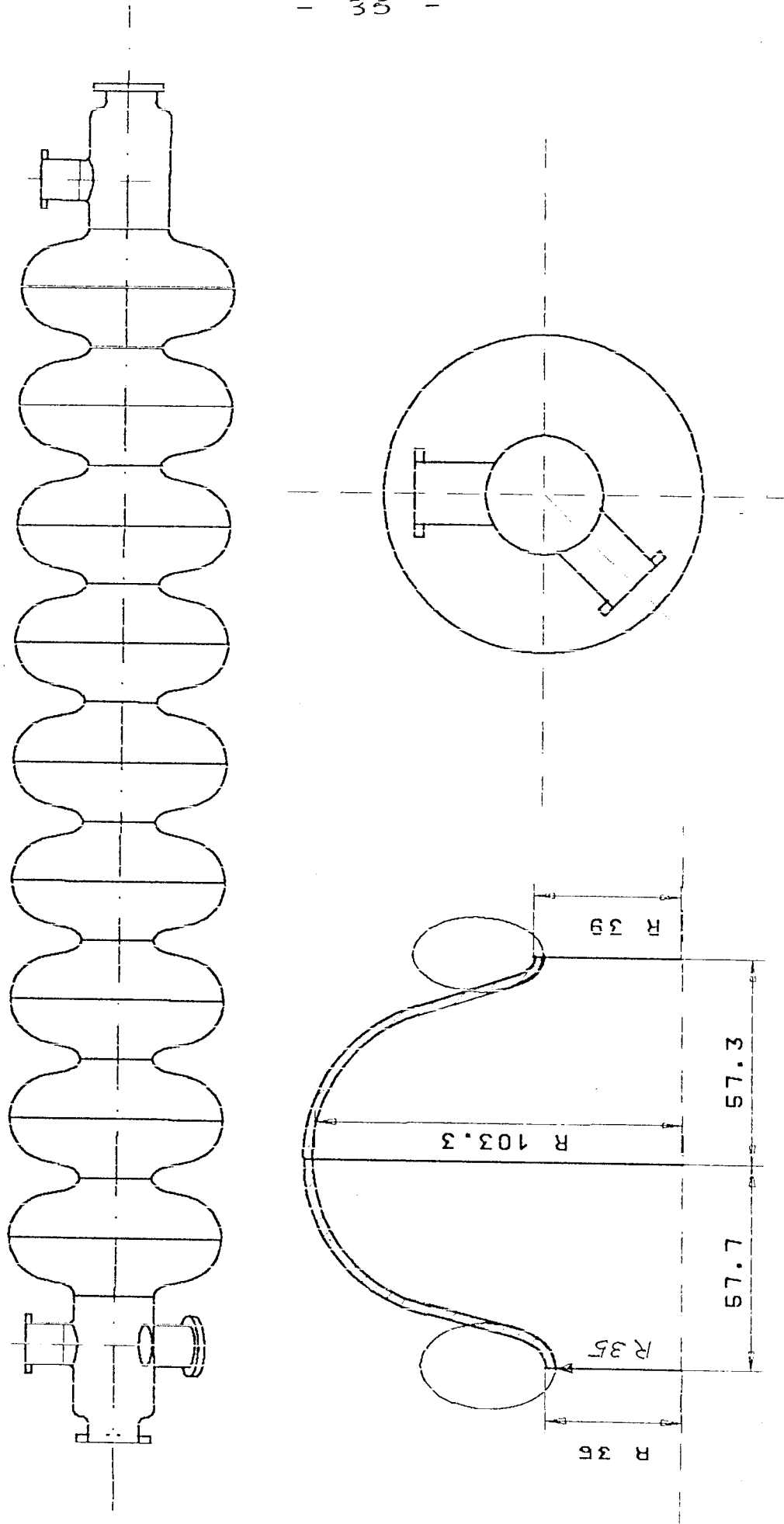


Fig. 4.1 Cavity geometry with coupling ports for small iris opening. Note the elliptical shape of the iris in the longitudinal plane.

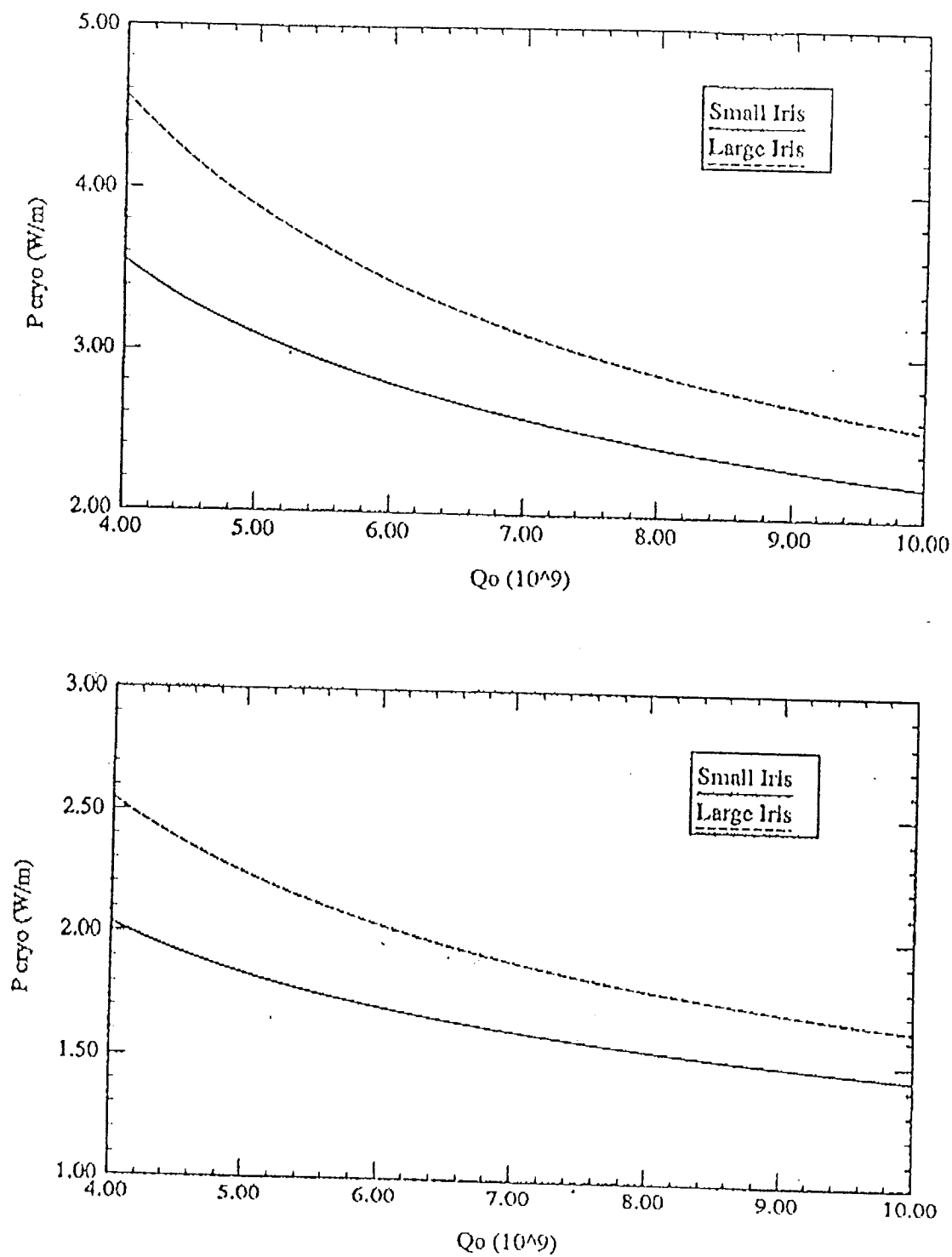
Table 4.1 - Cavity Parameters

Iris diameter (mm)	R/Q (Ω/m)	E_{pk}/E_{acc}	B_{pk}/E_{acc} (mT/MV/m)	cell to cell coupling (%)
92	740	2.6	4.9	5.4
70	973	2.0	4.2	1.8

Iris diameter (mm)	$k_{ }$, HOM $\sigma = 1 \text{ mm}$ (V/pC/m)	$k_{ }$, HOM $\sigma = 2 \text{ mm}$ (V/pC/m)	k_{\perp} , HOM $\sigma = 1 \text{ mm}$ (V/pC/m ²)	k_{\perp} , HOM $\sigma = 2 \text{ mm}$ (V/pC/m ²)
92	5.7	3.8	-	-
70	8.1	5.75	17.4	25.1

The small iris aperture has a clear advantage for the gradient but the overall refrigerator load has to be analysed in more detail. The total power dissipated in the helium bath includes losses from the accelerating mode, higher order mode losses and the static heat load. The cavity dissipation which depends on Q_0 and R/Q will be higher for the large iris cavity but the HOM losses will be lower as compared to the small iris cavity. The cryogenic load versus Q_0 for both cavities and for two typical set of parameters is plotted in Fig. 4.2.

A loss factor of 5.75 V/pC/m (see Table 4.1) corresponds to 3.15 W/m (8 nC/bunch, $\sigma = 2 \text{ mm}$, 800 bunches per pulse, 10 Hz rep. rate) in the single passage limit. A comparison with URMEL calculations of individual resonances (R/Q values) up to 5 GHz (cut off of beam pipe) shows, that 60% of this power is generated above 5 GHz. Usually HOM couplers are optimized to damp individual resonances with high R/Q values below cut off of the beam pipe. In order to avoid, that excessive power is dumped at 1.8 K, a second very broadband absorber is needed. A 0.5 m long section of stainless steel beam pipe will



	top figure	bottom figure
gradient	25 MV/m	15 MV/m
number of particles / bunch	5 10^{10}	2 10^{10}
average collision frequency	8 kHz	8 kHz
bunchlength	2 mm	2 mm
static losses	1 W/m	1 W/m

Fig. 4.2 Cryogenic losses as a function of the fundamental mode Q_0 for two different cavities and for two field levels.

be placed at 70 K after a set of 8 cavities. The high surface resistance of stainless steel would absorb 90% of the propagating HOM power, so that only 10% will be dissipated in Helium. Under that condition the cryogenic load is about the same for the two iris apertures in case of a low gradient but is higher for the large iris in case of high gradient. We have therefore chosen the small iris cavity both for its gradient capability and for the refrigerator load. Detailed calculations are underway to confirm that alignment tolerances of at least 0.1 mm and vibration amplitudes greater than $0.5\ \mu\text{m}$ are acceptable for the chosen cavity geometry.

Number of Cells per Cavity

The maximum number of cells per cavity is imposed by the field flatness sensitivity to mechanical tuning errors and by the damping of the higher order modes.

The sensitivity to mechanical tolerances is determined by the spacing in frequency between the π -mode and its neighbour and this spacing is decreasing approximately with the square of the number of cells. With the 70 mm iris diameter and with 9 cells, the mode spacing is roughly 0.75 MHz which is acceptable.

External couplers must be mounted on the beam tubes of each cavity to prevent transient longitudinal and transverse emittance growth. It is desirable to achieve Q 's lower than 10^6 for the highest R/Q transverse modes since the constraints of the focussing and therefore the cavity and quadrupole alignment tolerances can be strongly relaxed. Other techniques as stagger tuning and polarization of dipole modes in different directions will also be used if the results of beam break up simulations show important improvements.

In the case of the non propagating modes, two families are of particular concern, the TM011-like mode because of its very high R/Q and the TM110-like mode because of its poor penetration into the beam tube. If we slightly enlarge the end iris and detune the end cell to overcompensate in particular the TM011-0 mode while keeping the accelerating TM010- π mode flat, the damping of a 9-cell cavity is found satisfactory.

Several propagating modes, although above cut-off, couple very poorly to the beam tube. Fortunately, the modes which are weakly damped, have a very low R/Q and preliminary calculations show that they will have no significant effect on the multibunch instabilities. We have hence to worry only about the trapped modes with high R/Q, of which two serious candidates both in the longitudinal TM012 passband and in the 5th dipole TE121 passband exist. A beam tube reduction or a proper cavity to cavity spacing are the two simplest ways to cure these trapped modes.

A judiciously positioned diameter reduction to cut off the propagation of the TM012 and TE121 waves can have two beneficial effects. The position of the reduction is adjusted so that the excitation of the end cells and hence the coupling field in the beam tube are enhanced and the maximum field of the standing wave pattern is fixed at the coupler

location at the same time. Although this method is very efficient to get rid of the trapped modes, the main drawback is an increase of about 20% of the loss factor as the reduction behaves like a step for the beam. Without beam tube reduction, it is essential for the dangerous trapped modes that the HOM dampers, which are assumed to couple mainly with the radial electric field for the longitudinal modes and with the axial magnetic field for the transverse modes, sit near the peak of the weakened standing wave pattern of these fields. First calculations show that this requirement for both trapped passbands can be fulfilled with a proper choice of the distance between two adjacent cavities. In this case, the beam tube reduction could be avoided, but measurements on copper prototypes are needed to confirm this solution.

Mechanics

The cavity in the cryostat is subject to forces resulting from the hydrostatic pressure, the Lorentz force and the forces needed for tuning. We have to make sure that the cavity at room temperature can withstand an operation pressure of 2 bar without permanent deformation and that the mechanical stress during cell deformation for tuning does not exceed the yield strength of the material. Calculations assuming a yield strength $\sigma_{0.2}$ of 40 N/mm^2 indicate that a cavity wall thickness of 2.5 mm fulfills these requirements. However we plan to do stress measurements on samples of the actual niobium material to be used.

All cavity frequency perturbations have to be kept as small as possible in order to relax the RF control problem and not to increase the needed RF power. The main sources of frequency perturbations are the Lorentz force which increases quadratically with the accelerating gradient, the mechanical vibrations or microphonics and the Helium bath pressure variations. The cavity will be made as stiff as possible but still retain a sufficient tuning range to cope with the frequency uncertainty after cooldown. Various cavity stiffening schemes are being investigated and mechanical calculations including stresses, mechanical resonances and electromagnetic fields with 3-dimensional mechanical structure codes are underway. One method to make the structure more rigid is to use reinforcing Nb rods fixed to all cells of the cavity. The longitudinal bars can be attached to the cavity via braces welded to the equators. However, this stiffening scheme will provide only a limited reduction of Lorentz force detuning.

First calculations of the effect of Lorentz force at 25 MV/m show that the shape of the cavity is affected in two ways: the diameter at the equator is slightly enlarged, the surface near the iris is bent inwards. Fig. 4.3 demonstrates the deformation (please note the enlargement factor of 50000 for the changes). Stiffening of the iris area may be needed to reduce Lorentz force detuning from the present value of $1.3 \text{ Hz} / (\text{MV/m})^2$.

Moreover the cavity frequency sensitivity to helium bath pressure variations will be lower with the stiffening structure. The helium vessel will be designed in such a way that the bellows will change the cavity length and compensate the frequency shift due to cryostat pressure variations. The bath pressure frequency shift is then expected to be far below 20 Hz/mbar.

4.2 Tuner and Couplers

Tuner

The cavity tuning system must have a sufficient range to cope with the frequency changes after cooldown as well as a setting precision compatible with a bandwidth of about 350 Hz. A fast tuning device may excite the mechanical vibration modes of the cavity and this would make the control loop unstable. We will therefore only install a slow tuning system. The elastic deformation of the cavity is performed by means of 3 cold stepping motors located inside the insulating vacuum. Reliability tests to check the behaviour of the gear trains running in vacuum are in progress. In order to achieve a tuning accuracy of the order of 1 Hz, the mechanical system must be carefully designed and the cavity structure maintained permanently under stress to minimize backlash.

Once the cavity is equipped with the stiffening system, tuning is provided by the half end cells only. Therefore a correct excitation of the endcells must be guaranteed. As only two cells are deformed for tuning, the field flatness decreases proportionally to the frequency shift. Fig. 4.4 shows the ratio of maximum E_{acc} (in one cell) to the average E_{acc} for the 9-cell cavities as a function of tuning. If both end cells are tuned equally a tuning range of ± 120 kHz corresponds to a field unflatness of less than 5%. The extreme case of only one end cell tuning has to be excluded because of large field unflatness. The available tuning range will be sufficient to make up for the cavity frequency dispersion after cooldown.

Main Coupler

The main coupler has to handle pulsed RF-operation with a pulse length of ~ 1.33 ms, a repetition rate of 10 Hz and a peak RF-power of 208 kW per cavity.

During the beam pulse (800 μ s) the coupler has to operate under matched (or slightly overcoupled) conditions for 25 MV/m and a beam current of 8.2 mA, which leads to an external Q of $3 \cdot 10^6$.

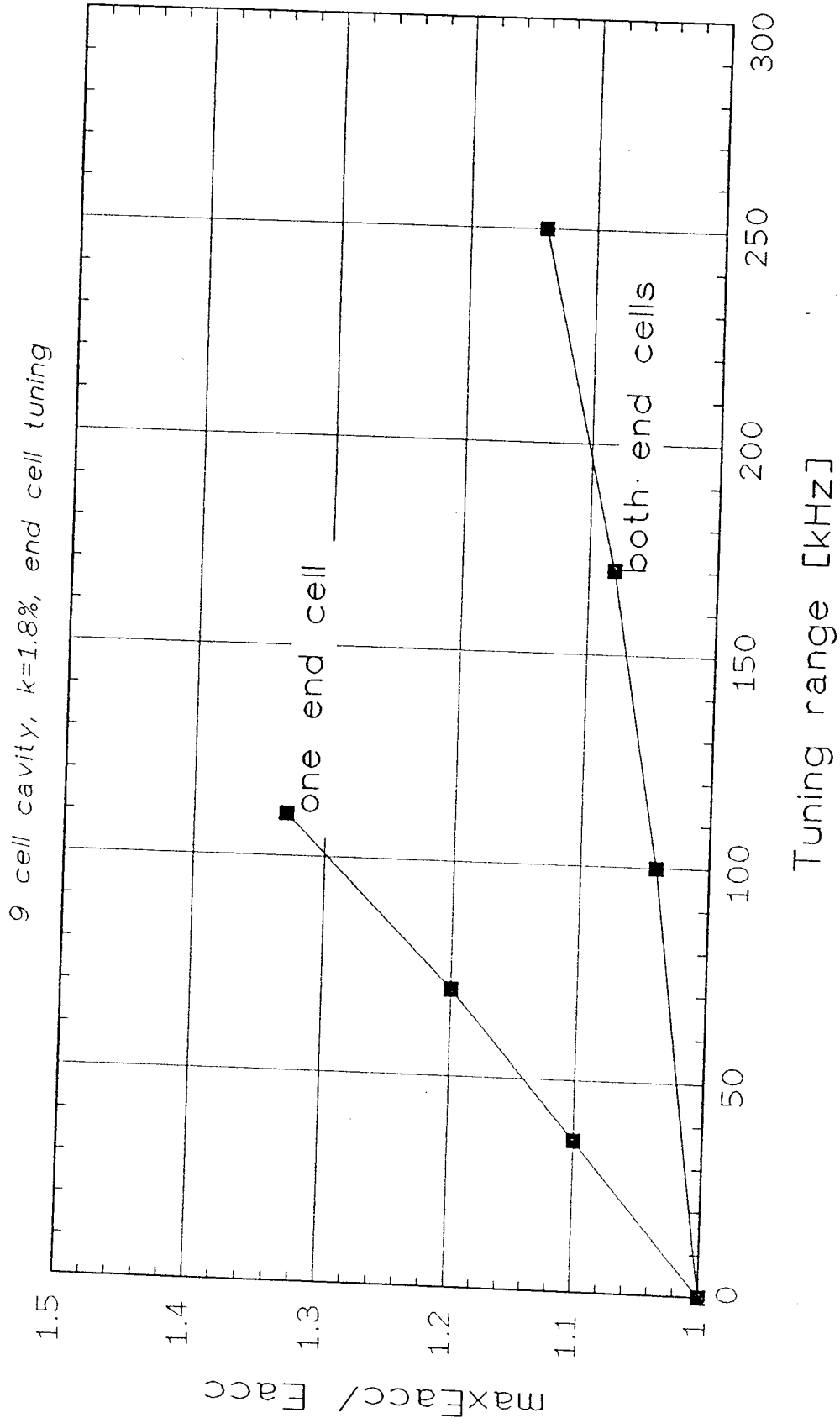


Fig. 4.4 Variation of field flatness due to tuning of one end cell or due to symmetric tuning of both end cells..

Before each beam pulse the empty cavity has to be filled with RF energy up to the nominal field level E_{acc} . This corresponds to a highly unmatched condition and the RF coupler has to withstand during the filling period standing wave conditions with almost 100% power reflection. After switching off the RF power the cavity empties its stored energy via the main coupler and a circulator into an external RF load.

The coaxial coupler is located at the cavity beam tube with an antenna as coupling element. A coaxial line of 40 mm diameter is considered sufficient for handling the pulsed 208 kW peak power. The inner conductor is held by a cold (70 K) ceramic window. The outer conductor is made from a stainless steel pipe (wall thickness 0.5 mm) which has a copper plating of 5 μm to reduce RF heating.

With the present layout of cavities and cryostats there will be a displacement of the cavities with respect to the outer cryostat vacuum vessel of up to 15 mm. As it is desirable to have a fixed external RF distribution system, the coupler has to handle this displacement.

Another constraint for the main coupler is related to the mounting and assembly procedure foreseen for the cavities. Part of the coupler should be mounted in the clean room and allow an UHV tight sealing of the cavity. The outer part of the coupler has to be mounted after installation of cavities in the cryostat vacuum vessel. This constraint is fulfilled by the use of two RF windows; one at 70 K and placed as near to the cavity as needed and a second window at room temperature. The inner window will not only act as a radiation screen to the 2 K level, but will also allow a separate vacuum between windows. This decreases the risks connected with window failures.

At present, two coupler versions are considered, which are shown in Figs. 4.5 and 4.6, respectively.

In one version a cylindrical RF window (see Fig. 4.5) is used. Lateral mobility is obtained by two bellows in the outer and inner conductor respectively. The demountable inner conductor is screwed to the rigid metal cover of the RF window which also holds the external part of the inner conductor. For this layout heat conduction and RF losses from the whole length of the inner conductor are absorbed at the 70 K level. The cold cylindrical window is a mechanically strong element and its position provides some protection against scattered X rays from the cavity and the beam.

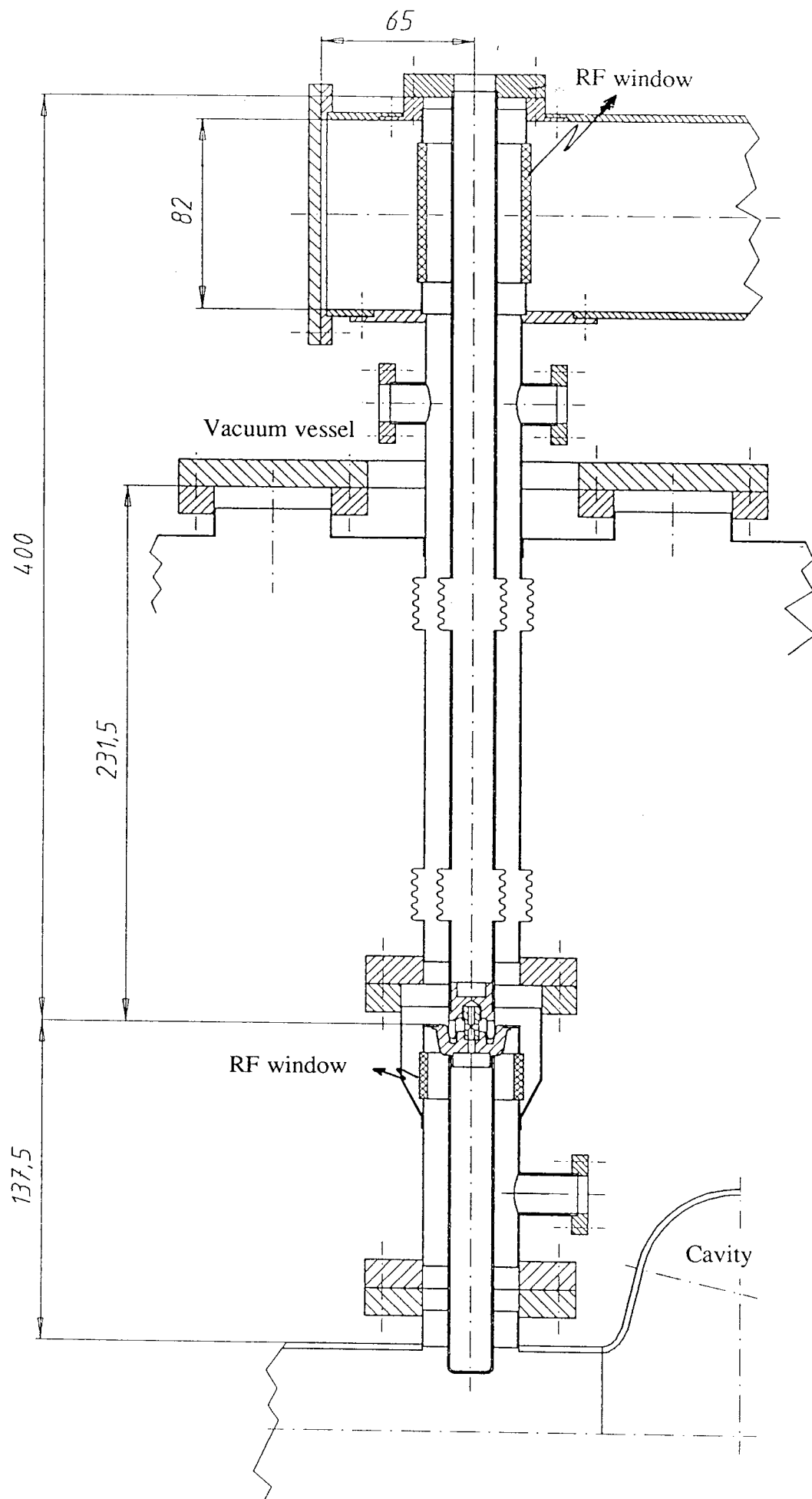


Fig. 4.5 Proposal for input coupler with cylindrical RF-window.

A second, similar alternative is shown in Fig. 4.6. Lateral and radial mobility are obtained by two bellows on the outer conductor and one on the inner. A third bellow on the outer conductor provides coupling adjustment via a mechanism external to the vacuum vessel and allows the waveguide to remain fixed. A conical or coaxial ceramic window located at 70 K serves as the intercept for heat conduction and RF losses.

It is foreseen to process the main couplers (in pairs) at high power level before installation.

The recent success of high power processing has opened the possibility for such a treatment in the test set-up where a large RF peak power will be available. The method is particularly valuable because it could be used in situ. The present experience with HPP indicates that an external Q of $3 \cdot 10^6$ as needed for the beam power matching is an optimum for the RF processing. But it would present an additional requirement for the input couplers which then have to handle peak power levels in the MW range. It is foreseen that the input couplers under design have to handle these extreme conditions.

Higher Order Mode Coupler

With a bunch separation of 1 μsec it is expected that external Q values below 10^6 for the most dangerous transverse HOM will be sufficient to avoid emittance dilution. The most dangerous longitudinal HOM (TM011), however, needs a damping with $Q_{\text{ext}} \leq 10^5$ to limit power extraction from the beam to safe values.

An extrapolation of mode damping in LEP and HERA (4 cell cavities) to cavities with 9 cells shows that even for the badly coupling TM012 mode an external Q of the order of 10^6 can be reached and that all dangerous dipole modes will have external Q below 10^5 .

Because of the pulsed RF- and beam operation it may be sufficient to operate HOM couplers with indirect cooling, i.e. without bringing liquid helium in their interior. However, present experience in CW operation shows that indirect cooling may not be sufficient for the conditioning phase of cavities and couplers when vacuum electronic phenomena like multipactor and field or photo emission may occur and cause additional losses. Multipactor analysis must accompany coupler design.

The use of polarized cells for stabilizing dipole modes in azimuthal direction is considered and will allow to reduce the number of HOM couplers from 4 to 2. In fact, because of field asymmetries it will always be necessary to have one HOM coupler on each beam tube.

Fig. 4.7 shows two different HOM coupler types presently used for mode damping of superconducting cavities in storage rings. One has a completely welded construction. The superconducting inner parts are cooled by conduction. The other type is dismountable, cooling is done by injecting liquid Helium. The dismounting flange is not exposed to fundamental mode fields.

Fig. 4.8 shows the spectral distribution of dominant HOM's in a 9-cell 1.3 GHz cavity. One can see that enhanced coupling is needed at three frequencies: 1.8 GHz for dipole modes, 2.5 GHz and 4 GHz for monopole modes. The two resonances around 3 GHz have fields existing only in the beam pipe where damping by the HOM couplers is very effective.

The storage ring HOM couplers of Fig. 4.7 are already designed to have resonant

[illegible]

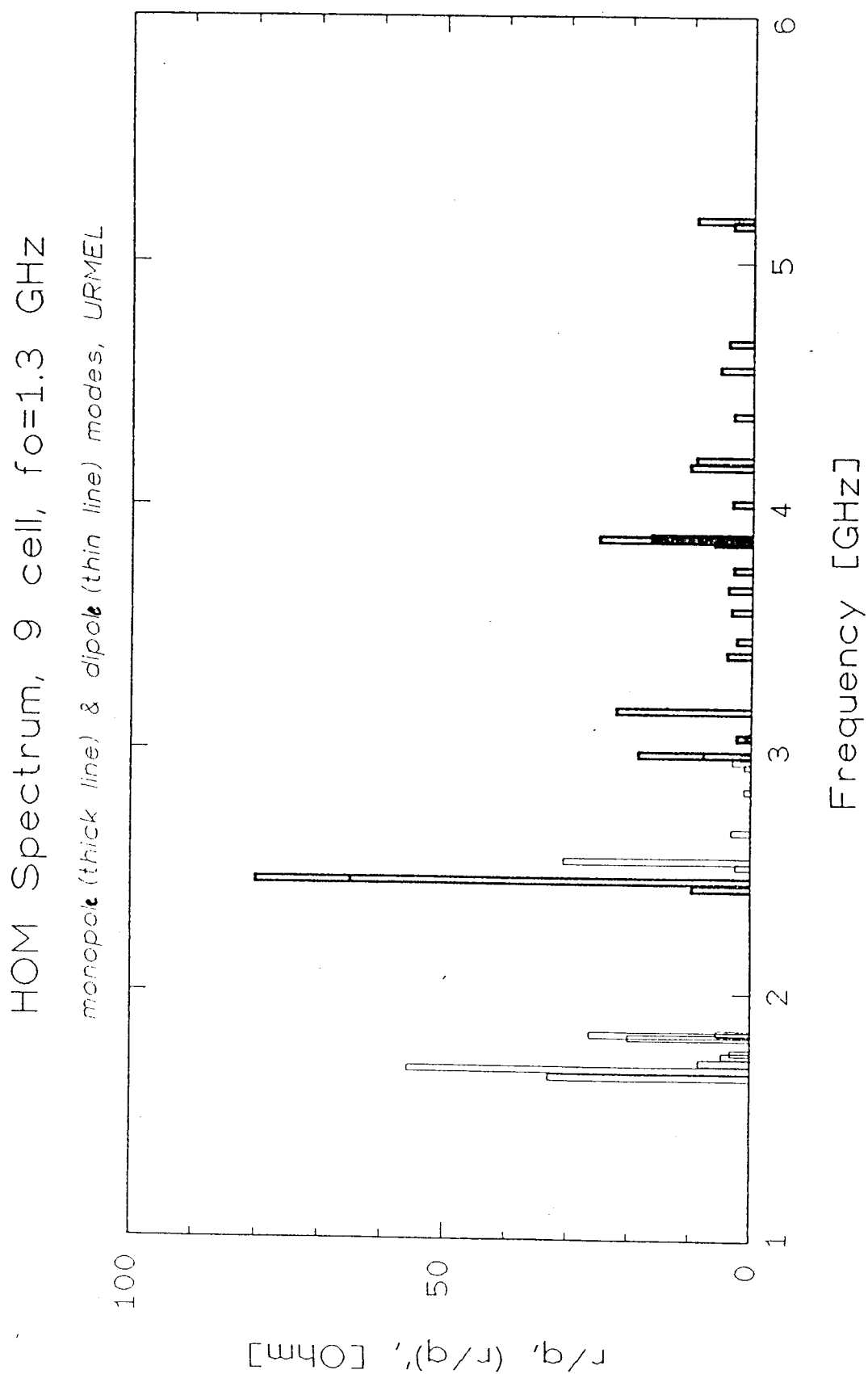


Fig. 4.8 Dominant higher order modes of the 9-cell, 1.3 GHz cavity..

enhancement coupling at the mentioned frequencies. Values for Q_{ext} are more than a factor 10 better (at 4-cell cavities) than needed for the 9-cell 1.3 GHz resonator. On the other hand the fundamental mode field at the HOM coupler is enhanced by a factor 5 (25 MV/m versus 5 MV/m in a storage ring). Fundamental mode suppression will be a dominant problem of HOM coupler design and operation.

4.3 Cryostat

General Remarks

There are three major aspects which determine the design of the cryostat for a superconducting linear accelerator:

- Low static heat leak.
- The layout must provide reliable and stable operation of the cavity system.
- The production cost per meter of the linac structure must be minimized.

A promising technique to achieve accelerating fields above 15 MV/m is the furnace treatment of the cavity at 1500⁰ C. This requires that the cavities be manufactured from solid Niobium, including connecting parts like flanges for couplers, cavity to cavity connections, and reinforcing bars.

On existing structures, helium leaks to the beam vacuum are almost exclusively due to leaky flanges which are situated in the helium surrounding the cavities. Reliability can therefore be gained by avoiding any flange inside the liquid helium. Therefore flanges to the beam vacuum are placed in the insulating vacuum instead. This also constitutes a cost reduction as penetrations of the Helium vessel are avoided.

The main cost reduction of the cavity cryostat, however, is due to the uniform structure of a linear accelerator. Up to now superconducting cavities have been built for storage ring applications in rather short units with many warm to cold transitions and as separate cryogenic units. For a linear accelerator, techniques and experiences from the large scale production of superconducting magnets for HERA and the Tevatron can be used. Combining cavities to long modules which are combined again to longer sections without warm to cold transitions is a straightforward way of reducing cost. This principle induces a number of small changes which bear on the cost, like the reduction of the number of supports, pump connection flanges, etc. In some cases cheaper materials can be used, for example the vacuum vessel will be built from normal steel instead of stainless steel and the radiation shields will be made from aluminium instead of copper.

Cavity and Helium vessel

Fig. 4.9 shows the Niobium cavity structure. On either end of the 9-cell cavity there are Niobium plates on the beam tube which establish the ends of the Helium vessel. The total Niobium weight of the cavity amounts to about 20 kg.

Fig. 4.10 shows the cavity within the completed Helium vessel. A stainless steel collar will be welded to the end plates of the cavity. The transition is made by an intermediate ring of Titanium. The stainless steel collar contains a hole for the two phase Helium supply line of 100 mm diameter. A stainless steel cylinder constitutes the outer wall of the Helium vessel. At one end the cylinder contains a bellow which allows the tuning of the cavity by a set of three stepping motors. They are placed at one end of the Helium vessel outside of the liquid Helium. For the magnetic shielding two options are considered: one inside and another outside the helium-vessel. The shielding has to reduce external fields below 30 mG.

On each cavity there is one input coupler and two higher order mode couplers (one on either side of the cavity) which are located at the cutoff tube of the cavity. They are placed outside the Helium vessel to avoid flanges in liquid Helium. Recent tests performed at Saclay have shown that cooling of beam tubes and coupler ports is adequate. In Fig. 4. 11a a layout of the flange connection for the couplers is shown. For RF control an additional pick-up probe must be investigated.

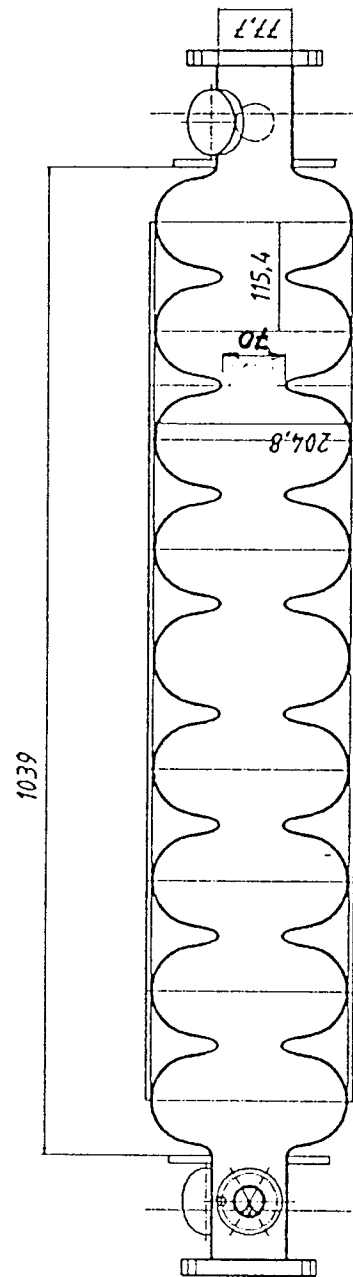


Fig. 4.9 9-cell cavity with Nb-parts

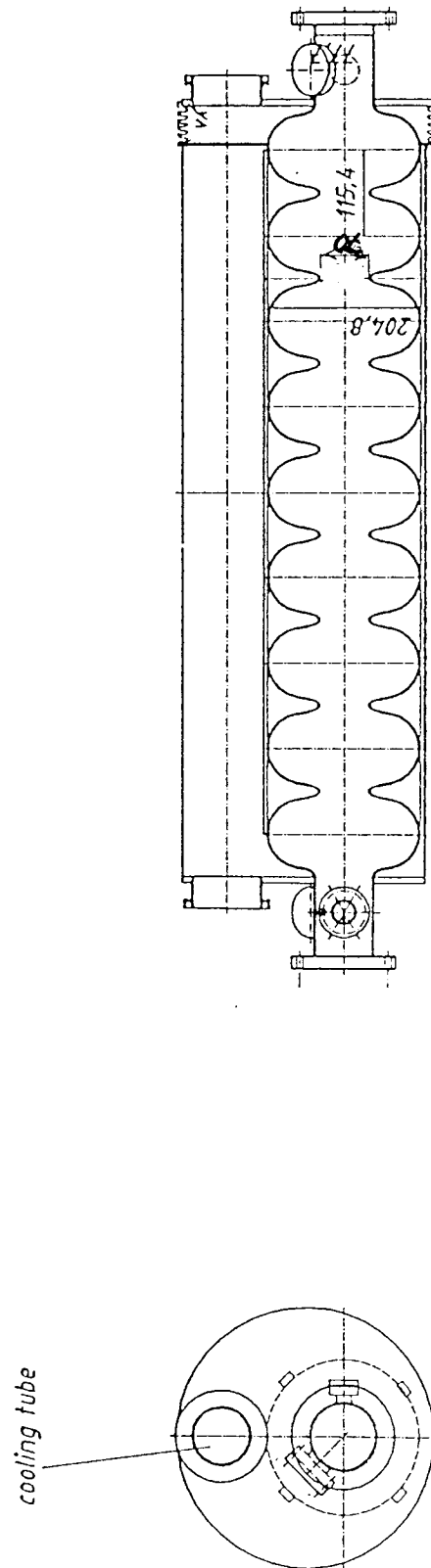


Fig. 4.10 9-cell cavity welded into its stainless steel He-vessel.

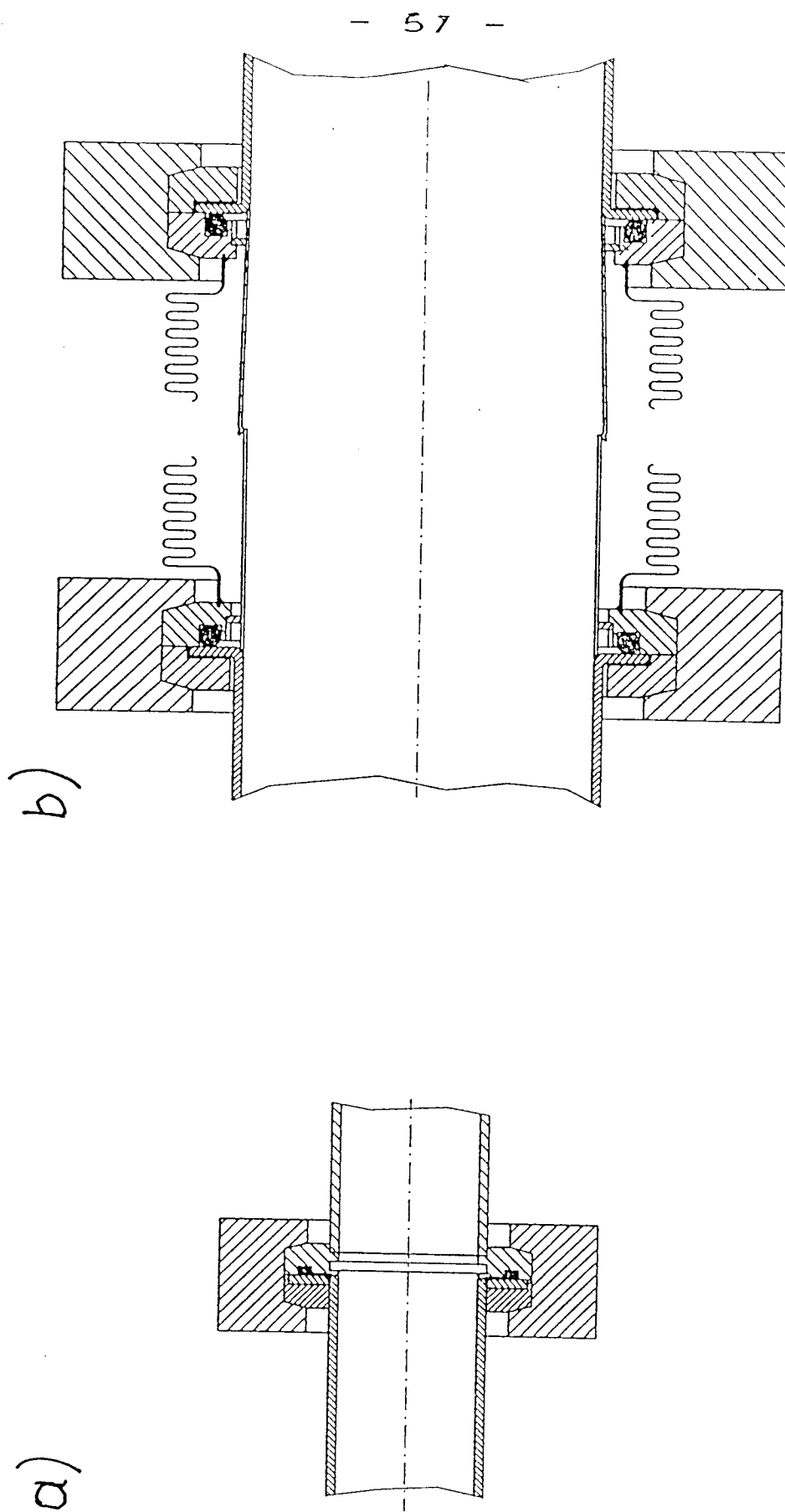


Fig. 4.11 Flange connections a) for couplers b) between cavities with bellows and RF joint.

Cryostat Module

Eight cavities constitute a cryostat module (see Fig. 4.12). The cavities are connected by a short beam pipe containing a bellow which allows for the necessary shrinkage during cooldown and separate tuning of cavities. The bellow is bridged by a RF-screen (see Fig. 4.11b). The distance of adjacent cavities corresponds to $3/2 \lambda$, resulting in a total cavity length of 1.39 m. The 300 mm diameter return pipe for the 2 K Helium serves as mechanical support for the cavities. The input coupler side of each cavity is fixed to this pipe, the other side can slide. The 300 mm pipe is supported from the vacuum vessel at three points. One post in the middle constitutes a fixpoint and a hanging support is foreseen at both ends (see Figs. 4.13a and 4.13b). Fig. 4.14 illustrates a support post, based on technology developed for the SSC dipoles, which meets the heat load budget and the structural requirements of the test cell cryostat. The sag of the supporting tube can be kept to a few tenth of mm at a wall thickness of 6 mm. The lowest resonance frequencies of the tube lie between 12 and 20 Hz. An alternative support structure which uses four supports to minimize axial motion of the input couplers is also being studied.

Whether the supporting tube should be above or below the cavity is still under study. Fig. 4.15 shows a cryostat cross section with the return pipe above the cavity vessel which is preferred from a cryogenics point of view.

Around the cavities there are two radiation shields made from aluminium: the inner shield will be cooled by the 4.5 K return line, the outer one by the 70 K supply line. Penetrations of the shields are done at right angles to the shield to ease efficient shielding of radiation.

The total weight of a cryomodule will be 2.1 t.

Quadrupoles, beam position monitors and steering elements needed for the operation of a linear accelerator might be incorporated in the cryostat module or form a separate optics module. In both schemes the quadrupoles and the correction elements are superconducting and will be cooled by the 4.5 K circuit.

The space required by the optical elements can be efficiently used to absorb higher order mode power which propagates through the beam pipe. The power can be absorbed inside the quadrupole at the temperature of the 70 K return line (see Fig. 4.16).

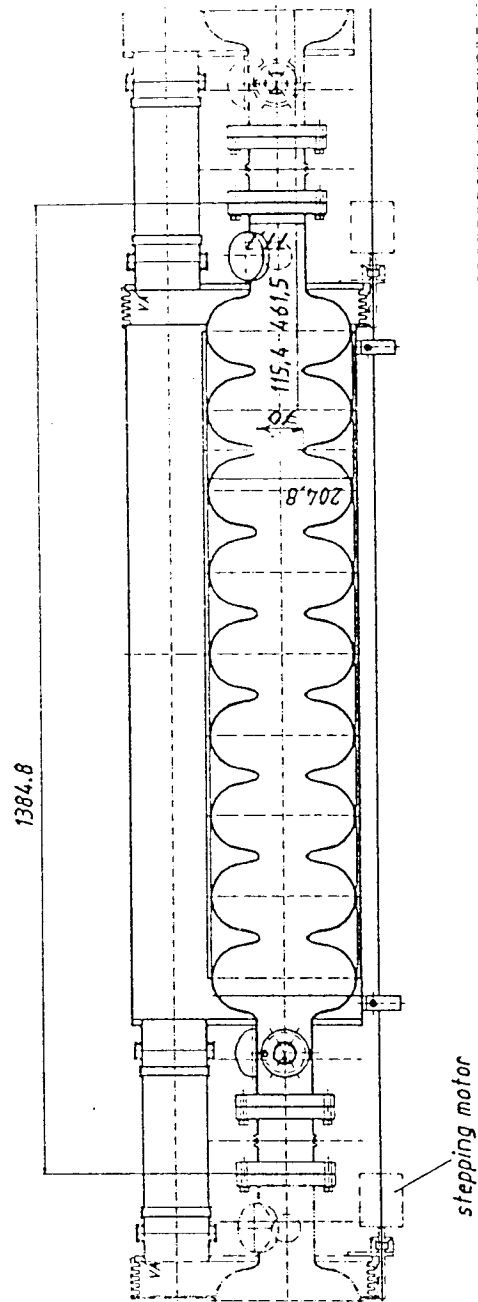
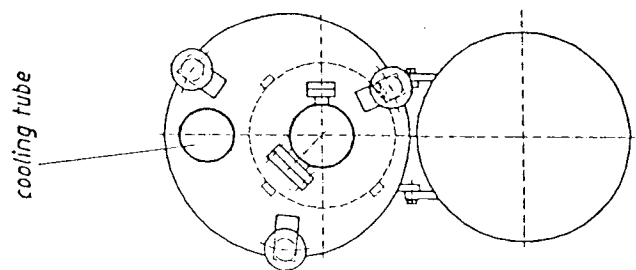
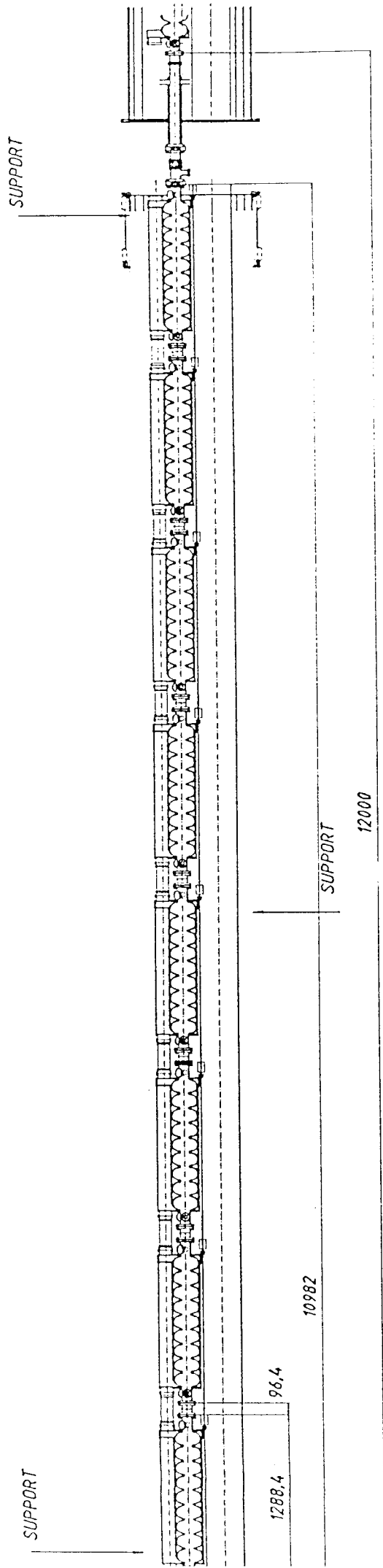


Fig. 4.12 a) Eight cavity module b) Cavity, He-vessel and supporting (He-return) tube.

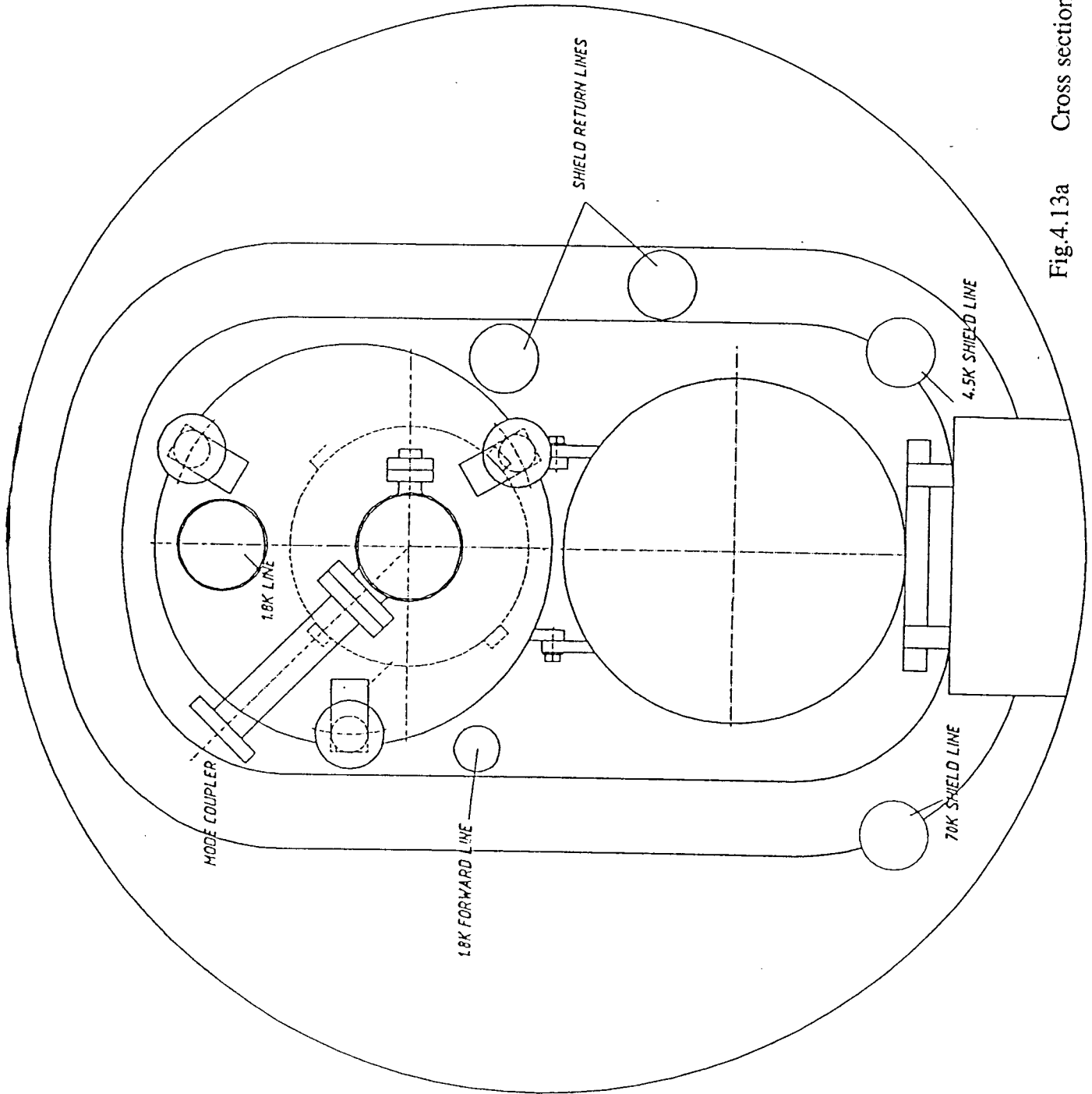


Fig.4.13a Cross section of cryomodule at middle support.

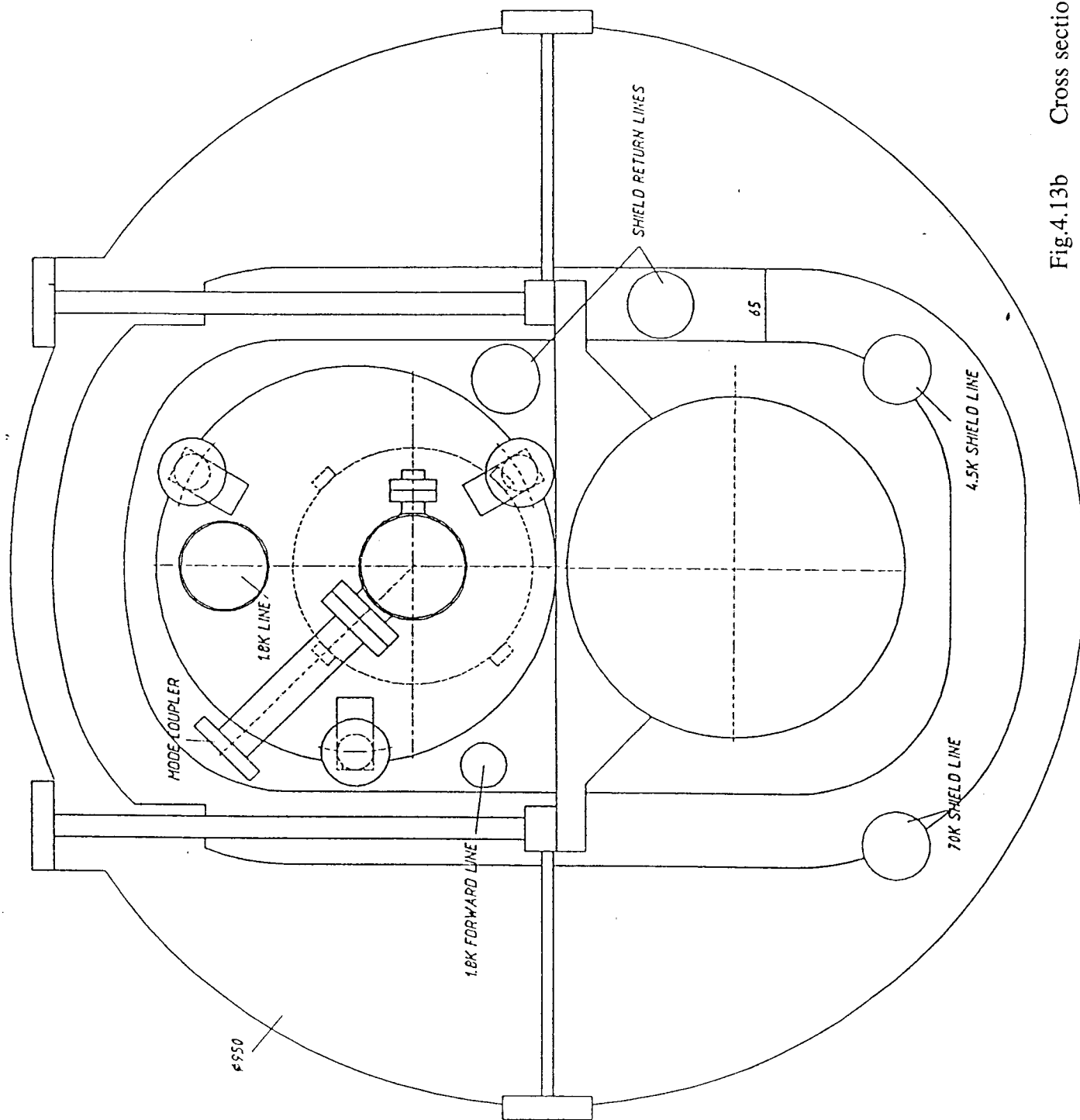


Fig.4.13b Cross section of cryomodule at end support.

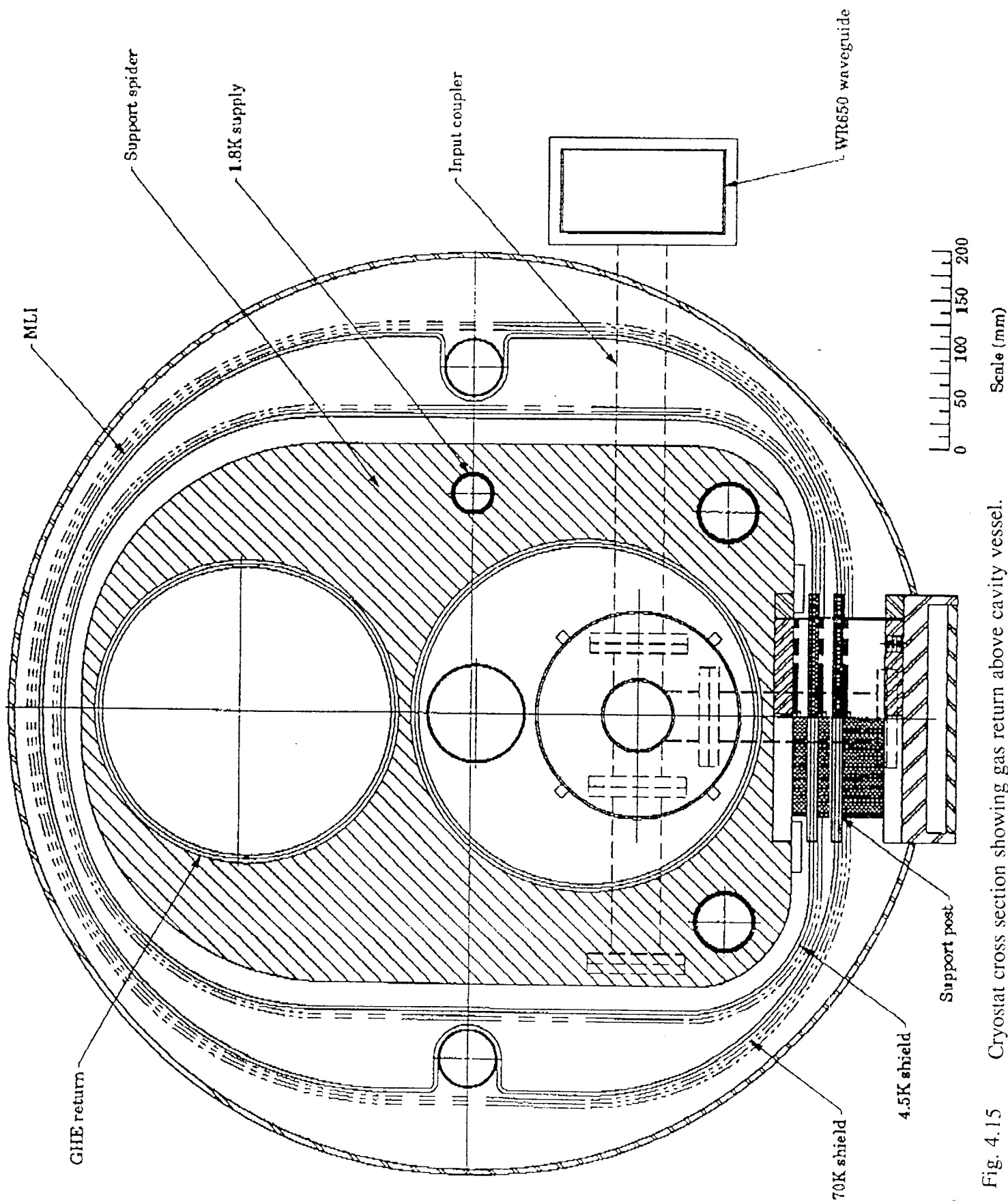


Fig. 4.15 Cryostat cross section showing gas return above cavity vessel.

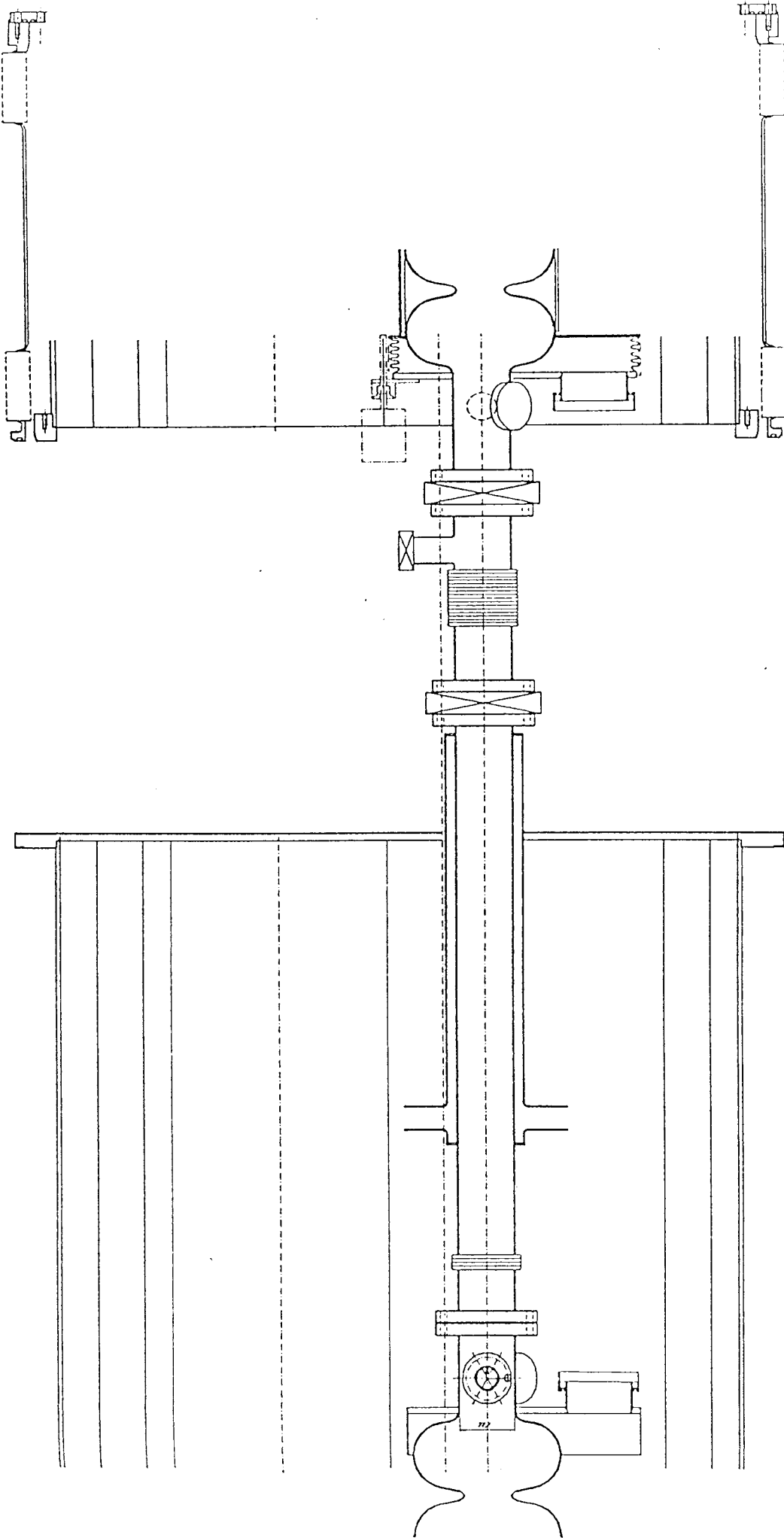


Fig. 4.16 Interface between two cryomodules with HOM absorber. This space may also be used for quadrupoles, steering magnets and beam monitors.

Vacuum System

There will be three different regions of vacuum: beam line vacuum, insulating vacuum and input coupler vacuum.

There are manual gate valves on the beam pipe on both sides of a module which allow the installation of a pre-evacuated module (see Fig. 4. 16). These valves will only be used during the preparation of a module installation or during an eventual replacement of a module. Due to the furnace treatment of the cavities the Hydrogen content of the Niobium and thus the H_2 outgassing rate will be minimized. The transition pieces of stainless steel between the cavities and the modules will be vacuum fired at $1050^{\circ}C$ to reduce H_2 desorption of these parts as well.

Contamination of the cavity surfaces by Hydrocarbons will be essentially avoided due to careful handling in the clean room. All pumpdown will be done with oil free turbomolecular pump stations. To reduce the coverage of the cavity walls by molecules (for instance H_2O) which increase the residual losses, the assembled inner part of a module can be baked as a whole in a simple furnace to $150^{\circ}C$ before alignment of the module. The connecting tubes between modules will be baked prior to installation and vented with dry nitrogen. During installation the beam pipes between adjacent modules (Fig. 4.16) will be connected inside a local "clean room" attached to the neighbouring flanges. Due to these treatments and precautions the outgassing rate of the cavity modules will be small so that only modest pumping speed is required to obtain an average beam line vacuum of 10^{-7} mbar (predominantly H_2) at room temperature. In fact one pump of 60 l/sec per 144 m section will be sufficient. At the moment, standard ion getter pumps are planned for this purpose. When the cavities are operated at cryogenic temperatures, connections between beam vacuum and room temperature parts must be kept to a minimum to avoid cryopumping of gas desorbed from the warm parts. Thus the connections to holding pumps will be valved off after cooldown of the cavities. During operation at 2 K the pressure in the cavities will be immeasurably small.

The insulating vacuum will be established by one turbo pump station at every section (144 m). This station will be continuously connected to the insulating vacuum for control purposes and to maintain the vacuum during warm up cycles. A vacuum barrier is foreseen between every

section. The vacuum vessels of adjacent modules are connected by sliding sleeves (see Fig. 4. 16) which contain bellows to allow for fabrication tolerances of the vacuum vessel and alignment of the modules. The connection to the cryogenic feed boxes of the test facility will be done in the same way. The test modules will have a flange on each sleeve to connect a pump station.

The high power input coupler is connected to the beam vacuum up to the 70 K window only. Thus the H_2 outgassing of this part of the coupler is negligible. The region up to the next window at room temperature requires a vacuum better than 10^{-6} mbar to avoid RF sparking. A connection to the insulation vacuum is not advisable as its pressure may be above this level due to leaks in the Helium vessels. Therefore the input couplers of a module will be pumped separately by a small ion getter pump. Having vacuum on both sides of the ceramic increases the operational safety against window failures.

Cryogenic Circuits

The cryogenic circuits are the same as in the system designed for the linear collider.

The two phase Helium (30 mbar) is supplied by a 100 mm diameter pipe between the individual He-containers of each cavity: 12 x 8 cavities are connected in this way and form one section (144 m). A 40 mm diameter pipe parallel to the cavities serves as supply for each section. The 300 mm diameter pipe (also used as support system for the cavities) is the suction line for one string (1750 m) and has connections to the end of each section.

All quadrupoles of one string are cooled by the forward flow of the 4.5 K line (ϕ 60 mm). The return flow (ϕ 60 mm) is used for cooling of the inner radiation shield and the interception points of the input couplers.

The 70 K circuit of one string (ϕ 60 mm) is used for the cooling of the outer radiation shield, the intercept of the input coupler line at the position of the cold window and the HOM absorber at the quadrupole beam pipe.

Alignment

A bunch traveling off axis through the cavity structure will generate transverse wake fields which will result in transverse forces leading to growth of transverse emittance and a reduction of the luminosity. Therefore precise fabrication of the cavity and alignment of the whole structure is very important. First calculations on the effect of transverse wakefields due to misalignment indicate a required positioning tolerance of a few tenth of a mm for the cavity field axis with respect to the neighbouring quadrupoles.

There will be reference points on either side of each cavity which indicate the position of the field axis. Once the cavities are mounted on the 300 mm support tube, survey fixtures will be connected to the reference points and the cavities can be positioned with respect to a straight line with a precision of 0.05 mm. The support tube will be suspended in the same way as in the vacuum vessel. The survey fixture closest to the middle fixpoint of the module will remain on the cavity. It serves, together with the survey fixtures on the cavities at the ends of the module, to adjust the supports and to transfer the field axis to reference points on the vacuum vessel. These steps can be done with an accuracy of 0.1 mm.

At least on the first two modules the survey fixtures will stay on all cavities during further assembly and will remain visible in the space between the cavity vessel and the support tube inside the 4 K shield (see Fig. 4.13). This allows checking of the alignment during assembly and installation. From the experience with the HERA magnets we expect the misalignment caused by handling of the module to be less than 0.1 mm. By view windows in the cryogenic boxes of the test facility the motion of the cavities during thermal cycles can be measured. Again from the experience with the HERA magnets we expect deviations from the calculated motions of less than 0.1 mm. Thus in total we expect the positioning error of the cavities to be less than 0.2 mm. (Note, that the quadrupoles will be aligned to a higher precision.)

Heat Load

The power dissipated at 2 K during operation of the cavity (duty cycle of 1.3%) is 1.35 W/m. This includes losses in the input couplers and power dissipation of higher modes. The static heat flow originates from heat conduction through the supports of the module, the input couplers, RF cables for HOM couplers and RF probes and cables from the various diagnostic

systems, part of this heat flow is intercepted at the 4.5 K level.

The dynamic heat load on the 70 K shield line is given by the losses in the input coupler and the dissipation of the power contained in traveling modes within the beampipe. The static heat flow due to the support structure, couplers, cables and radiation amounts to 4.6 W/m (see Table 4.2) at 70 K.

Table 4.2 - Heat Load Budget for Test Module

Static Losses

Load per Meter	2K Watt	4.5K Watt	70 K Watt
Radiation		0.35	2.0
Supports	0.05	0.2	0.5
Input Coupler	0.15	0.3	1.5
HOM Absorber		0.1	
Power Lead		0.1	
Cables	0.2	0.2	0.6
Sum	0.40	1.25	4.6

Total Losses for $Q=3 \cdot 10^9$ and 15 M V/m

Load per Meter	2K Watt	4.5K Watt	70 K Watt
RF Load	0.73		
Input Coupler	0.15	0.5	2.0
HOM Load	0.22	0.1	2.0
Radiation		0.35	2.0
Supports	0.05	0.2	0.5
Power Lead		0.1	
Cables	0.2	0.2	0.6
Sum	1.35	1.45	7.1

Losses for 12m Module containing 8 Cavities

	2K Watt	4.5K Watt	70 K Watt
Total Load	16.2	17.4	85.2
Static Load	4.8	15.0	55.2

4.4 Production and Assembly

For the cavity production sheet material of high quality Niobium ($\text{RRR} \geq 300$) with a thickness of 2.5 mm will be used. Industrial manufacture of complete 9-cell cavities is foreseen including deep drawing of half cells, chemical polishing, electron beam welding and welding of the stiffening bars. The following preparation process at DESY which is summarized in Table 4.3 features all the precautions presently identified as useful to produce good quality cavities. Fig. 4.17 shows a schematic layout of the corresponding infrastructure.

First a buffered chemical polishing is done on the inner side of the cavity in order to remove a layer of approximately $20\text{ }\mu\text{m}$, followed by high-pressure rinsing (100 bar) with ultra-clean water (Fig. 4.18) and drying. Automized handling of the cavities for these steps is foreseen and the chemical facility (Fig. 4.19) should be located in the clean room of class 10000. To avoid contamination, from here on all operations which expose the inner surface of the cavity have to be done in a clean room of class 100.

The first preparation is followed by a RF acceptance test in a vertical bath cryostat at a temperature of 1.8 K, to determine the Q-value and the maximum gradient. A high peak power processing of the cavity can be done in the vertical cryostat to increase the accelerating field. If needed further improvement of the cavity performance by a heat treatment (1500°C) in an ultra-high vacuum furnace housed in the class 100 clean room is foreseen. This step is useful both for minimizing field emission and for purifying the Niobium (Titanification). This procedure would be followed by a second cold measurement in the vertical cryostat, to verify the expected increase of Q-value and maximum accelerating field. Also at this test a high peak power RF processing of the cavity could be performed.

Before the cavity leaves the clean room all flanges will be closed by valves in order to keep the cleanliness of a qualified cavity. The sealed off cavity then will be welded into the helium vessel. A third cold test may be intended to check that no degradation of performance occurs in a horizontal cryostat when the cavity is welded into the helium tank and equipped with its final couplers. If also at this stage high peak power processing must be possible the main power coupler has to be designed correspondingly.

It should be pointed out that the whole complexity of this flow diagram may not be justified for a cavity mass production. Of course superfluous steps can be bypassed when better knowledge

INSPECTION

- Visual inspection
- Mechanical measurements

TUNING

- Preparation for clean room
- Degrease, removal of 5-10 μm
- Rinsing and drying
- Transport
- Field measurements and tuning
- Transport

CHEMICAL TREATMENT

- Preparation for cleanroom
- Degrease, removal of 20 μm
- Ultraclean rinsing and drying

FIRST VERTICAL RF TEST (+ HPP Processing)

- Mount flanges
- Pumpdown, leaktest
- Transport
- Insertion in vertical cryostat
- Pumpdown, cooldown
- Q and field measurements
- Warmup
- Dismounting
- Transport

FURNACE TREATMENT

- Preparation for cleanroom
- Dismount flanges
- Mount fixture for furnace
- Furnace treatment
- Removal from furnace

SECOND VERTICAL RF TEST (+ HPP Processing)

- Mount flanges
- Pumpdown, leaktest
- Transport
- Insertion in vertical cryostat
- Pumpdown, cooldown
- Q and field measurements
- Warmup
- Dismounting
- Transport

ASSEMBLY HELIUM VESSEL

- Preparation for cleanroom
- Dismount flanges
- Put on protective covers
- Transport
- Welding of Helium vessel
- Pumpdown, leaktest
- Transport

FINAL HORIZONTAL RF TEST (+ HPP Processing)

- Preparation for cleanroom
- Dismount protective covers
- Mount final couplers
- Pumpdown, leaktest
- Transport
- Mount tuning
- Insertion into horizontal cryostat
- Pumpdown, cooldown
- Q and field measurements
- Warmup
- Dismounting
- Transport

CAVITY CONNECTION

- Preparation for cleanroom
- Mounting of cavity on support
- Assembly of 8 cavities on support,
including beampipe connection, valves
- Pumpdown, leaktest
- Transport

CRYOSTAT ASSEMBLY

- Mount magnetic shield, weld Helium pipes, mount alignment
- Mount shields and superinsulation, mount piping and cables
- Mount external parts of coupler
- Insertion into vacuum vessel, alignment, welding

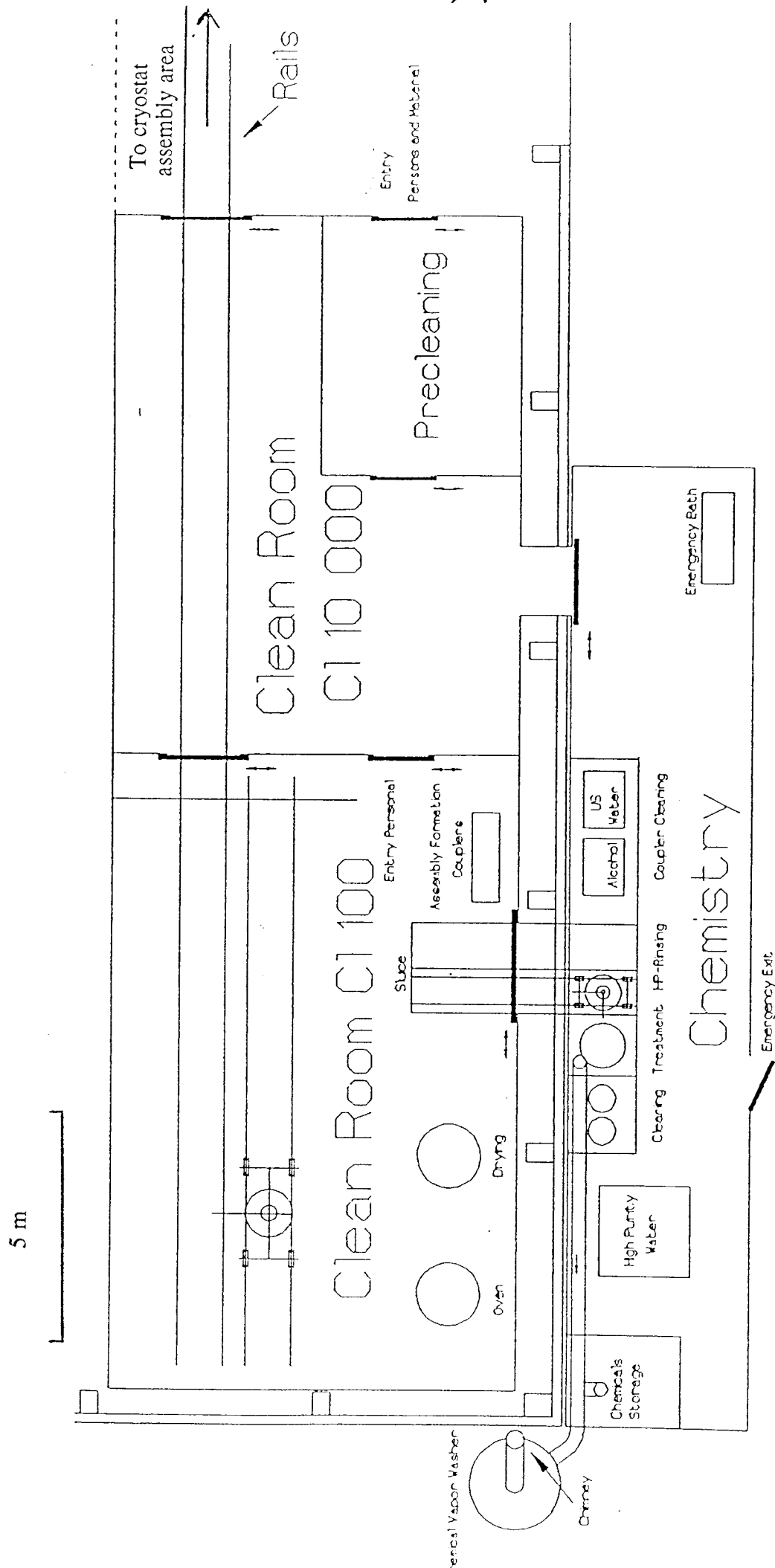


Fig. 4.17 Infrastructure for cavity treatment and assembly.

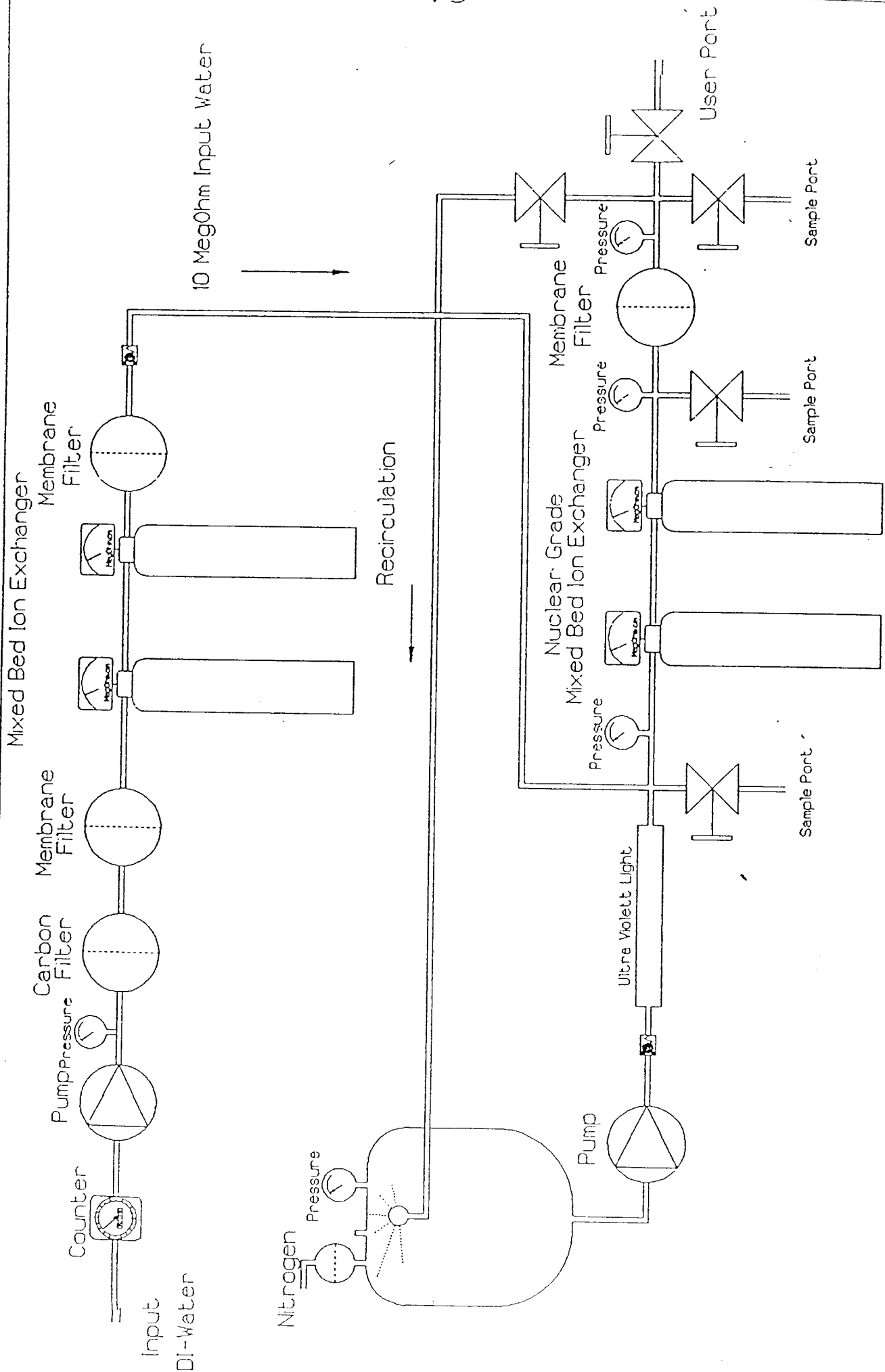


Fig. 4.18 Ultra clean water installation.

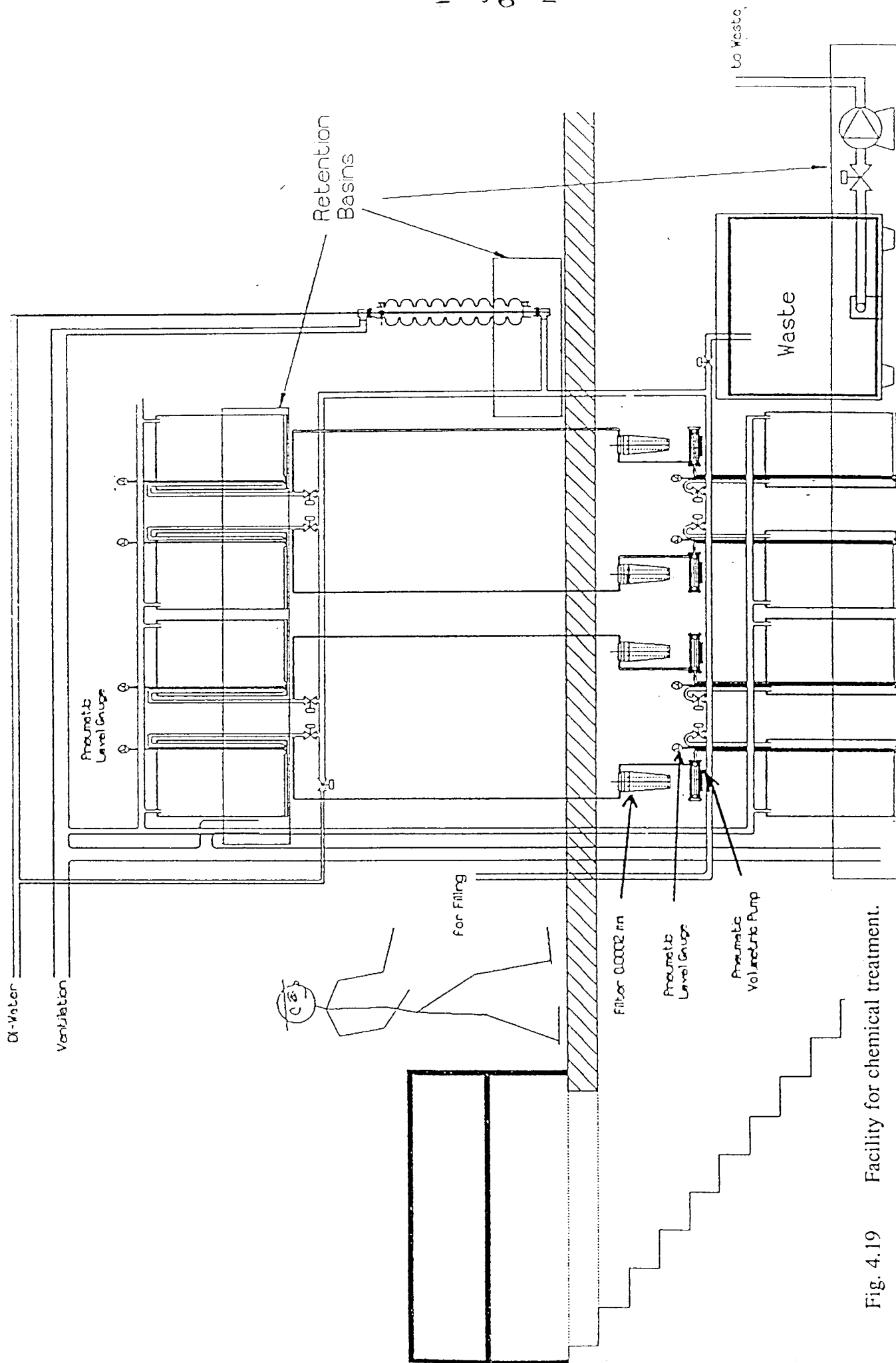


Fig. 4.19 Facility for chemical treatment.

has been gained after treating some cavities.

Finally the assembly of 8 cavities i.e. the installation of connection pipes between the cavities and manual gate valves at either end of the module will be done in the clean room (class 100). Subsequent work on the module as completing the Helium tubing, alignment, mounting the outer parts of the input couplers, mounting the step motors etc. is performed under normal workshop conditions. The inner parts of a cryostat module including the radiation shields will be assembled as an unit which will be inserted into the vacuum vessel as a whole.

Heat Treatment

Before installation in the furnace (see Fig. 4.20) the cavity is cleaned as if in preparation for an RF test. This will include a one hour soak in nitric acid, a chemical etch for 1-2 minutes to clean the inside and outside surfaces, thorough rinsing, and clean room drying. After assembly inside the titanium lined box (see Fig. 4.21) the cavity is suspended in the furnace with Nb covers at the beam holes to protect the RF surface from coating with Ti.

To outgas the furnace the pressure is allowed to reach $7 \cdot 10^{-6}$ mb below 500°C , $1.3 \cdot 10^{-6}$ mb to 1000°C and $3 \cdot 10^{-7}$ mb to 1400°C . After reaching temperature the vacuum improves to 10^{-7} mb or better. (All pressures are referred to the cold regions of the vacuum system). After 4-8 hours at $1400\text{-}1500^{\circ}\text{C}$, the heat treatment is complete. Temperatures are measured by a pyrometer calibrated in a separate run against a thermocoupler. The furnace cools down for 36 hours. The vacuum is let up with filtered nitrogen and the cavity removed in a clean room, and disassembled from the titanium liner.

The field flatness is checked and restored if necessary in a clean room. To remove any dust introduced while removal from furnace or the tuning stage, the cavity is rinsed (100 bar) and dried as usual.

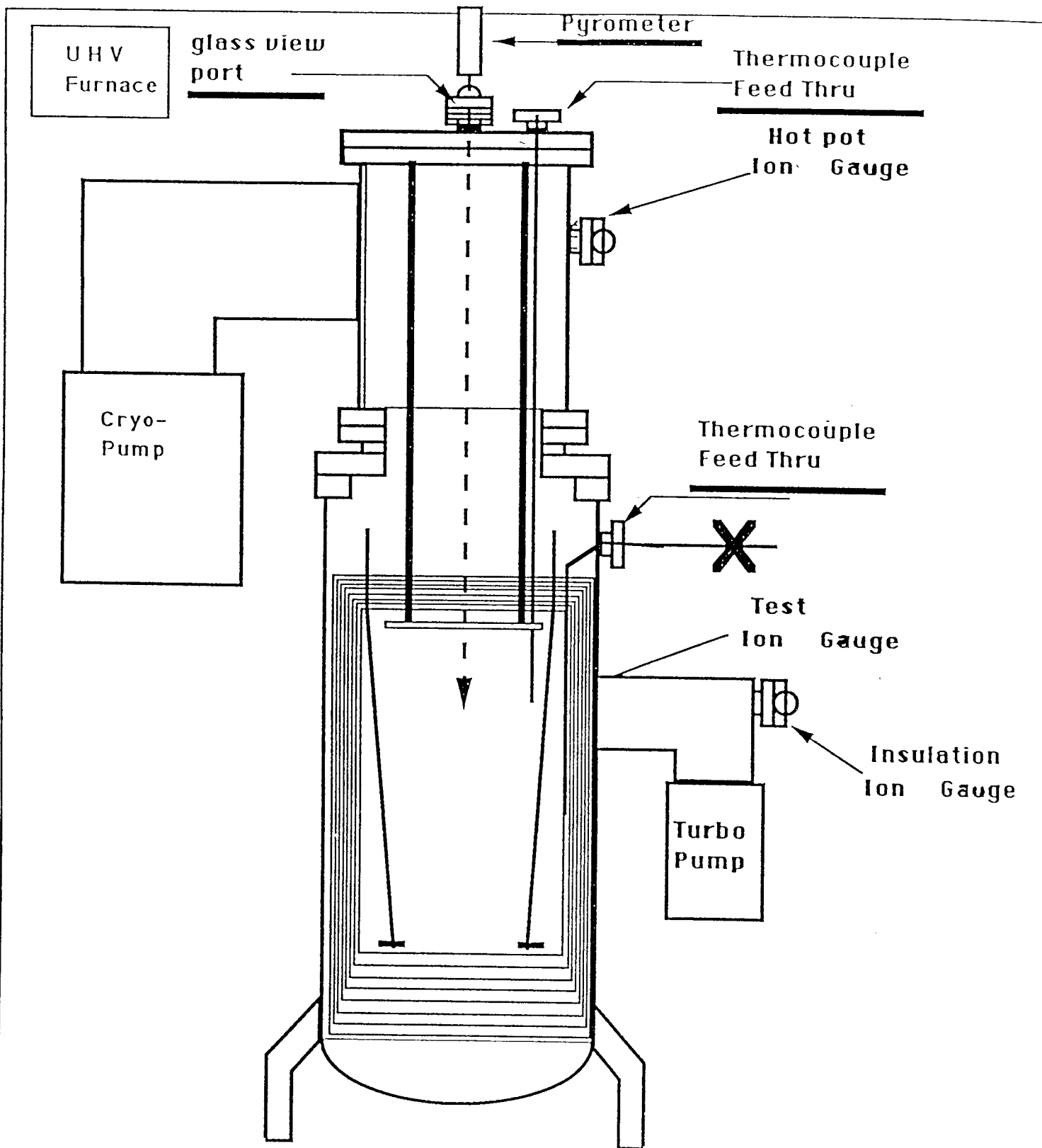
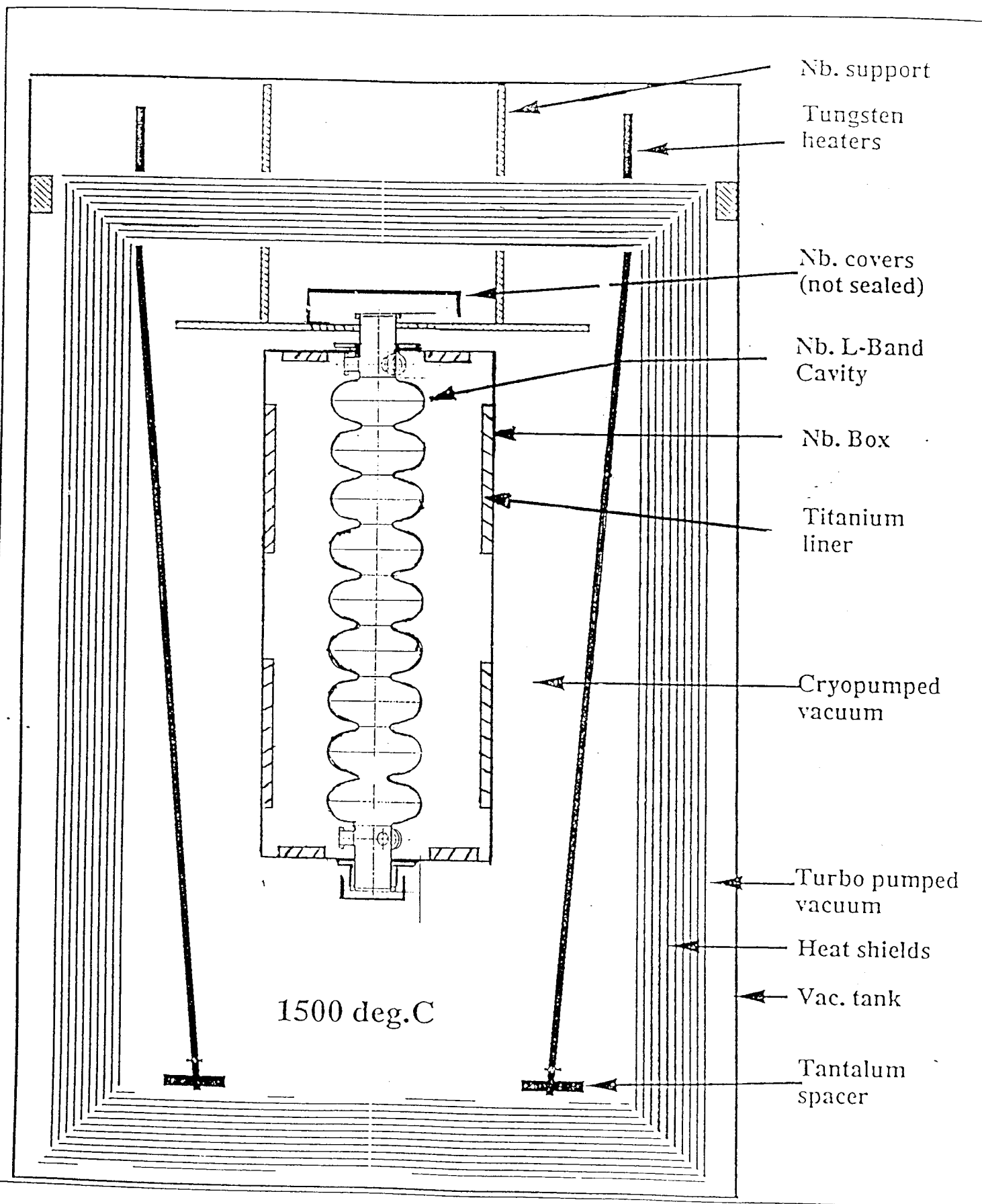


Fig. 4.20 Layout of UHV furnace for high temperature treatment.



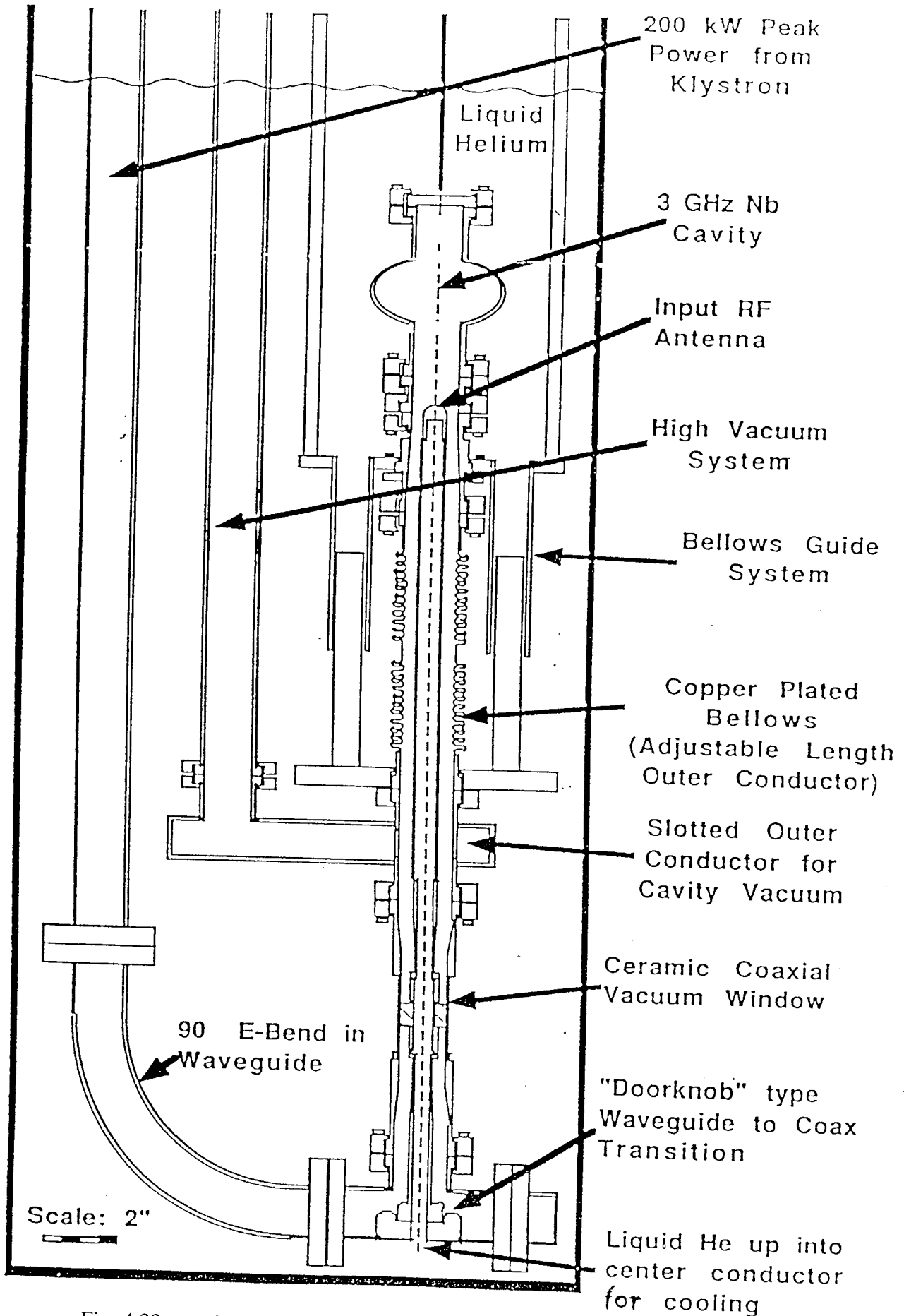


Fig. 4.22 Schematic layout of HPP processing set up.

Infrastructure

To summarize, the infrastructure needed for the cavity production and assembly at DESY involves many items: automatic chemical treatment facility (Fig. 4.19), 100 bar rinsing (Fig. 4.18), vertical and horizontal cryostats, 1 MW klystron and variable coupler for HPP (Fig. 4.22), ultra high vacuum furnace (Fig. 4.20, 4.21) and large clean rooms. More detailed specifications can be found in the appendix.

5. Test Facility

5.1 General Layout

Besides the string of 4 cryomodules with its RF and cryogenic systems the test facility includes an electron injector and beam analysis stations. A schematic diagram is shown in Fig. 5.1.

Beam analysing stations will be installed behind the injector and behind the cryomodule string. Each of them will have a set of specific beam diagnostics.

5.2 Injector

The injector must be able to deliver a beam at an energy of at least 5 MeV. The bunch population and frequency depend on the kind of experiment to be made. Two types of injectors which will be installed successively are proposed. The first one, easier to design, will serve for testing acceleration and RF to beam energy transfer. The second one will approach the TESLA bunch specifications and - requiring more studies - could be built in a second step.

The minimum energy required for injection into the string of four cryomodules must satisfy two conditions:

- The beam has to be transmitted through the 48 m long test set-up without losses and without debunching under space charge forces. The strong focussing effect of SW cavities on a low energy beam has to be taken into account (as an example for $E = 2$ MeV and $E_{acc} = 15$ MV/m, the focal length is 1 m).
- For studies on beam-cavity interaction it is desirable to transmit the beam through one cryostat without acceleration.

First simulations, including space charge forces, show that these conditions will be met if the energy of the incoming beam is above 5 MeV.

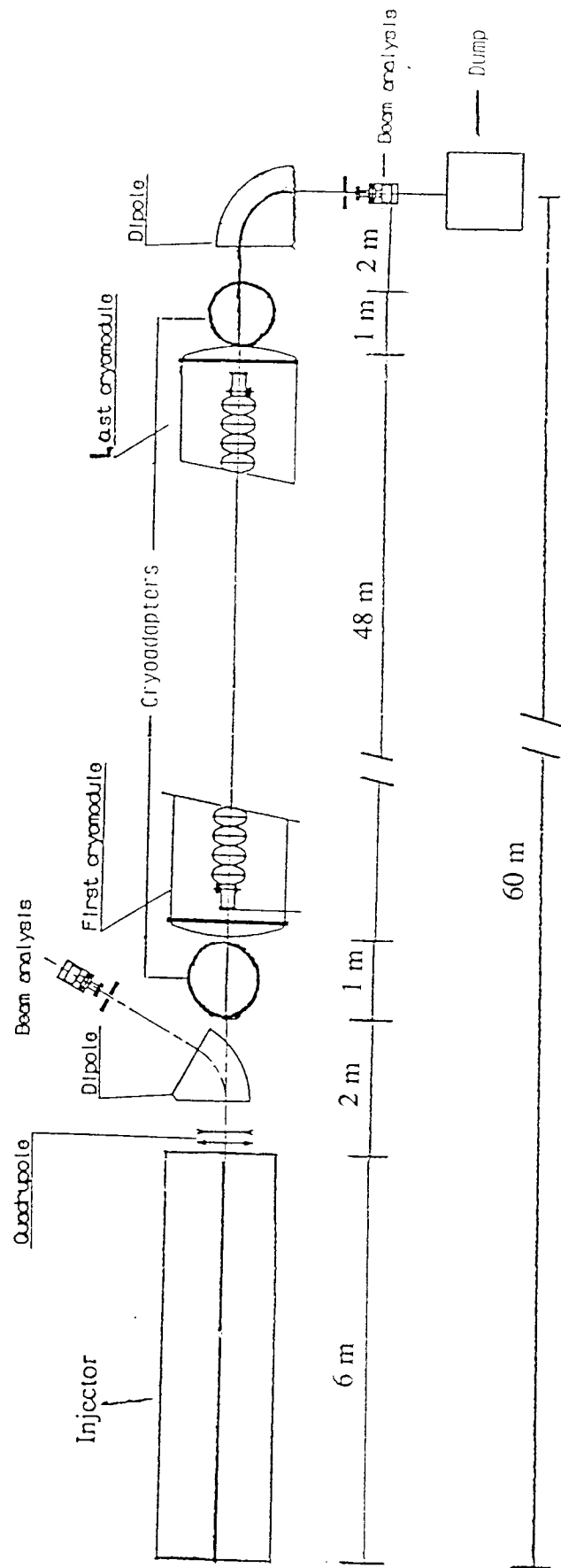


Fig. 5.1 Schematic layout of Test Facility including an injector, 4 cryomodules and beam analysis systems.

Injector 1 : Low bunch charge (Fig. 5.2)

The possibility of producing a beam with the correct properties with respect to acceleration, energy resolution and stability has to be demonstrated with a test facility. The main difficulties come from the pulsed mode of operation of eight cavities under heavy beam loading, with high gradient and fed by a common klystron. Most of these problems can be studied with a beam of equivalent charge per pulse (8 mA during 800 μ sec), regardless of the bunch population. We therefore propose to build an injector able to deliver a pulse current of up to 10 mA during 800 μ s with a bunch frequency of 1.3 GHz ($4 \cdot 10^7$ electrons per bunch). These characteristics are rather standard and do not present any special design problems.

For another kind of measurements to be performed with this injector, it is required to deliver a beam with the same time structure as TESLA (i.e. bunches 1 μ s apart). This can be done by applying to the gun control electrode during a 800 μ s macropulse a train of 1 MHz micropulses of a duration shorter or equal to the RF period (0.77 ns). If micropulses as short as 0.77 ns cannot be produced, 1 ns pulses (already produced with such guns) could be compressed by velocity modulation in a subharmonic 216 MHz TM010 cavity installed behind the gun. For such a moderate compression, only a low modulating voltage would have to be applied, and would limit the deterioration of the longitudinal emittance. The peak current in the micropulses will be increased, despite space charge forces, as much as permitted by the focussing and bunching scheme. $5 \cdot 10^8$ electron bunches seem possible and would result in a 80 μ A macropulse current.

The injector No. 1 consists of a 300 kV electron gun, a chopping system, a prebunching cavity and a capture cavity. It is very attractive to use a standard 9-cell cavity as capture cavity, since it will not only save design work but also offer a test bench for the cavity prototype. For an incoming 300 keV beam, satisfactory capture efficiency is obtained with accelerating fields ranging from 8 to 20 MV/m. The maximum output energy would be 6.6 MeV with 8 MV/m and 14 MeV with 15 MV/m. A separate klystron is recommended to feed this cavity in order to allow a flexible optimization of the injector characteristics.

The overall length of this injector would be about 6 m.

Injector 2: High bunch charge (Fig. 5.3)

The problems connected with wakefields and HOM power dissipation are of fundamental importance for the design of a SC collider. They must be studied by using a beam with very high charge per bunch.

Given the HOM loss factor of 5.75 V/pC/m, about 25 W will be lost in one 8-cavity cryostat by the TESLA beam. The most crucial unknown parameter is the fraction of this power which will be dissipated in the 2 K components. This fraction could be determined in the test facility by calorimetric measurements if the total HOM power generated by the beam is sufficiently high. Calculations predict that about 1/4 of the total HOM power will be extracted by these couplers. The rest, corresponding to the high frequency part of the spectrum, is supposed to propagate and to be partly dissipated at the ends of the cryostat in absorbers at higher temperature. These absorbers could be installed in separate cryostats to permit low level calorimetric measurement. This power can be correctly evaluated above a level of about 0.5 W. Assuming that only half of the high frequency spectrum power is dissipated in these parts (a pessimistic hypothesis), the beam should loose a total HOM power of more than 3 W. If the proposed time structure of the beam is used, it requires a bunch population of at least $2 \cdot 10^{10}$ electrons.

Though single bunches of such density have already been produced using classical technology, the challenge here is to produce a train of 800 such bunches, spaced 1 μ s apart, in the same RF pulse. It is interesting to notice that in the real machine, the bunch length can in principle be shaped by a bunch compressor at the exit of a damping ring. In the test facility, the same requirement has to be fulfilled by the injector alone.

In principle, another combination of bunch frequency and population with the same $N^2 \cdot f_c$ product could be used but this would not alleviate the design very much.

Two approaches have been considered.

The first, based on the technology of RF guns with photocathodes, would require a SC cavity at low frequency, because of the long pulse and high charge per bunch. A scheme using this technology has been proposed by INFN and Wuppertal. It consists of a 2+1/2-cell cavity at about 500 MHz housing an alkali antimonide photocathode. An optional decoupled single cell of special

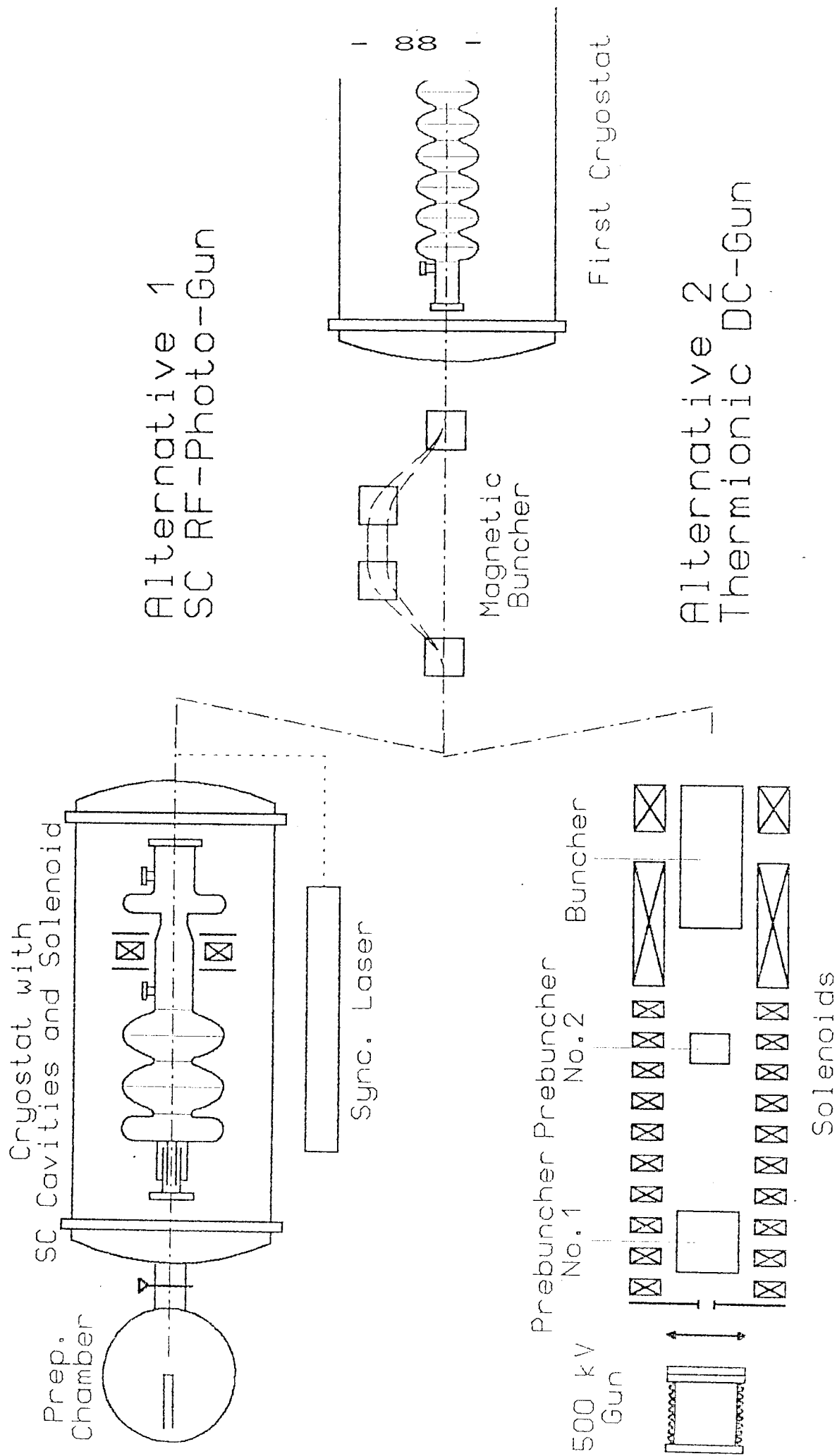


Fig. 5.3 Two possible designs of injector 2 (high bunch charge).

geometry can be added enhancing the efficiency of the compressor while conserving the beam quality. An output energy of above 8 MeV is expected. The interaction between SC cavity and photocathode is now under experimental investigation at Milano and Wuppertal. First results obtained at Wuppertal prove that cavity and photocathode can be operated together without destroying their qualities each other. A laser illuminating the photocathode with appropriate pulse structure could be developed from existing RF guns.

A scheme using a classical gun of 500 keV has been studied at Saclay. Such a high voltage value is justified by the fact that space charge effects decrease with beam energy. Pulses of 1 ns after prebunching by a series of subharmonic frequency NC cavities can be injected into a capture cavity. This capture cavity can be either NC or SC.

A NC one would permit the use of continuous solenoid focusing but would require a structure able to dissipate a power of about 40 kW/m, a non trivial value. Solenoids are convenient to find a compromise between longitudinal and transverse emittances. Using a 5-cell copper cavity fed by a 2 MW peak power klystron it would be possible to obtain a 7 MeV beam with a bunch length less than 2 mm.

A SC capture cavity has no power dissipation problem but imposes the use of SC solenoids between single cells.

In all cases the required bunch length can be obtained only after magnetic compression.

Both approaches - RF gun and classical gun - need a considerable amount of R & D before their feasibility is established and several laboratories have programmes in progress on these items. The continuation of such programmes is essential to establish the feasibility within the next two or three years.

5.3 Cryogenics

Introduction

The R + D - programme for superconductive RF-cavities requires equipment being capable for production and handling of liquid and gaseous helium at temperatures down to approximately 1.8 K. It is proposed to modify existing research equipment, including a 4.4 K / 900 W refrigerator in the DESY experimental hall 3 to meet our requirements. The details of the proposed system are described below.

Requirements

The test facility will be equipped with three cryostats for single cavity tests. Two of them will be arranged vertically and one horizontally all connected permanently to the distribution system. The option for one further cryostat will be provided.

A parallel line will supply a group of up to 4 cryomodules of 12 m length each. A layout of the facility including the mutual position of the individual components is given in Fig. 5.4.

The refrigeration requirement of the cryomodules dominates the cooling capacity to be supplied. Since the RF-losses both of the modules and of the cryostats are much higher than static losses, it will always be possible to keep one or several test cryostats cold in standby.

Although there is a strong tendency to operate a future linac TESLA at a minimum temperature of 2.0 K, the test facility should be capable of operating at 1.8 K. This will keep open the option for a final decision after having performed model measurements under both conditions.

According to the present state of knowledge the following amount of refrigeration capacity must be available:

at 1.8 K	200 W
at 5.0 K	200 W
at $70 < T < 80$ K	700 W

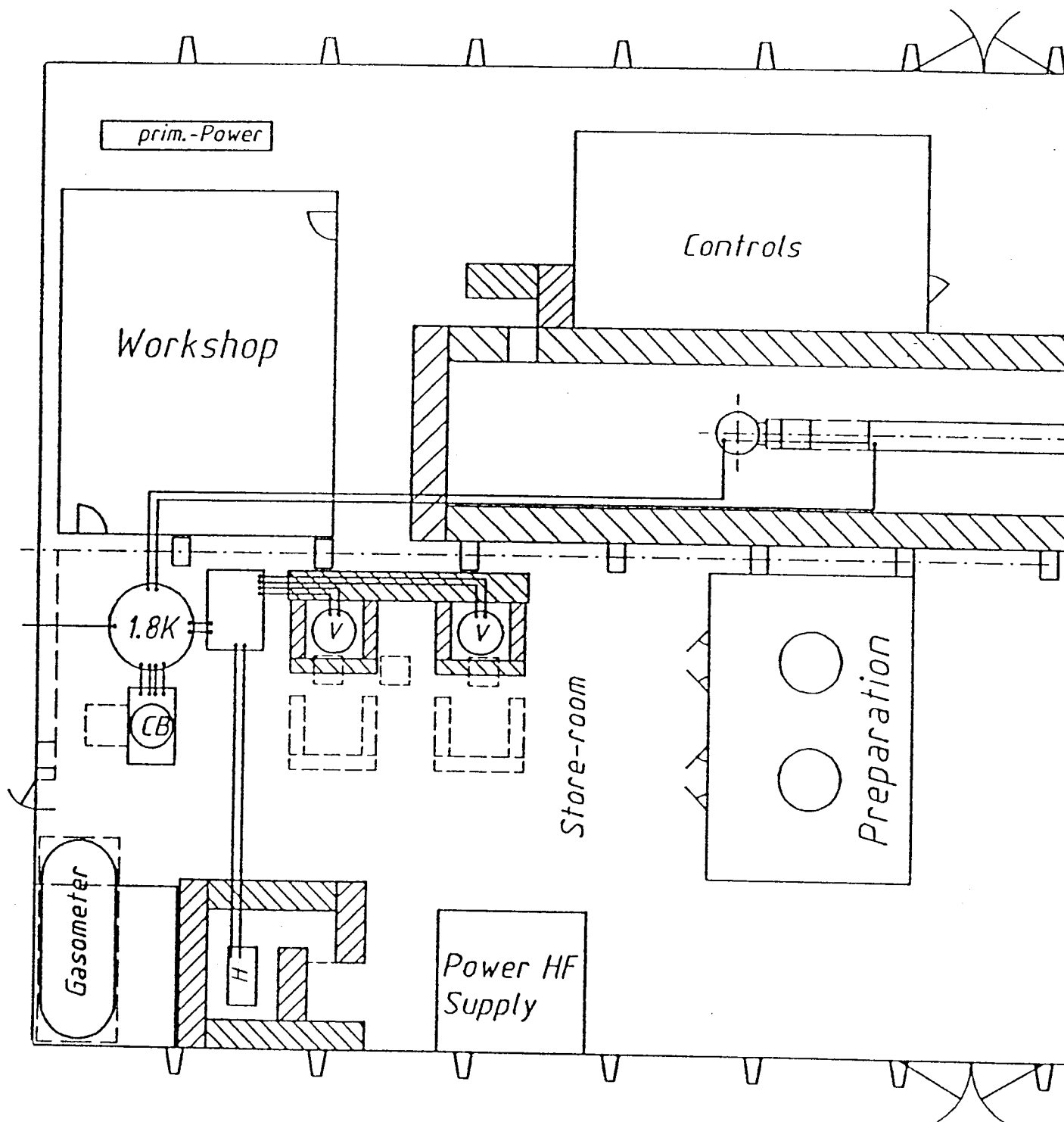


Fig. 5.4 Arrangement at DESY of cryogenic equipment for test facility.

The value for the 70/80 K temperature level is defined by the existing 900 W DESY refrigerator which can supply only 70 K at minimum for the shield cooling gas circuit.

This capacity would allow to run the cryomodules with RF power and to keep at least the heat shields of the 3 cryostats at their operation temperature.

Cryogenic Circuit

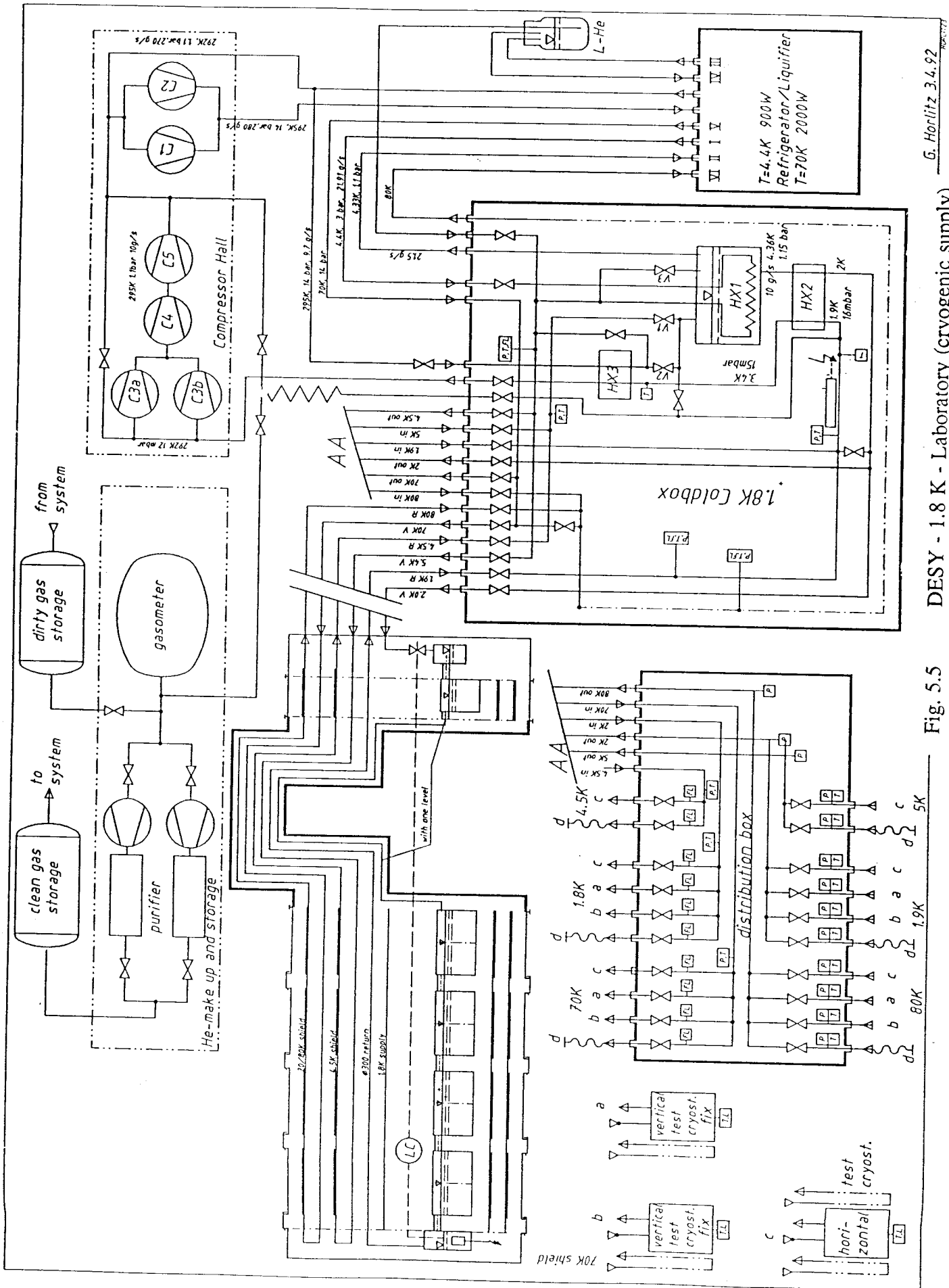
The cryogenic circuit is based on an existing DESY refrigerator / liquefier with refrigeration capacity of about 900 W at 4.4 / 4.5 K and 2000 W shield cooling gas supply at 70 K to be returned at 80 K. The circuit is shown in Fig. 5.5. The refrigerator supplies cold helium at a pressure of about 3.0 bar and a temperature of 4.4 K at plug I. The helium (mass flow rate about 0.022 kg/s) is transferred to the adjacent 1.8 K cold box where it is re-cooled to 4.4 K in the bath heat exchanger HX 1.

Before being expanded into the two phase section of HX 1, the whole 4.4 K massflow is passed through the 5 K heat shields in the cryostats. After having absorbed the heat load of these shields, the helium returns at about 5.4 K to the 1.8 K-box and expands through valve VI, being partially liquefied at a temperature of 4.4 K and a pressure of 1.15 bar. The vapor is returned through plug II into the refrigerator where it is handled in the standard way.

From the liquid section of HX 1 a 1.15 bar / 4.4 K liquid flow of about 0.01 kg/s is forced into the heat exchanger HX 2 where it is subcooled to about 2 K by means of the 1.9 K vapor returning from the cryostats. (It is assumed that the equilibrium vapor temperature is increased from 1.8 K in the cryostats to 1.9 K due to transfer losses).

The 1.15 bar / 2 K helium is transferred to the distribution box adjacent to the 1.8 K box where it is expanded through the supply valves into the cryostats. The final pressure will be 16 mbar at $T = 1.8$ K. The vapor returns to the 1.8 K box, where it is heated in HX 2 to about 3.5 K. In order to return the 16 mbar helium to the 1.15 bar suction level of the main circuit compressors (C1) and (C2), room temperature vacuum pumps (roots pumps in the first stage, liquid ring pump or screw compressor in the second and third stage) have been chosen.

Before entering the first pumping stage, the cold 3.5 K return gas is heated to room temperature in HX 3 by means of a counterflow of warm gas. The massflow rate of the heating gas is approximately the same as in the 1.8 K circuit. It is cooled down and expands into the 4.4 K / 1.15 bar two phase circuit. By this arrangement a large fraction of the enthalpy of the 3.5 K gas can be returned at pressure / temperature conditions of the lower temperature end of the refrigerator. The operating mode of the latter is then almost refrigeration. Only a small amount of liquefaction power will be required due to the unbalance of the two gas streams in HX3, caused by differences in enthalpies and specific heat capacities in the high pressure and the low pressure



DESY - 1.8 K - Laboratory (cryogenic supply)

Fig. 5.5

G. Horlitz 3.4.92

branch. Other options such as a cold compressor or low temperature expander are being investigated.

The flow rate of the DESY refrigerator at maximum cooling power of 900 W amounts to 0.04655 kg/s. After extraction of 0.02191 kg/s for the 1.8 / 4.4 K circuits the remainder of 0.02464 kg/s corresponds to an excess refrigeration of about 476 W. This will be reduced to about 400 W due to the unbalance in HX3.

The 70 K shield cooling flow is available at plug V. It passes the 70 K heat shields in all boxes being in operation and the flow returns at $T \approx 80$ K through plug VI of the refrigerator. (In the case of a new refrigerator the shield gas supply temperature would be specified to 40 K instead of 70 K).

The vacuum compressors have to be installed in the existing compressor building. Fig. 5.6 shows the distribution of the equipment on the floor.

Instrumentation and control system

The total number of sensors for pressure, temperature, mass flow and liquid levels amounts to about 420. Most of them have to be equipped with electrical signal converters for data handling by means of a process computer system.

Computer equipment for the data handling and process controls is provided. The equipment proposed does not only do the controls for the 1.8 K circuits but it operates also the 4.4 K refrigerator and other devices of the 1.8 K laboratory. The existent process control system of the DESY refrigerator cannot be used anymore. (An optional new one could be purchased without this equipment).

5.4 RF System

Pulsed RF Power Generation

The peak RF power needed for one 9-cell cavity at full gradient (25 MV/m) and beam intensity is 208 kW. There are commercially available klystrons operating at 1.3 GHz which can deliver the total RF power of 4.5 MW during pulse-lengths of up to two ms at a 10 Hz repetition rate. One such klystron can supply two cryounits of eight 9-cell cavities each with RF power.

For the test facility four klystrons are needed. Two are used for the four cryounits, another one for cavity high power processing and main coupler processing. For the preaccelerator (see the injector section) an additional lower power klystron is required.

The present design uses conventional pulsed cathode klystrons without modulating anode. For the test facility a Pulse Forming Network (PFN) in conjunction with a pulse transformer will be used, because it is a proven solution. Hard tube modulators have been considered but even with a modulating anode klystron large capacitors at the 130 kV level would be necessary. A stored energy corresponding to about 25 times the energy needed per pulse must be supplied in order to keep the voltage droop during the pulse on the two percent level. The same is true for a series cathode modulator tube which, in addition, would have to support the full cathode current of about 70 A. There is only a very limited choice of such tubes.

Another problem arises from the fact that the pulsed input electric power for the RF system of the whole 500 GeV linac is of the order of 8 GW (klystron efficiency 50%). For the pulse duration of 1.33 ms this results in the average power of 106 MW. It is prohibitive to draw this amount of pulsed energy directly from the mains without appropriate energy storage and averaging.

A possible modulator solution is the power supply depicted in Fig. 5.7a. At the voltage level of 10 kV the network L1, C1 (5H and 1.5 mF) reduces the fluctuations of the charging current of the subsequent PFN below the 5 percent level. By discharging the PFN into the pulse transformer a 2 ms 130 kV pulse is generated every 98 ms. The amount of energy stored in the PFN is comparable to the total amount of energy needed for the klystron beam per pulse, i.e. about 18 kJ for one klystron. - The PFN pulse length has been chosen to be 2 ms in order to give sufficient flexibility and reserve beyond the needed 1.33 ms of RF pulse duration. - The parameters of the modulator are summarized in Table 5.1.

The capital investment and operating cost of the RF system for the final linac using the PFN

Table 5.1 - Parameters of the Klystron and Modulator

Cavity peak power	208 kW
Cavities per klystron	16
Klystron peak power	4.5 MW
Pulse length	2 ms
RF energy/pulse	9 kJ
Klystron voltage	130 kV
Klystron current	70 A
Impedance	1.9 k Ω
Modulator peak power	9.1 MW
Transformer ratio	13 : 1
PFN stored energy	18 kJ
PFN voltage	20 kV
Switch current	0.9 kA
PFN impedance	8.33 Ω
Klystron efficiency	50%
Repetition rate	10 Hz
Average power-kly/mod	90 kW/220 kW
DC power supply	10 kV/22 A
Pulse flatness	$\pm 0.5\%$
Voltage regulation	$\pm 0.5\%$
PFN sections	24
PFN L	417 μ H
PFN C	6 μ F
Pulse rise time	$\leq 100 \mu$ s

could be imagined where n PFNs are charged up successively by one common charging network. It will be necessary to evaluate alternative modulator designs including unconventional solutions in order to provide minimum cost alternatives.

One alternative consists of storing electrical energy in a superconducting coil. However, transfer of a part of the stored energy to the klystrons (with an intermediate pulse transformer) requires switching of the high current in the coil at a 10 Hz rate. An appropriate switch and superconducting cable suitable for a dB/dt of 20 T/s corresponding to a pulse current droop of 2% within 2 ms need to be developed. A principle electrical circuit is shown in Fig. 5.7b.

For the test facility it is proposed to design and construct a Superconducting Magnetic Energy Storage coil (SMES) capable of supplying 2 klystrons in parallel. The stored energy of this coil will be 1 MJ at a current of 1000 A. The output voltage will be 20 kV. The same pulse transformer as in the conventional scheme with split primary winding will be used. The output voltage of the DC converter will be 300 V.

The switch S will consist of about 10 Gate Turn Off thyristors (GTO) or standard thyristors with a quench (chopper) circuit connected in series.

The superconducting coil wound as a solenoid requires a low loss a.c. cable as is already under development for power applications. A non-conducting cryostat will be used to avoid eddy current losses.

From this setup we will learn about the performance of the series connected switch elements, the 20 kV handling and the fast pulsed SMES.

For a future linac and operation of up to 80 klystrons from one SMES - a number which may fit best to the distributed refrigerators - the following items still remain to be developed:

- a switch capable of commuting 40 kA at 20 kV at a 10 Hz rate
- a superconducting cable for 40 kA fast pulse operation and minimum cryogenic losses.

Other technologies might imply pulsed power supplies or high frequency choppers to avoid the large low frequency pulse transformer.

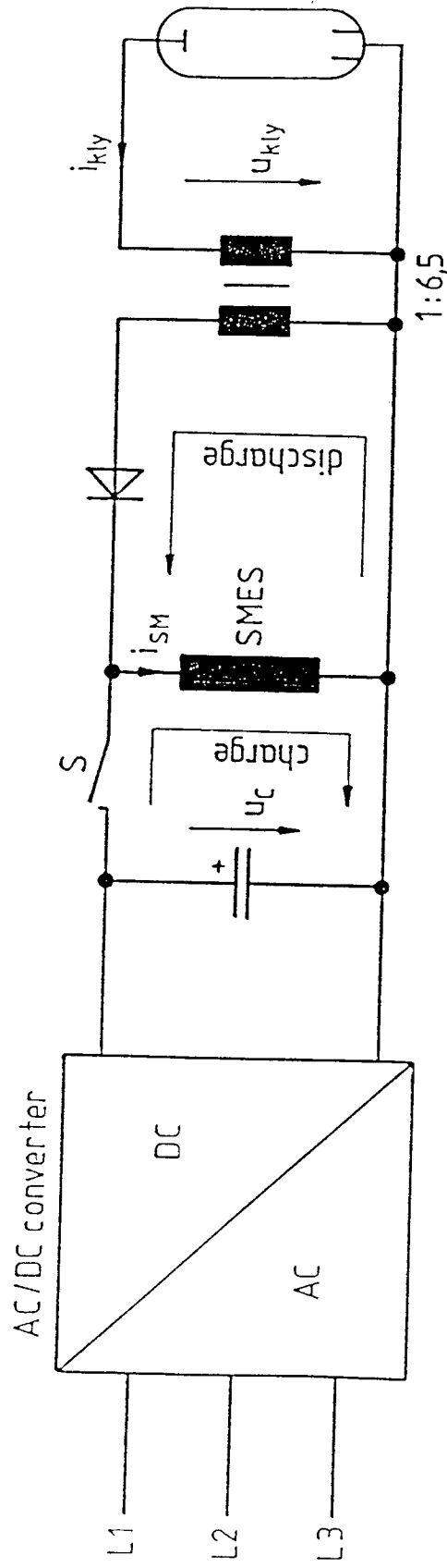


Fig. 5.7b Schematic electrical circuit of the Superconducting Magnetic Energy Storage (SMES) coil circuit coupled to a klystron through a pulse transformer.

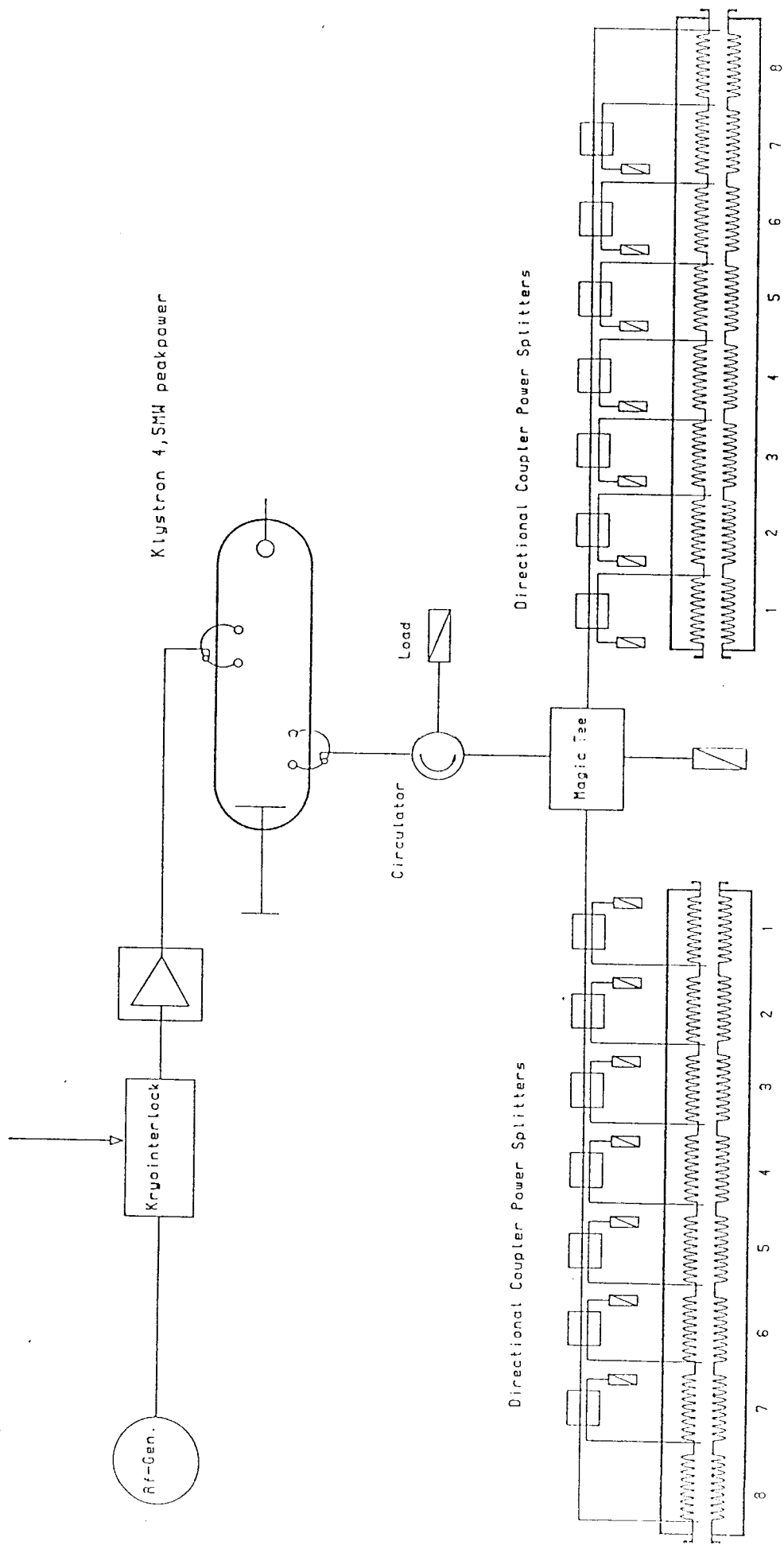


Fig. 5.8 Layout of the RF distribution scheme. One 4.5 MW klystron feeds two cryounits. There are eight 9-cell cavities in each unit. The coupler hybrids branch off equal amounts of power into the individual cavity. An interlock circuit which switches off the RF drive in the case of a quench or for other reasons like phase- or amplitude errors is also indicated. In total four cryounits are planned.

Date		Name	AF Distribution
Gen. 1	22.11.91	A. Keller	
Gen. 2	22.11.91	R. Goss	
Projekt: Futura			
Gen. 1			
Gen. 2			
Gen. 3			
Gen. 4			
Gen. 5			
Gen. 6			
Gen. 7			
Gen. 8			
Gen. 9			
Gen. 10			
Gen. 11			
Gen. 12			
Gen. 13			
Gen. 14			
Gen. 15			
Gen. 16			
Gen. 17			
Gen. 18			
Gen. 19			
Gen. 20			
Gen. 21			
Gen. 22			
Gen. 23			
Gen. 24			
Gen. 25			
Gen. 26			
Gen. 27			
Gen. 28			
Gen. 29			
Gen. 30			
Gen. 31			
Gen. 32			
Gen. 33			
Gen. 34			
Gen. 35			
Gen. 36			
Gen. 37			
Gen. 38			
Gen. 39			
Gen. 40			
Gen. 41			
Gen. 42			
Gen. 43			
Gen. 44			
Gen. 45			
Gen. 46			
Gen. 47			
Gen. 48			
Gen. 49			
Gen. 50			
Gen. 51			
Gen. 52			
Gen. 53			
Gen. 54			
Gen. 55			
Gen. 56			
Gen. 57			
Gen. 58			
Gen. 59			
Gen. 60			
Gen. 61			
Gen. 62			
Gen. 63			
Gen. 64			
Gen. 65			
Gen. 66			
Gen. 67			
Gen. 68			
Gen. 69			
Gen. 70			
Gen. 71			
Gen. 72			
Gen. 73			
Gen. 74			
Gen. 75			
Gen. 76			
Gen. 77			
Gen. 78			
Gen. 79			
Gen. 80			
Gen. 81			
Gen. 82			
Gen. 83			
Gen. 84			
Gen. 85			
Gen. 86			
Gen. 87			
Gen. 88			
Gen. 89			
Gen. 90			
Gen. 91			
Gen. 92			
Gen. 93			
Gen. 94			
Gen. 95			
Gen. 96			
Gen. 97			
Gen. 98			
Gen. 99			
Gen. 100			
Gen. 101			
Gen. 102			
Gen. 103			
Gen. 104			
Gen. 105			
Gen. 106			
Gen. 107			
Gen. 108			
Gen. 109			
Gen. 110			
Gen. 111			
Gen. 112			
Gen. 113			
Gen. 114			
Gen. 115			
Gen. 116			
Gen. 117			
Gen. 118			
Gen. 119			
Gen. 120			
Gen. 121			
Gen. 122			
Gen. 123			
Gen. 124			
Gen. 125			
Gen. 126			
Gen. 127			
Gen. 128			
Gen. 129			
Gen. 130			
Gen. 131			
Gen. 132			
Gen. 133			
Gen. 134			
Gen. 135			
Gen. 136			
Gen. 137			
Gen. 138			
Gen. 139			
Gen. 140			
Gen. 141			
Gen. 142			
Gen. 143			
Gen. 144			
Gen. 145			
Gen. 146			
Gen. 147			
Gen. 148			
Gen. 149			
Gen. 150			
Gen. 151			
Gen. 152			
Gen. 153			
Gen. 154			
Gen. 155			
Gen. 156			
Gen. 157			
Gen. 158			
Gen. 159			
Gen. 160			
Gen. 161			
Gen. 162			
Gen. 163			
Gen. 164			
Gen. 165			
Gen. 166			
Gen. 167			
Gen. 168			
Gen. 169			
Gen. 170			
Gen. 171			
Gen. 172			
Gen. 173			
Gen. 174			
Gen. 175			
Gen. 176			
Gen. 177			
Gen. 178			
Gen. 179			
Gen. 180			
Gen. 181			
Gen. 182			
Gen. 183			
Gen. 184			
Gen. 185			
Gen. 186			
Gen. 187			
Gen. 188			
Gen. 189			
Gen. 190			
Gen. 191			
Gen. 192			
Gen. 193			
Gen. 194			
Gen. 195			
Gen. 196			
Gen. 197			
Gen. 198			
Gen. 199			
Gen. 200			
Gen. 201			
Gen. 202			
Gen. 203			
Gen. 204			
Gen. 205			
Gen. 206			
Gen. 207			
Gen. 208			
Gen. 209			
Gen. 210			
Gen. 211			
Gen. 212			
Gen. 213			
Gen. 214			
Gen. 215			
Gen. 216			
Gen. 217			
Gen. 218			
Gen. 219			
Gen. 220			
Gen. 221			
Gen. 222			
Gen. 223			
Gen. 224			
Gen. 225			
Gen. 226			
Gen. 227			
Gen. 228			
Gen. 229			
Gen. 230			
Gen. 231			
Gen. 232			
Gen. 233			
Gen. 234			
Gen. 235			
Gen. 236			
Gen. 237			
Gen. 238			
Gen. 239			
Gen. 240			
Gen. 241			
Gen. 242			
Gen. 243			
Gen. 244			
Gen. 245			
Gen. 246			
Gen. 247			
Gen. 248			
Gen. 249			
Gen. 250			
Gen. 251			
Gen. 252			
Gen. 253			
Gen. 254			
Gen. 255			
Gen. 256			
Gen. 257			
Gen. 258			
Gen. 259			
Gen. 260			
Gen. 261			
Gen. 262			
Gen. 263			
Gen. 264			
Gen. 265			
Gen. 266			
Gen. 267			
Gen. 268			
Gen. 269			
Gen. 270			
Gen. 271			
Gen. 272			
Gen. 273			
Gen. 274			
Gen. 275			
Gen. 276			
Gen. 277			
Gen. 278			
Gen. 279			
Gen. 280			
Gen. 281			
Gen. 282			
Gen. 283			
Gen. 284			
Gen. 285			
Gen. 286			
Gen. 287			
Gen. 288			
Gen. 289			
Gen. 290			
Gen. 291			
Gen. 292			
Gen. 293			
Gen. 294			
Gen. 295			
Gen. 296			
Gen. 297			
Gen. 298			
Gen. 299			
Gen. 300			
Gen. 301			
Gen. 302			
Gen. 303			
Gen. 304			
Gen. 305			
Gen. 306			
Gen. 307			
Gen. 308			
Gen. 309			
Gen. 310			
Gen. 311			
Gen. 312			
Gen. 313			
Gen. 314			
Gen. 315			
Gen. 316			
Gen. 317			
Gen. 318			
Gen. 319			
Gen. 320			
Gen. 321			
Gen. 322			
Gen. 323			
Gen. 324			
Gen. 325			
Gen. 326			
Gen. 327			
Gen. 328			
Gen. 329			
Gen. 330			
Gen. 331			
Gen. 332			
Gen. 333			
Gen. 334			
Gen. 335			
Gen. 336			
Gen. 337			
Gen. 338			
Gen. 339			
Gen. 340			
Gen. 341			
Gen. 342			
Gen. 343			
Gen. 344			
Gen. 345			
Gen. 346			
Gen. 347			
Gen. 348			
Gen. 349			
Gen. 350			
Gen. 351			
Gen. 352			
Gen. 353			
Gen. 354			
Gen. 355			
Gen. 356			
Gen. 357			
Gen. 358			
Gen. 359			
Gen. 360			
Gen. 361			
Gen. 362			
Gen. 363			
Gen. 364			
Gen. 365			
Gen. 366			
Gen. 367			
Gen. 368			
Gen. 369			
Gen. 370			
Gen. 371			
Gen. 372			
Gen. 373			
Gen. 374			
Gen. 375			
Gen. 376			
Gen. 377			
Gen. 378			
Gen. 379			
Gen. 380			
Gen. 381			
Gen. 382			
Gen. 383			
Gen. 384			
Gen. 385			
Gen. 386			
Gen. 387			
Gen. 388			
Gen. 389			
Gen. 390			
Gen. 391			
Gen. 392			
Gen. 393			
Gen. 394			
Gen. 395			
Gen. 396			
Gen. 397			
Gen. 398			
Gen. 399			
Gen. 400			
Gen. 401			
Gen. 402			
Gen. 403			
Gen. 404			
Gen. 405			
Gen. 406			
Gen. 407			
Gen. 408			
Gen. 409			
Gen. 410			
Gen. 411			
Gen. 412			
Gen. 413			
Gen. 414			
Gen. 415			
Gen. 416			
Gen. 417			
Gen. 418			
Gen. 419			
Gen. 420			
Gen. 421			
Gen. 422			
Gen. 423			
Gen. 424			
Gen. 425			
Gen. 426			
Gen. 427			
Gen. 428			
Gen. 429			
Gen. 430			
Gen. 431			
Gen. 432			
Gen. 433			
Gen. 434			
Gen. 435			
Gen. 436			
Gen. 437			
Gen. 438			
Gen. 439			
Gen. 440			
Gen. 441			
Gen. 442			
Gen. 443			
Gen. 444			
Gen. 445			
Gen. 446			
Gen. 447			
Gen. 448			
Gen. 449			
Gen. 450			
Gen. 451			
Gen. 452			
Gen. 453			
Gen. 454			
Gen. 455			
Gen. 456			
Gen. 457			
Gen. 458			
Gen. 459			
Gen. 460			
Gen. 461			
Gen. 462			
Gen. 463			
Gen. 464			
Gen. 465			
Gen. 466			
Gen. 467			
Gen. 468			
Gen. 469			
Gen. 470			
Gen. 471			
Gen. 472			
Gen. 473			
Gen. 474			
Gen. 475			
Gen. 476			
Gen. 477			
Gen. 478			
Gen. 479			
Gen. 480			
Gen. 481			
Gen. 482			
Gen. 483			
Gen. 484			
Gen. 485			
Gen. 486			
Gen. 487			
Gen. 488			
Gen. 489			
Gen. 490			
Gen. 491			
Gen. 492			
Gen. 493			
Gen. 494			
Gen. 495			
Gen. 496			
Gen. 497			
Gen. 498			
Gen. 499			
Gen. 500			
Gen. 501			
Gen. 502			
Gen. 503			
Gen. 504			
Gen. 505			
Gen. 506			
Gen. 507			
Gen. 508			
Gen. 509			
Gen. 510			
Gen. 511			
Gen. 512			
Gen. 513			
Gen. 514			
Gen. 515			
Gen. 516			
Gen. 517			
Gen. 518			
Gen. 519			
Gen. 520			
Gen. 521			
Gen. 522			
Gen. 523			
Gen. 524			
Gen. 525			
Gen. 526			
Gen. 527			
Gen. 528			
Gen. 529			
Gen. 530			
Gen. 531			
Gen. 532			
Gen. 533			
Gen. 534			
Gen. 535			
Gen. 536			
Gen. 537			
Gen. 538			
Gen. 539			
Gen. 540			
Gen. 541			
Gen. 542			
Gen. 543			
Gen. 544			
Gen. 545			
Gen. 546			
Gen. 547			
Gen. 548			
Gen. 549			
Gen. 550			
Gen. 551			
Gen. 552			
Gen. 553			
Gen. 554			
Gen. 555			
Gen. 556			
Gen. 557			
Gen. 558			
Gen. 559			
Gen. 560			
Gen. 561			
Gen. 562			
Gen. 5			

a) An error in cavity tuning.

It can be caused by microphonic effects and radiation pressure in the cavity and thermal expansion of the wave guide between the circulator and the cavity.

It is believed that by stiffening the cavity structure with appropriate bars and by tuning only the two end half-cells the phase jitter of the cavity voltage due to vibrations and microphonic noise can be reduced to ± 1 degree.

However, radiation pressure presents a particular difficulty since the cavity tune changes during RF filling. These changes may differ from one cavity to the next.

For the full gradient of 25 MV/m radiation pressure is expected to detune the cavity of present design by 800 Hz. In order to avoid complicated tuning procedures during the cavity RF filling time this value should be reduced to about 180 Hz which corresponds to half the loaded cavity bandwidth. The potential for frequency programming the RF source during cavity filling will also be investigated.

- The thermal effect on the waveguides can be minimized by adjusting the tuners only after thermal equilibrium has been reached. This effect would favour a tree like RF distribution scheme where all waveguide path lengths are equal and all cavity phases move in parallel. As stated above, one could change to such a distribution scheme if the linear one turned out to be impractical.
 - The tuning offset for each cavity can be properly adjusted by setting to maximum cavity voltage. We propose to derive the input to the cavity tuner loop during the last 100 μ s of the RF pulse by a sample and hold circuit.
 - An important task of the test facility will be to demonstrate that the tuning error can indeed be kept reasonably small. The error in cavity voltage resulting from the expected overall tuning error of ± 5 degree (16 Hz) - ± 10 degree (32 Hz) is 0.7% - 3%. For a half linac with $N = 10000$ cavities these errors have to be divided by $N^{1/2}$ since the tuning errors of different cavities are uncorrelated. Therefore the estimated contribution of tuning errors to the beam energy spread is $\leq 0.03\%$.
- b) Errors due to voltage fluctuations of the klystron RF.
- A common amplitude feedback loop around all cavities fed by one klystron, i.e. a loop

which stabilizes the scalar sum of the cavity voltages, could ensure a voltage stability better than 1% during the acceleration time of about 1 ms.

For 625 uncorrelated klystrons this error will result in an energy spread $\leq 0.04\%$

c) Errors due to phase fluctuations of the klystron RF.

A phase loop minimizing the phase jitter between the klystron output (or the phase signal of one cavity) and the RF generator signal should ensure a phase stability better than ± 1 degree. Since the contribution of individual cavities to the total phase error is highly reduced by statistical arguments and since the afore mentioned amplitude loop also corrects voltage fluctuations resulting from individual cavity tuning phase errors the generation of a vector sum signal of all cavities coupled to one klystron as a reference signal is not necessary.

d) Errors in relative phase between beam and cavity RF voltage.

The proper timing of the beam relative to the cavity RF voltage can be defined by first tuning the beam-loaded cavity to maximum RF voltage. Subsequently the phase of the klystron induced cavity voltage is varied until a minimum in total cavity voltage is obtained. Ideally, the magnitudes of klystron induced cavity voltage and beam induced one should be equal. Then, the total cavity voltage is zero at the correct phase which therefore can be detected with a precision of better than one degree. A slow phase loop must stabilize the klystron RF phase relative to the beam signal to a similar precision over longer periods of time. The input signals to this loop can be the RF voltage signal from one cavity and a filtered beam monitor signal.

Assuming a maximum phase error of ± 5 degrees for an individual klystron the total energy spread for 625 klystrons then will amount to 0.015%. The test facility must therefore demonstrate that the long term phase stability is indeed smaller than 5 degrees.

e) Errors in the injection phase.

An error in injection time is more critical since its effect on the energy spread is not reduced by statistics. An error of ± 5 degrees in the injection phase (corresponding to a time jitter of 10 ps) gives an energy deviation of 0.4% which is much larger than the sum of all previously discussed contributions.

In order to obtain a total energy spread of 0.1% the error on injection phase must be reduced to ± 1 degree corresponding to an energy deviation of 0.015%.

It should be noted here that errors in the injection time on the microsecond time scale will cause energy fluctuations too, even if the injection phase angle is correct. This is due to the

which is still rising during acceleration of the beam whereas too late injection will have the opposite effect.

The amplitude loop should, however, be able to handle also this effect.

Block diagrams of the phase-, amplitude- and tuner loop are shown in Fig. 5.9 and a synchronization scheme for beam injection is shown in Fig. 5.10.

f) Fluctuations of the bunch charge.

The RF power in the cavity taken away by the beam depends linearly on the beam current. Without feedback an energy error of $\pm 0.1\%$ would necessitate maintaining the total charge over the 800 bunches of one RF pulse to less than $\pm 0.2\%$. However, with amplitude feedback charge fluctuations of a few % could be tolerated.

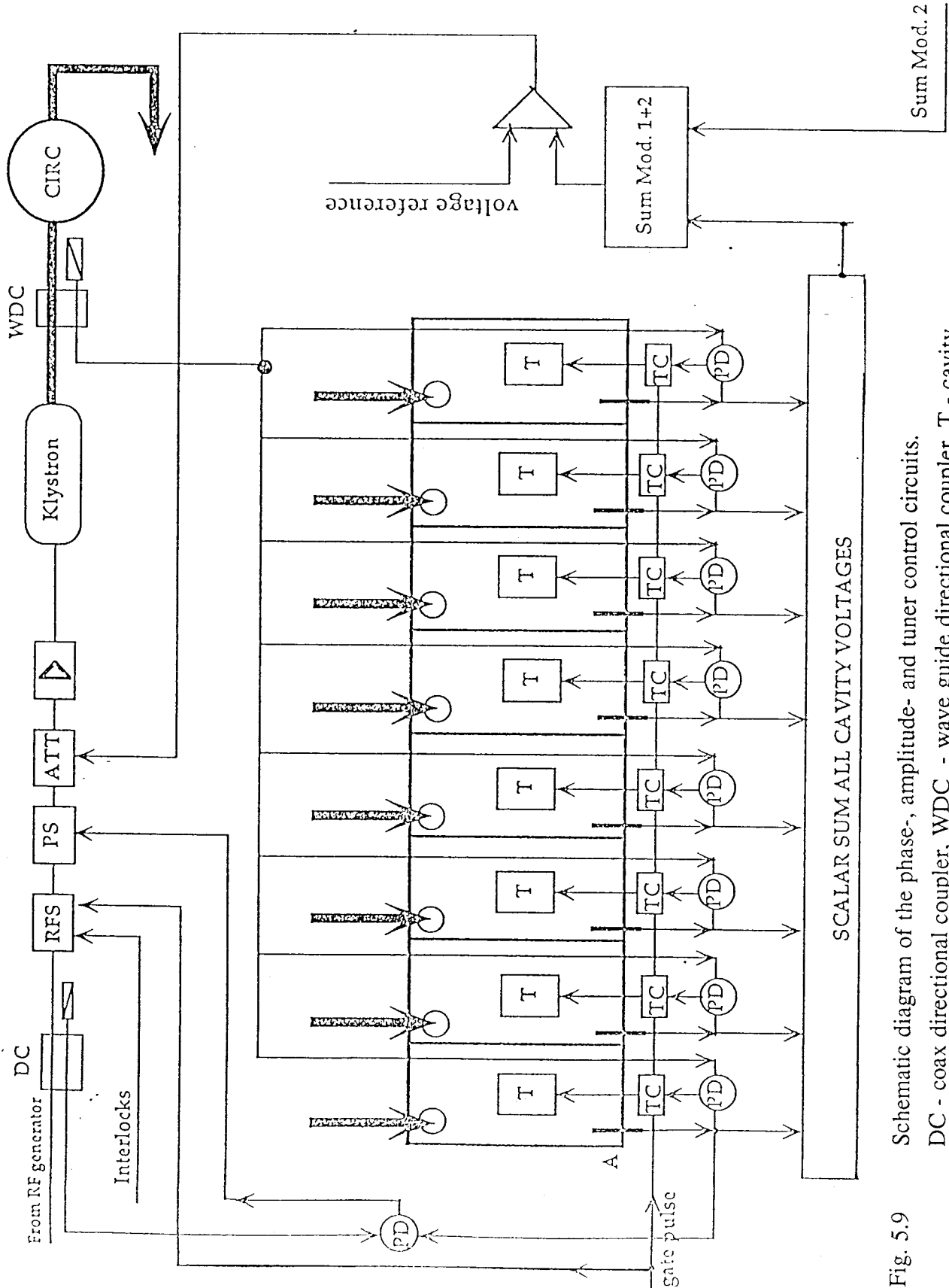


Fig. 5.9

Schematic diagram of the phase-, amplitude- and tuner control circuits.

DC - coax directional coupler, WDC - wave guide directional coupler, T - cavity tuner, TC - gated tuner control, PD - phase discriminator, RFS - RF switch, PS - variable phase shifter, ATT - variable attenuator, CIRC - circulator.

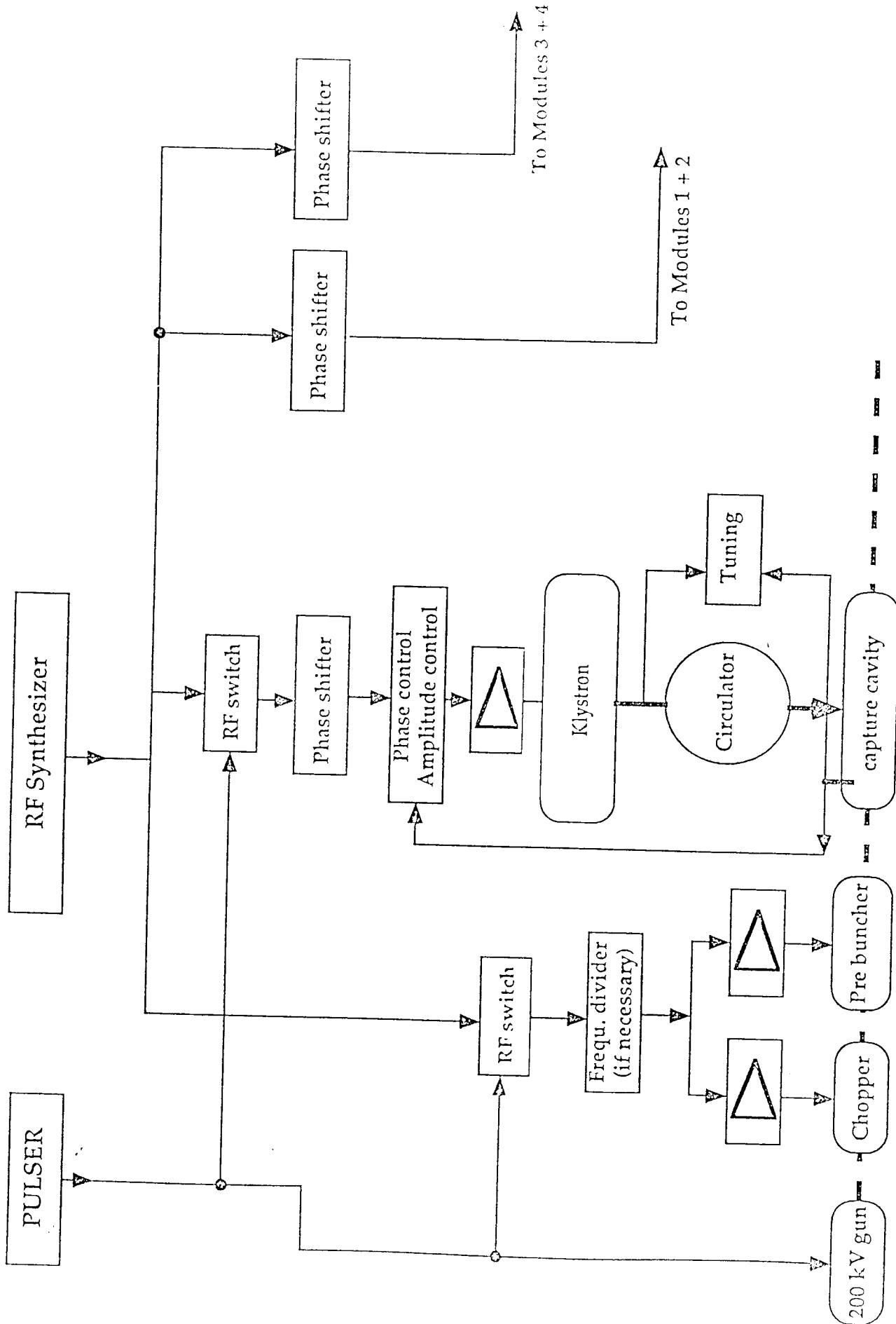


Fig. 5.10 Synchronization scheme for beam injection.

5.5 Diagnostics

The behaviour of the cavities and the RF system operating at very high field under pulsed operation, with and without beam, is of fundamental importance for the design of a SC collider. Therefore, the cryomodule and the beam line have to be equipped with adequate diagnostics.

Cryomodule instrumentation

Specific diagnostic equipment must be available in order to carry out the measurement program.

- First one will measure the static heat load and determine Q_0 using a calorimetric method. These measurements necessitate an instrumentation which must be sufficiently accurate to measure power dissipation of a fraction of a Watt.
- Measurement of Q_0 by the RF method. This measurement requires a variable coupler. Designing this coupler is under exploration. If available, it would also be used to adjust the field levels in different cavities separately and to compensate variations in the external Q values.
- The option of high power processing has to be made available. Present experience with high power processing shows that with a fixed coupler set at $Q_{\text{ext}} = 3 \cdot 10^6$, a pulse length of 1 msec and a peak power of 208 kW one can reach an accelerating field of 28 MV/m at the end of the pulse. For RF processing higher fields are needed requiring peak power of 1 MW. This RF power is available but it would be necessary to change the RF distribution system and it would impose an important additional requirement on the input coupler.
- Thermometers, working in superfluid helium, will be fixed on the cavities. This will permit a constant monitoring of power dissipation and long term stability of Q. The beam tube temperature should also be monitored. Additional thermometers for monitoring temperatures at the 4.5 and 70 K level will be installed.
- A monitoring of field emitted electrons will be made available on each cavity. The electron current collected by the pick-up electrodes gives after filtering a useful information on electron loading. In addition, several X-ray detectors will be mounted in the cryostat to monitor field emission.

- RF beam position and long pulse current monitors: They will give non-destructive information.
- X-ray detectors associated with some beam size limiting apertures will give informations on beam alignment and can also trigger a beam loss interlock system.
- A bunch length measurement will be necessary for tests with short, high intensity bunches. It could consist of a transition radiation or a Cerenkov light radiator associated with a streak camera. The time resolution required is about 2 ps. It will be installed in front of the first cryomodule.
- Vacuum instrumentation for measurements of pressure and residual gas composition.

5.6 Experimental Programme

For the realization of the programme experimental tests have to be performed at various stages of the programme. The main guide lines for cavity performance tests are given in chapter 4.4.

Single Cavity Tests

For single cavity tests, at least two vertical test cryostats and one horizontal test cryostat are foreseen. Besides the usual testing of quality factors, accelerating fields, field emission and quench behaviour, the frequencies of fundamental and higher order modes will be determined and the possibility of high power processing (HPP) with a variable coupler will be explored. These tests will be performed on the naked cavity without He-vessel, HOM couplers and tuning system.

For the first cavities (at least) a test in the horizontal test cryostat should be performed on cavities equipped with HOM couplers, welded He-vessel and tuning system. We plan to investigate the influence of the horizontal position on cavity performance. The addition of the He-vessel and tuning system will allow already a first check of tuning range and speed, setting precision and the influence of vibrations and mechanical resonances of the cavity-He-vessel system. The influence of stiffening bars and rings on the pressure sensitivity can be studied as well as the detuning due to radiation pressure at pulsed high power, high field conditions. The system behaviour at different bath temperatures between 1.8 and 2 K will be checked.

An excitation of the cavity by low power pulsed RF via the HOM couplers will allow investigation of its broadband behaviour. The tuning of the HOM filters can be checked.

The horizontal cryostat test may also allow a more detailed study of RF electron trajectories and X-ray production.

In this simplified layout the quench behaviour of cavities at high fields can be studied and first tests on the handling of quenches and adequate protection systems can be performed involving not only RF signals but also He bath pressure and cavity vacuum .

Tests of cryounits without beam

Each cryomodule will contain eight 9-cell cavities with all auxiliaries like main couplers, HOM couplers, tuning systems and RF-probes, support and alignment system and cryogenic feedlines. In addition a SC quadrupole, steering magnets and beam monitoring will be integrated in the layout.

In order to perform precise Q_o -measurements, $Q_{ext} = 10^9$ should be achievable whereas for high power processing $Q_{ext} = 10^6$ will be necessary so that the filling time of the cavity can be shortened to avoid quenches.

The RF measurements have to be performed first on individual cavities for determining the field level and the Q_{ext} of the main coupler. During this measurement all other cavities have to be detuned at maximum.

In a next step the combined operation of a few or all cavities has to be performed and all RF controls regulations and interlocks have to be studied under pulsed high field conditions.

The transmission of HOM modes along the cavity string can possibly be studied already at this stage e.g. by injecting HOM via one HOM coupler in the system. The behaviour of trapped modes in the presence of neighbouring cavities may also be investigated.

Similarly reacceleration of field emitted electrons in neighbouring cavities can be investigated.

Other RF tests may involve the transmission of the fundamental mode at the HOM couplers, and the detuning of cavities by many bandwidths under full power conditions. Tests with and without circulators should also be performed.

The cryomodule will also allow the following tests:

- Behaviour of the full system with respect to vibrations and shock excitation of the cavities.
- Influence of cooling conditions at particular operating temperatures.
- Alignment precision, stability and reproducibility for cavities and quadrupoles.
- Quality of the magnetic shielding (to about 30 mG).

Particular attention has to be given to a quench protection system; it will have to integrate not only RF signals from all cavities but also informations from the cryogenics, the cavity vacuum and from the tuners. A fast and reliable system operating under high RF power and high field conditions with msec-pulses will be a major challenge. It should also allow the return to normal operation of a quenched cavity without switching off other cavities.

Tests of cryounits with beam

A schematic layout of the whole test set up is given in Fig. 5.1. It includes besides the four cryomodules an electron injector, beam analysis stations, appropriate diagnostic systems and the RF and cryogenic systems.

The system will have an overall length of approximately 60 m. Adequate focussing elements have to be included in the beam lines and the possibility for off-axis steering of the beam should be given.

The beam line has to handle essentially two operation modes:

A first class of experiments is related to the acceleration of an 8 mA beam for which the bunch population and repetition rate can be chosen in some convenient way. Accurate measurement of the energy and energy dispersion of the beam is important and allows to study problems related to controls and regulation in the presence of pulsed high RF power and of strong transient beam loading. With only 8 cavities we cannot rely on statistical effects to reduce the energy spread induced by phase and amplitude errors; it is therefore important to reduce all contributions to the energy spread caused by other reasons.

The damping of transverse HOM can be evaluated with a beam experiment. The method consists in determining the regenerative BBU current threshold. The cavity mode is excited by an RF generator through an antenna and the radiated power at another probe is measured for different beam currents. The Q of the mode is deduced from a modelization of BBU. Another method would be to modulate the beam with a broadband stripline kicker and measure with a pick-up the beam transfer function. Further calculation is needed to get an order of magnitude of this effect.

It may be possible to increase the HOM power deposited in the system by exciting resonantly some longitudinal modes. With a bunch population of $5 \cdot 10^8$ electrons and an external Q of 10^5 , a peak RF power of 100 mW could be expected.

The operation with this beam will also allow to test the main couplers under TW and SW conditions at high power. The quench protection system can be studied with beam including the influence of beam fluctuations, fast beam losses and fast RF-switch off. This can define a safe interlock range which is still compatible with the regular operation of many cavities.

A second class of experiments and in particular the ones related to HOM losses and wake fields will need a much more ambitious high charge per bunch injector with short bunch lengths. Some flexibility in the length, time separation and repetition rate would be very desirable.

We mention the following tests:

- Transfer of full pulse RF power to the beam at design bunch length.
- Measurement of energy dispersion and energy stability.
- Evolution of emittance and phase relations along the beam line.
- Measurement of HOM power absorbed by the HOM couplers and the part escaping the cavities via the beam tubes. Transmission and absorption of the HOM power along the beam line, in other cavities and in the dedicated HOM absorbers. Measurement of the fraction of HOM losses absorbed at 2 K.
- Measurement of total loss factor of the cryostat by measuring the increase in energy dispersion of a single bunch passing through the cryostat without acceleration.
- Measurement of transverse wakes by injecting the bunch off axis.
- Beam stability from bunch to bunch and beam path stability.
- Check of cavity alignment by measuring the production of transverse modes.

6. Further R & D Towards TESLA Goals

Over the last decade, steady improvements in the understanding of field limitations multipacting and thermal breakdown, along with invention of methods to control them have been the foundations for continuous advances in SRF cavity performance. More recently we have begun to understand the nature of field emitters, isolated some of the sources and forged new approaches to defeat field emission. Our ability to control the number of emitters has improved substantially, along with development of new tools to provide cleaner surfaces, and to eliminate emitters in situ by processing. Advances towards the needed capabilities of TESLA will only be realized if efforts already in progress continue to seek ways of upgrading the performance and reliability of cavities.

A healthy level of basic R & D activities prevails in laboratories engaged in the development and utilization of SRF. A thorough discussion of the R & D plans of each of the institutions participating in this proposal is given in Appendix. Here we summarize some of the general themes that will be addressed.

Encouraging results on the benefits of heat treatment and HPP will be buttressed with increased statistics using the multi-cell structures presently available. Controlled exposures that test the survival of the benefits of HT and HPP will be carried out to establish a protocol for the assembly of the cavities. It should preserve the emission free surface through the many operations necessary between laboratory tests and beam line operation. These questions will be emphasized in the on-going work at Cornell. It will be very important to extend the HPP technique to 1.3 GHz, the intended RF frequency for TESLA. This work will be carried out at the DESY TTF. Work on high power RF processing at 1.5 GHz has already started at Saclay with promising results.

That it is occasionally possible to reach 18 MV/m with standard chemical surface preparation techniques encourages us to believe that, with better understanding and improvements, even these standard techniques may in the future approach the desired performance. A few areas of improvement already targeted are: filtering of acids, chemical treatments in a dust-free room, high pressure (100 bar) water rinsing after chemistry, automated chemistry to preserve uniform treatment from cavity to cavity and to minimize contamination, and measures to improve the cleanliness of the vacuum system of the RF test set-up. Work in these areas is in progress at Saclay and CERN. Improved procedures will be incorporated in the TTF at DESY as successes are realized.

It will also be important to continue the quest to deepen the basic understanding of the

behaviour of superconducting surfaces in RF fields, for it is these initiatives that will ultimately open the way to bring SRF technology closer to its ultimate potential for Nb, i.e. gradients of 50 MV/m at Q values over 10^{10} .

Along these lines, Wuppertal and Saclay have installed state of the art field emission microscopy equipment to study the nature of active emission sites using DC fields. Cornell is studying, using microscopy, the fate of emitters that have undergone RF processing. Thermometry based diagnostic techniques are being used at Wuppertal, CERN, Saclay and Cornell to carefully study the loss mechanism in SRF cavities and to reveal the nature of anomalous losses. Thermal modelling of the heating of the RF surface under various conditions is being studied at DESY, Saclay and Cornell. Efforts to improve the heat transfer between the Nb-He interface are in progress.

The purity and thermal conductivity of Nb has been improved by Russian companies, who are now making available Nb a factor of 2 to 5 superior than Nb used hitherto for making cavities to improve performance by providing the ultimate in high thermal stability, as well as to reduce structure cost. CERN, Saclay and INFN are exploring sputter coating of Nb on 1.3-1.5 GHz cavities. The route of hydroforming a multi-cell copper cavity from one piece of copper has already been proven, e.g. at CERN.

Over the longer range, a close watch on the basic studies and RF characterization of new materials like Nb_3Sn , NbTiN , or even the high T_c superconductors is worthwhile. It will be important to keep in reserve the possibility, although remote at present, of gradients higher than 50 MV/m for upgrades to TESLA. Higher T_c materials such as NbTiN , Nb_3Sn and YBaCuO are under investigation at CERN, Saclay and Wuppertal.

All of these activities will be of generic importance to TESLA and all will receive a strong impetus from their respective funding agencies and their own laboratories when the collaborative TTF project is launched.

APPENDIX 1

Possible R + D at CERN

For a reliable production of cavities a number of problems has to be solved. It is not possible to detect with the naked eye small defects, which are however large enough to produce quenches at fields well below the specified field. Welding from the outside with a reliability high enough for a production of thousands of cavities needs to be proven.

The study of electron emission as the main cause for field limitations must be intensified. The heat treatment at high temperature is a drawback in the construction of cavities. The niobium is becoming very soft, the flanges have to be niobium instead of the more reliable stainless steel conflat flanges, and the thermal treatment adds to the cost. The means for surface cleaning have to be improved for very clean surfaces. Other means for obtaining similar results must be explored.

An order of magnitude in Q value at 4.2 K could be gained if it were possible to produce layers of NbTiN or Nb₃Sn. The accelerator then could run at 4.2 K reducing the operating cost and allowing for an increase of the duty factor.

Therefore it is proposed to define a Research and Development program which could contain the following points:

- Development of an automatic inspection device for the detection of defects on the niobium sheets and the half cells. It might be necessary to improve the surface finish, to be able to distinguish fatal defects from the normal variations of the niobium crystal structure. We will look for instruments for such a purpose that are already available in industry.
- It is necessary for a production of cavities to be able to inspect the interior and to repair defects found. As it is probably not possible to introduce the electron beam gun into the cavity, from time to time projections of little niobium spheres near the weld will appear if the cavity is welded from the outside. An articulated computer controlled manipulator should be developed, with a head that could for example contain a laser scanning microscope, a mechanical engravers tool and a power laser beam, passing through the same light path as the laser scanning microscope, for remelting of the damaged surface.

for remelting of the damaged surface.

- Although welds are not important for losses it would be best from a cost point of view, if all welds could be avoided on the cavity. Therefore it is proposed to study alternative techniques as e.g. hydroforming. A development of hydroformable niobium tubes should be initiated in industry. With this method of fabrication the production cost of niobium cavities can probably be reduced.
- The benefits of high pressure water rinsing, high temperature annealing and high power processing have been well established. An increased statistics using multi-cell cavities and studies on the influence of various parameters like e.g. air exposure should be continued.
- An improvement of the surface cleanliness is of the greatest importance. For example a heat treatment of a thin inner layer of only a few μm with a laser beam should give similar results as the oven treatment, conserving the mechanical properties of the deformed niobium, and giving the possibility to use different flanges. Cleaning with plasma discharge and high power UV-light and oxygen can probably improve the surface cleanliness. These methods are successfully used in the semiconductor industry.
- Finally plasma and laser assisted chemical vapor deposition and diffusion techniques are promising for the development of layers with a higher T_c like NbTiN and Nb₃Sn. Although such a development is probably rather long, the gain that could be obtained is making such an effort worthwhile to undertake.

The INFN - ARES Research Program

The ARES Collaboration is funded by INFN and includes researchers and technicians from the following INFN sections and laboratories: Laboratori Nazionali di Frascati, Milano, Tor Vergata and Genova.

The ARES collaboration has started building up experience in the field of SC RF through the construction and commissioning (started at the end of '91) of a 25 MeV superconducting Linac (LISA), to be operated mainly for a FEL experiment, and by producing in collaboration with the national industry prototype 500 MHz cavities for LISA and, through a collaboration with CERN, prototype industry-fabricated 350 MHz sputtered cavities. Work on 4 GHz cavities has also been carried out in Genova.

Its program for 1992 includes completion of the commissioning and operation of LISA and also some R & D topics directly related to future linear colliders, and in particular to TESLA, summarized in the following.

- Development of techniques to hydroform and sputter (Nb) 1.3 GHz cavities. This program will start in 1992 with main contributions coming from Tor Vergata, LNF and Milan. A basic research set-up in Tor Vergata is funded, while cavity production in Milan is at present under review.
- Feasibility study on a superconducting RF gun capable - in association with a magnetic compressor - of producing the beam structure required by TESLA. First prototyping of some parts, at present partly funded, is foreseen for the end of 1992.

The production of high quantum efficiency photocathodes to be operated in a SC environment is funded and underway, in collaboration with industry and the University of Wuppertal. It is mainly centered on Milan with contributions from LNF.

R & D Studies at GECS (Saclay-Orsay)

Field emission

1. Studies in DC, at room temperature, with dedicated facilities:
 - a) Plane parallel gap housed in UHV, enabling the measurement of the Fowler-Nordheim characteristics (including the very low current regime) of 1 cm^2 sample cathodes. This facility has a rapid turnover of samples, and can be used for testing the effect of various surface treatments (anodization, electropolishing, other coatings..).
 - b) Scanning electron microscope equipped with a needle probe anode for in situ microscopic study of emitters.
2. Studies in RF, with a mushroom TM020 cavity in preparation at Orsay.

Improvement of the cavity Q value

There is at Saclay a theoretical and experimental effort on dissipative phenomena in RF superconductivity (trapped flux, thermoelectric currents, granular superconductivity, special resonators for measuring the surface resistance of samples..).

Thin films

Saclay concentrates on the deposition of Nb and NbTiN on copper substrates by (reactive) magnetron sputtering (many recent advances). Sputtering capabilities for samples and for cavities exist in the laboratory, together with characterization facilities (T_c , R_s , H_c , λ , chemical and X-ray analysis...).

Chemical treatment of cavities

1. Development of an automated chemical process.
2. Research of improved chemical treatments in order to suppress H contamination.
3. Dust contamination and storage of cavities.

Thermal behaviour of cavities

1. Model calculations.
2. Thermometry in superfluid Helium.
3. Thermophysical properties of materials (Kapitza conductance, thermal conductivity).

CORNELL / FERMILAB R & D for TESLA

High Power Pulsed RF Processing

Tests will continue on 1-cell, 2-cell and 9-cell cavities at 3 GHz using the maximum available power of 200 kW. 1-cell cavities will be tested with thermometry diagnostics, and dissected after HPP. Emitters studied with thermometry will be processed with HPP and the sites will be examined microscopically. We also hope to determine the number of emitters processed as a function of field level. The 9-cell cavities will be used to increase the statistics of results on high gradients with HPP, and to study the best parameters for processing. We also plan to apply HPP to a heat treated cavity. A collaboration between Fermilab and Cornell has been set up to start HPP tests on 1.3 GHz cavities as soon as possible. 2 x 5-cell cavities of the TESLA shape, including polarization, are under fabrication. Another 2 x 5-cell cavities of the LEP-DESY shape have been ordered from industry which has dies at 1.3 GHz already available. Fermilab is building a cryostat insert to allow HPP up to 1 MW RF peak power. Negotiations are underway for a loan of a 4 MW · 300 μ s klystron from Boeing with modulator included. This klystron will be set up at Cornell. It is hoped that RF cold tests can start within a one year time frame. Thermal modelling of breakdown in pulsed RF fields will be carried out using a programme developed at DESY.

Heat Treatment

Tests will continue on 6-cell cavities at 1.5 GHz to increase the statistics of high gradient results with heat treatment. 3 GHz 9-cell cavities made at Cornell will also be heat treated and tested at Wuppertal. When higher RRR Nb is available, 1-cell cavities will be made and tested with heat treatment.

Basic Studies on Field Emission

The mushroom cavity will be used to study the nature and number of emission sites as a function of surface treatment and different materials. Experimental and theoretical analysis of starburst features found at the site of processed emitters will continue. Experiments to compare He processing and RF processing of emitters will be carried out.

R & D for SRF at DESY

Hydrogen contamination of Niobium

We will continue our investigation on the Hydrogen contamination of Niobium. Recent work on samples shows, that the content of Hydrogen can be decreased by chemical treatments. The problem is to produce a smooth surface at the same time. It is planned to continue the work on samples before a 500 MHz cavity is treated by this method.

In addition two 500 MHz cavities will be built. One will be treated by the "CERN" chemistry to investigate the benefit of this method. The other cavity will be fabricated including the final 800 C degassing procedure. It is the aim to work out a fabrication method for new 500 MHz cavities as well as to find a cure for the existing (and polluted) HERA cavities.

High power input window

The gradient of the HERA superconducting cavities is limited by the power rating of the input window. The level of 100 kW should be increased to 200 kW. A prototype of a improved design has been tested up to 300 kW. More experimental evidence is needed, however, to ensure a safe operation at this power level. For this purpose a new high power test set up is under construction. Regular tests will start in May 1992.

Sputter coating of ceramics for windows

The experience with the 500 MHz input windows show, that an anti-multipactor coating of the ceramic is essential but critical. So far all our 20 windows have been sputtered at CERN. It is planned to establish an own sputter facility to investigate different coating materials.

Input window for TESLA

For the TESLA cavities an input line design has to be developed: 1.3 GHz, 208 kW, 1.33 ms, 10 Hz rep. rate, coaxial design. A laboratory test model is under construction, first measurements will start in spring 1992. It is planned to finish a high power version before end of 1992.

Higher order mode coupler for TESLA

Several ideas of new coupler schemes for TESLA cavities are investigated. Two 9-cell cavities (Cu) from an earlier 1 GHz project are available at this time. The shape is close to the TESLA design so that first measurements started already. Results can be expected during spring 1992.

R & D for TESLA at Wuppertal

Based on the research and development of superconducting cavities with high fields and low losses since the early seventies, these activities will be continued at Wuppertal with the emphasis on further improvements of SRF for future linear electron accelerators like TESLA. Because of the available infrastructure, the SRF properties will be studied mainly at 3 GHz.

Our work will focus on 3 GHz 1-cell and 9-cell cavities built from niobium with the highest available purity grade. This includes russian Nb with an RRR of more than 500, which can be postpurified with a titanisation to RRR values far above 1000. The thermal breakdown and field emission loading of such cavities will be investigated as a function of standard and improved preparation techniques like chemical and heat treatment, combined with ultrapure water and methanol rinsing, and dust-free assembly conditions. High resolution thermometry and X-ray mapping in superfluid helium will be extensively used to measure the residual loss distribution and to localize and characterize the remaining defects and field emitters. In addition, the effect of RF and He processing with 400 W in cw or pulsed operation can be studied. Thermal model calculations will be performed for the analysis of the experimental data. The overall goal of these measurements consists in the exploration of the ultimate field limitation of 1-cell as well as in an improved reliability of high gradients and Q-values in 9-cell Nb cavities.

Valuable hints for the improvement of the surface preparation techniques as well as a deeper understanding of the enhanced field emission process are expected from our sample investigations with a scanning field emission microscope which has been installed recently. High resolution images of the field emitters and their in-situ current distribution shall be obtained by means of an integrated scanning tunneling microscope and a high resolution SEM.

Our recently started experiments with a superconducting photoemission gun will focus on the investigation of interactions between superconducting cavities and highly efficient photocathodes. We intend to determine operational conditions with maximum gun performance but minimum quality degradation of both components. In addition the preparation of several cathode materials and their behavior in various residual gas compositions will be studied. Based on our experience a complete design for a prototype photoemission source for TESLA will be developed in collaboration with the INFN group at Milano.

Since granular high-temperature oxide superconductors show too much RF losses at high

field levels, we also plan to continue the successful work on Nb_3Sn layers made of Nb cavities by the vapor-diffusion technique, which have been stopped 1988 because of the HTSC development. Nevertheless, Nb_3Sn would enable at 1.3 GHz TESLA operation at 4.2 K. Moreover, the theoretically expected magnetic field limitation is about twice as high as for Nb. Therefore, we will start to coat high purity Nb samples and some of our best single-cell Nb cavities with Nb_3Sn to evaluate the potential of this material by means of the experiments described above.

The beamtubes with coupler ports are fabricated from the same niobium quality with similar care and inspected in the same way. The surfaces of the flanges should not have any scratches radially, in order to ensure leakfree connections. All flanges with scratches have to be reworked.

From the half cells cavity cells are made by welding with electron beam welding preferably from the outside. It is important to find welding parameters that do not produce projections on the inner surface. In general it can be said, that a defocussed broad beam with high current and low voltage produces best results. Each weld and its surroundings have to be inspected on the inside for fissures, holes and projections. Defects that cannot be removed with a cutting tool by hand, make the cell unusable. Cells are then welded together with electron beam welding. Good stress free alignment before welding is essential for good welds and respect of the mechanical tolerances. The vacuum in the electron beam welder must be oil free and at least 10^{-6} mb. After welding the beam tubes to the cavity in a similar way, all welds are again inspected.

The full cavity is inspected for dimensional tolerances.

At DESY

After reception tests, which comprise visual inspection, verification of dimensions, vacuum test, measurement of resonance frequency and field flatness, the cavity is degreased in a similar way as above.

From here onwards all operations which expose the inner surface of the cavity have to be done in a clean room!

At the entrance into the clean room all parts of the cavity and its support are cleaned by spraying with dustfree DI-water and at least 3 bar pressure.

A chemical polishing, as described later in more detail, is done on the inner side of the cavity in order to remove a layer of 20 μm . The chemical polishing installation is located in a class 10000 clean room. All operations have to be controlled automatically for optimum reproducibility. A first rinsing with high quality DI-water of at least 10 $\text{M}\Omega\cdot\text{cm}$ resistivity, and filtered to 0.22 μm follows immediately the chemical polishing. The cavity is then filled three times with DI-water.

The connections to the chemical polishing machine are removed, and the cavity is installed for the final rinse with very high purity water and under a pressure of at least 100 bar. At least 800 liters of water are used for this final rinse. This operation takes place in the sluice to the class 100 clean room. From now onward the cavities are handled in a semiautomatic way by manipulators in order to avoid contamination. The operation takes place in a carefully controlled laminar clean room environment of class 100.

The cavity is dried by pumping with an oilfree vacuum pump with a liquid nitrogen cold trap. A steady flow of filtered nitrogen, which is fed into the connection between the cavity and the pump, provides an additional protection against backflow of contaminated air.

After drying the cavities are closed for the first cold test. They are connected to a clean vacuum system with electropolished interior surfaces. (Indium seals should be avoided). A turbomolecular pump and a primary pump are used, with an oil vapour absorber and an automatic valve between them. No ion getter pumps are used, to avoid contamination with titanium dust. Venting will be done by a clean capillary tube with filtered nitrogen directly through the end flange of the cavity. The Q versus E and the Q versus T curve can then be measured. In this way a rather complete diagnostic of the cavity can be performed.

The high peak power processing is done in the vertical cryostat, to bring the cavity up to the maximum possible field. The feasibility of this processing implies a variable coupler ($Q = 10^6 - 10^{10}$) and a high power klystron (1-2 MW).

If necessary, a heat treatment in a clean ultrahigh vacuum oven at 1500° C follows. The cavity is enclosed in a multilayer titanium box for avoiding a degradation of the niobium heat conductivity by diffusion of nitrogen and oxygen rest gas into the bulk. In order to avoid contamination after this treatment, the aperture of the furnace is located in the clean room (class 100). This heat treatment will be followed by a second vertical cold test.

It is essential to keep the cavity qualification after a successful testing, and thus to avoid contamination during the (dis) mounting of the cavity. To achieve this, the test inserts must be equipped with two metal valves closing the cavity. After a successful testing, the insert and the cavity are filled with pure filtered argon, the valves are closed, and the isolated cavity can then be dismantled with the valves and stored without risk of contamination. This arrangement is compatible with a variable coupler on the lateral port of the cutoff tube of the cavity.

The isolated cavity (still under argon atmosphere) is then welded to its helium tank, brought back into the clean room after the standard rinsing and drying, and is equipped with its definitive couplers

A third cold test may then be intended to check that no degradation of cavity performance occurs in a horizontal cryostat.

Cavity installation then continues in the clean room (class 100); the cavities are joined together on a supporting bench by a semiautomatic manipulating device. At this stage, the valves used for cavity storage are removed. The cavities joined together and equipped with vacuum valves, main and HOM couplers and filled with clean argon are rolled in the class 10000 clean room and here loaded onto the outside transport chariot. The assembly chariot does not leave the clean area. The joined cavities are then transported out of the clean area. In the hall they will be assembled into a cavity cryomodule, which will then be brought to the test facility for a first performance test.

Cleaning

The cavities have to pass a very thorough cleaning, each time they enter the class 10000 clean area. In a cleaning sluice the outside of the cavity is cleaned with a vacuum cleaner and with filtered compressed air or nitrogen to avoid contamination of the clean area. All parts and tools needed in the clean area are processed in a similar way.

Before the first chemical polishing a degreasing will be done with fresh and warm (60°C) alkaline detergent, assisted with 20-40 kHz ultrasound. The detergent is filtered before use by a $1\text{ }\mu\text{m}$ membrane filter. Only high quality detergents will be used. After degreasing the cavity is rinsed by spraying with filtered ($0.22\text{ }\mu\text{m}$) DI-water of at least $10\text{ M}\Omega\cdot\text{cm}$ resistivity.

Each time the cavity (or any other piece) enters the class 100 clean room, an intensive rinsing by spraying with high purity $18\text{ M}\Omega\cdot\text{cm}$ water filtered to $0.04\text{ }\mu\text{m}$ is done. The interior of the cavity is sprayed with at least 500 liters of water and with a pressure of 100 bar. The water is sprayed through three nozzles that produce each a solid cone of water. A turning rinsing head is introduced into the cavity (axis vertical) from below. Loose covers on all openings permit also the flanges to be rinsed. The final filter is mounted on the rinsing cane after the flexible teflon hose and the swivel joint. All tubes have to be electropolished stainless steel or titanium. From this rinsing onwards, and until the cavity is closed, the cavity should not be approached. Clean,

especially designed manipulators will do in a semiautomatic way all operations on the cavity. The rinsing and the handling will be the performance determining operations of the cavity.

Chemical Treatment

The chemical treatment is designed to remove all surface defects, that are detrimental for the cavity performance. This operation involves a very dangerous mixture of concentrated hydrofluoric acid, nitric acid and phosphoric acid. It is the phosphoric acid and the temperature that determine the speed of the dissolution of niobium and the rise of temperature of the acid mixture. A mixture of 1 volume part hydrofluoric acid, 1 volume part nitric acid, and 2 volume part phosphoric acid has proven to be a reasonable compromise. The starting temperature of the mixture should not exceed 18⁰ C for avoiding a runaway reaction.

The design of the installation uses ideas developed at CERN and at Saclay. The cavity with its axis vertical is connected to a computer controlled machine, where the chemical products are never opened to the outside. The chemicals are pumped with slow volumetric pumps to elevated containers. From there they fall after opening of the respective valves by gravity into the cavity. After a preset time, another valve opens, and the chemicals are drained into the storage containers that are placed under the floor level. In an emergency this last valve can be bypassed by a manual valve, and the product being dumped into the retention container. Immediately after emptying of the chemicals, the cavity will be rinsed via an already mounted spraying cane with 0.22 μm filtered DI-water of 10 M $\Omega \cdot \text{cm}$ resistivity. The first rinsing water is drained into the retention container. The cavity is then filled three times with DI-water. Also this water is drained into the retention container. The connections to the chemical machine are removed, and the cavity is transferred to the high pressure rinsing station, where the final rinse under strict clean room conditions is performed.

Foreseeing four identical upper and lower containers with their volumetric pumps, provides ample freedom for the adaptation of the process according to new developments. One of these circuits can be used for including a nitric acid treatment for the removal of indium contaminations. It could also be interesting to try again the formerly so successful oxypolishing, which would need two circuits. However, for safety reasons it should be avoided to introduce alkaline process steps.

A moderate ventilation around the cavity and the containers, filters, and pumps keeps the environment completely clean of acid vapors. The ventilated air is passed through an alkaline acid scrubber.

All acidic waste liquids are collected in the retention container, which should have a much bigger volume of at least 800 liters. From this retention container the waste is pumped with a membrane pump into transport containers for removal. If necessary, the waste can be neutralized and the fluorides precipitated before transport.

All containers, valves, pumps, tubes, hoses, and filters are made of PFA. Where not available, PVDF or PTFE can be used. The tubes are stud welded. All machined surfaces are heated to weld a smooth surface. The chemicals are of reagent quality ("Selectipur" of Merck or equivalent) and filtered to $0.22\ \mu\text{m}$. In this way a high degree of safety on cleanliness can be obtained simultaneously.

Thus, the chemistry room contains:

- The installation for DI-water. One circuit with essentially unlimited supply of $10\ \text{M}\Omega\cdot\text{cm}$ water, and one supply with say 1200 liters of very high purity water.
- One stainless steel degreasing bath with filters pumps ultrasound and heating for the cavities and a smaller bath for the cleaning of couplers and other parts.
- One stainless steel tank with DI-water equipped with ultrasound and heating for rinsing of the cavity after degreasing and a smaller tank for rinsing of couplers and other parts.
- The chemical machine consisting of four circuits with upper and lower containers, made of PFA and of 100 liters content. From each lower container a small metering pump pumps the liquid through a filter into the upper container. In one circuit a counterflow heat exchanger before the filter permits to cool the acid mixture to below 18°C . The coolant is tap water. All containers are connected to the cavity, the retention (waste) container, and to the ventilation. The cavity is connected via the rinsing cane to the DI-water circuit. The machine is controlled by a processor or microcomputer, which also does the process logging.
- The final rinsing installation, which consists of a high pressure membrane pump, with the final filter and the rinsing cane. The rinsing is done in the sluice to the class 100 clean room.
- Two ventilation circuits. One circuit blows filtered clean room class 10000 compatible air

into the room. The other circuit ventilates the acid vapours through an acid scrubber to the outside. The balance between both circuits has to be such as to insure a slight overpressure in the room, avoiding contamination from the outside.

- Safety equipment as a safety shower, a safety bath filled with a 30° C slightly alkaline magnesium sulfate solution in water for rapid precipitation and neutralization in case of an accident with the acids. Breathing equipment, acid resistant clothes, goggles, boots etc. The upper and lower containers, the retention container and the place, where the cavity is connected to the chemical machine, are placed in acid resistant basins. The electrical installation must be compatible with a wet room and protection with differential safety switches must be foreseen.
- The inside surfaces of the room shall be water resistant. Stainless steel is the only metal permitted. Good drains must be installed to permit water spillage during manipulations.

High Purity Water Installation

The high purity water, needed for the final rinsing of the cavity and all other parts connected to it, is of vital importance for the final performance. The quality of the water has to be comparable to the standards used in semiconductor manufacturing. The cleaning is very much improved by creating a strong tangential flow of high speed very near the surface. This tangential flow is most effectively generated by a vertically (!) impinging water jet. Shearing forces are generated, that are able to remove even small particles attached by electrostatic forces to the surface.

The high purity water installation receives water from the DI-water distribution in the building. This water is passed through an activated carbon filter, a membrane filter, and a first mixed bed ion exchanger (two units in series). If necessary a pump for boosting the pressure is installed at the input. This is the external circuit. From here it enters via a check valve the internal circuit. The internal circuit consists of the following sequence of parts: a membrane filter, a UV-lamp for sterilization, a nuclear grade mixed bed ion exchanger with an addition of scavenger resin to remove non ionized compounds (again two units in series), a membrane filter to the user and a membrane filter to the 1200 liter storage tank. From the storage tank the water is circulated in the inner circuit by a low pressure magnetically coupled PVDF pump. All filters have a pore size of 0.22 μm . The tank above the water is filled with filtered clean nitrogen. Sample ports are foreseen at different points of the installation for surveillance and trouble shooting. Water meters,

pressure gauges, conductivity meters, and flow meters are appropriately installed to verify the correct operation of the installation. All parts are made from PFA, and were not possible from PVDF, PTFE, ss316 LN stainless steel, or titanium. The diameter of the tubing should not exceed 1/2 inch, to get a high speed of flow and to keep thus the tubing clean.

The water is passed into a high pressure hydraulically driven membrane pump as used in the chemically industry for metering of dangerous liquids. The pumphead is ss316 LN stainless steel, the membrane is a double Teflon membrane with a protection for membrane rupture. A pump with variable pressure of maximum 200 bar and a maximum flow of 15 liters per minute would be well adapted for this application. Via stainless pipes a pulsation damper and a membrane filter of $0.22\ \mu\text{m}$ and through a PTFE hose with a stainless steel braid the water enters the rinsing cane.

The rinsing cane enters the cavity vertically from below. The rinsing cane is moved vertically and around its axis by pneumatically driven motors. The waterjets are most efficient if they hit the surface vertically. Therefore three nozzles with 0 and $\pm 45^\circ$ are arranged such as to compensate their momentum. The nozzles are made of sapphire or tungsten carbide. The cane is ss316LN stainless steel electropolished inside and outside. If the cane has to be guided, it should pass through a water lubricated titanium bearing (titanium and stainless steel do not coldweld or freeze). After the Teflon hose and the swivel joint the final filter with a pore size of $0.04\ \mu\text{m}$ is installed in a titanium housing (for reducing the weight). Separately, also the outside of the cavity has to be rinsed with a similar device.

For the final rinsing the cavity is moved into a closed room, which is the chemistry side of the sluice into the clean room. After the rinsing the cavity remains for a predrying a short time in this part of the sluice and is then moved through an opening into the class 100 clean room.

For cleaning of all other parts, that enter the clean room a manual rinsing in a glove box can be done, similarly as it is done for the cleaning of laser windows for the fusion lasers.

For surveillance of the water quality and the efficiency of the rinsing the following instrumentation is needed. Resistivity meter temperature compensated, total organic carbon analyzer with a sensitivity down to a few parts per billion, a non volatile residue measuring instrument with the same sensitivity, a particle counter with a high sensitivity ($\leq 1\ \mu\text{m}$) head, and the equipment for monitoring bacterial growth. For detailed water analysis an external service can be used.

Clean Room Mounting

All those operations of assembly, where the cavity is open to air, must be done under strict clean room conditions. A clean room of class 100 with a size of 14 m length, 7 m width and 3 m height will be sufficient for these operations. The clean room is under slight overpressure, and can only be reached via a sluice from a clean room of class 10000. An emergency exit to be opened only from the inside, can be foreseen for safety reasons.

All parts that enter the clean room have to be cleaned with particle free DI-water of high quality. Only the material absolutely necessary for the operation, and compatible with cleanroom work should be in the clean room. Full protective clothing certified for class 100 clean room must always be worn (boots, pants, blouse, gloves, hair cap and a mouth protection). The particle count should be monitored and recorded continuously at least at three points. A competent firm should regularly service and clean the clean room. At least three technicians have to be fully trained for working in a clean environment. No untrained persons should have access to this area. The comfort of the people working in the clean room is important for obtaining good results. Air conditioning is therefore necessary.

Despite these precautions is it still possible to contaminate the cavity during mounting. Therefore all handling should be done by semiautomatic manipulators.

Also the clean room class 10000 has to be handled with great care. Protective closing here is also obligatory.